SOME STRUCTURAL STUDIES

ON

CHALCOGENIDES AND INTERMETALLIC COMPOUNDS

BY

ELECTRON DIFFRACTION

A THESIS

SUBMITTED TO

THE UNIVERSITY OF POONA

FOR THE DEGREE OF

DOCTOR OF PHILOSOPHY

BY

K. C. BARUA

Kamal Chandra

NATIONAL CHEMICAL LABORATORY

POONA-8.

OCTOBER 1966

C O N T E N T S

5

C H A P T E R - I

GENERAL INTRODUCTION

In the recent times epitaxially grown films have received much more attention than ever on account of their increasing importance in device applications and also because of the ease of preparations of single crystal films by epitaxial methods. The importance of vacuum deposited films in variety of purposes in research and industries was recognised long ago and this resulted in their well-known applications in the preparation of reflectors, anti-reflection coatings on lenses, paper capacitors, fluorescent screens, interference filters, multiple beam interferrometry, memories in computers and in many semiconducting devices. Some of the specialised uses of thin films in laboratory are for shadow casting, replica making by carbon or silicon monoxide films in electron microscopy. The wide applications of thin films in so many different fields have, however, been possible because of the development of efficient high speed vacuum pumps, suitable diffusion oils, gettering agents, demountable vacuum systems etc.

It is well-known that the properties of the thin films and of surface layers of solid differ considerably from those of the bulk materials. Consequently many physical and other properties, such as thermionic emission, surface

tension, adsorption and catalysis etc. are characteristic of surface layers. Even metallic conductors like sodium, potassium, rubidium and cesium etc. when deposited in thin film form, exhibit semiconducting properties (Mayer, 1959, 1961). It may be mentioned here that though many of the physical properties are structure-sensitive, very little attention has been paid to the study of structures of thin films, crystal growth process, development of orientations, phase changes etc. while working on electrical and optical properties of thin films grown on active and passive substrates. Vacuum deposited films can be obtained in a wide variety of structures from the irregular amorphous aggregates to single crystals by controlling the evaporating conditions, such as the rate of evaporation, substrate temperature, the state of vacuum etc. It is also feasible to have single crystal films grown epitaxially on single crystal substrates with desired orientations, shape and size etc. by appropriate evaporating conditions.

The discovery of diffraction of X-rays by crystal lattice (Friedrich, Knipping and Laue, 1912) gave the first direct method for determining the crystal structure of solids. Even though there are many advantages of this technique for the bulk structure, this method cannot be used for the study of surface layers and thin films. The diffraction of electrons by crystal lattice observed by Davisson and Germer (1927, 1928) and almost simultaneously

by Thomson (1928) provided a powerful tool for the study of structures of surface layers and thin films. The applications and the theory of scattering of electrons have been discussed by many workers (Finch and Wilman, 1937; Thomson and Cochrane, 1939; Raether, 1951, 1957; Pinsker, 1953; Vainshtein, 1964; Cowley and Rees, 1958 and others).

X-rays are scattered by the electron shells of the atoms, while atomic nuclei with their positive charges remain 'invisible' to them. A picture of the distribution of electron density within the crystal can be obtained from the Fourier treatment of experimental X-ray data, the peak in the electron density map corresponds to the atoms of the crystal lattice. Electrons are scattered by the intense electrostatic field due to the atomic nuclei modified by the electron clouds. The Fourier synthesis from electron diffraction data provides a picture of the potential distribution in the lattice, the maxima again coinciding with the nuclei. The scattering of X-rays by atoms is approximately proportional to the atomic number and hence light atoms in the presence of heavy ones present difficulties in resolving, particularly when the difference of atomic number is large. In the case of electrons the scattering amplitude is less dependent on the atomic number and hence lighter atoms are more easily resolved. The average absolute magnitude of the atomic amplitude of scattering of X-rays is approximately 10^{-11} cm. and that for electrons is about 10^{-8} cm. Since the intensities are proportional to the

square of the amplitudes, the corresponding intensities for the scattered waves of X-rays and electrons will be about $1:10^6$. To obtain a measurable intensity the specimen must be about 1 mm. in linear dimension in the case of X-rays and only about 10^{-4} to 10^{-5} mm. for electrons. However, in the latter case the thickness will be limited by the increase of effects due to inelastic and incoherent scattering, secondary scattering of the already-diffracted beams, absorption etc. Electrons with accelerating voltage of about 50-60 KV can penetrate crystalline films of a few hundred angstroms thickness, depending upon the atomic weight of the materials. During this process electrons do not lose appreciable amount of energy and hence the scattering is elastic and coherent. In the case of electron diffraction study by reflection a crystalline layer of 5-10 Å thickness is good enough to yield sharp diffraction patterns. The same film when put for the transmission pattern, electron beam traverses through the whole film thickness and hence gives the information which is characteristic of the total thickness penetrated by the beam, thus providing knowledge about the nature of the deposit as a whole. Often reflection patterns from the surface layers and the transmission patterns from the same film are different, thereby indicating the changes occurred during the crystal growth process. Any change in the crystal structure due to the change of evaporation conditions and other variables can all be detected by

this technique. Thus electron diffraction is an ideal tool, not only for the surface structure but also for the study of phase changes, orientations, twinning and other phenomena associated with the crystal growth process.

Crystal growth

In the case of an ideal crystal, atoms or ions occupy the minimum potential energy configuration. Due to the action of the interatomic forces the atoms or ions are clustered together to pack themselves closely, thus forming a three dimensional pattern. The crystal grows atom by atom, layer by layer, though growth of succeeding layers may and indeed generally does start before a layer is completed. Each atom, as it deposits on the substrate takes up a position compatible, in terms of potential energy with the surrounding conditions. The initial nuclei thus formed over the substrate begin to grow and further growth of the film is in general no longer directly influenced by the substrate. Since the growth takes place simultaneously either on the same or different layers, the atoms at the junctions are not in their maximum stability conditions, thus giving rise to defects such as dislocations, stacking faults, twinning etc. in the crystal.

Gibbs (1878) on thermodynamical ground suggested the first quantitative theory of the crystal growth process. Curie (1885) and Wulf (1901) followed it. The atomic theory

of crystal growth had been developed by many workers (Volmer, 1939; Kossel, 1927, 1928; Stranski, 1928, 1949; Becker and Doring, 1935, 1949 and Frenkel, 1945, 1946). Later on by taking into consideration the presence of imperfections and dislocations, Burton and Cabrera (1949), Burton, Cabrera and Frank (1951) developed the theory of crystal growth. Most recently Hirth, Hruska and Pounds (1964), Rhodin and Walton (1964), Bauer (1964) and van der Merwe (1964) have discussed the theories for vapour phase deposit films, their initial nucleation, growth process and interfacial misfit etc.

The morphology of a crystal may considerably be modified by the presence of impurities during its growth. Thus for example, if sodium chloride is allowed to grow from a neutral solution cubic crystals are obtained, but if it is allowed to grow in the presence of a little urea, octahedral crystals are formed and in the presence of gum-arabic dendritic growth of sodium chloride crystal is observed. In all the above cases, however, the atomic arrangement in the crystals remains the same.

Epitaxy

Royer (1928) used the term 'epitaxy' for the first time to signify the oriented growth of a crystal over another. An epitaxial film on a crystalline substrate means a single crystal film, the lattice of which has a definite orientation relationship with respect to that of the substrate. This

sort of growth of a crystalline film over another crystalline substance is known as oriented overgrowth or epitaxy. The epitaxial growth of crystals was observed in nature as early as 1902 by Wallerant and 1903 by Mugge.

Royer studied many cases of epitaxial growth. He observed that the deposit atoms or ions take up orientation as to follow the substrate structure such that there was a close fit between the two-dimensional network at the interface of the deposit-atoms and the atoms of the substrate. It is now proved beyond doubt that in the case of vapour phase deposits the substrate and the conditions of evaporation, such as temperature of the substrate, rate of deposition etc. have great influence on the growth process of the crystal. Royer found that in the cases of epitaxy there was a densely populated lattice row in the deposit parallel to the one of the substrate rows, provided their relative identity spacing did not differ by more than 15%. By treating the substrate as a two dimensional network, Frank and van der Merwe (1949) found a similar limit for the formation of epitaxial layers. The difference between the network spacing of the substrate and the deposit layer of atoms is generally expressed in terms of percentage misfits. The observations of Pashley (1956) indicated that a measure of similarity or a correspondence in the adjacent atomic patterns is a prerequisite for an oriented overgrowth. Quantitatively the misfit may be expressed by

$$f_i = (a_i - b_i)/a_i ; \quad i = 1, 2$$

where i = 1,2 refer to two suitably chosen interfacial directions, b_i and a_i being the normal spacings of corresponding atoms in the direction designated by i. For certain purposes the expression used is

$$f_i = (a_i - b_i) / \tfrac{1}{2}(a_i + b_i)$$

which is more natural way of expressing the misfit since the denominator is the arithmetic mean of the spacing in the direction i.

The situation as to the orientation role of the surface may be summerised as :

(a) Epitaxy of a given deposit can occur on a variety of substrates and does not necessarily depend on a close crystallography registry between the substrate and the deposit.

(b) General understanding of epitaxial growths depends on a detailed knowledge of the mode of nucleation and growth characteristic of each vapour-solid combination.

Now it is well-known from many experiments, that epitaxial growth of a crystal can take place even if the lattice misfit is as high as 50% (Pashley, 1956; Goswami, 1954) thus suggesting that van der Merwe's idea that the misfit larger than 15% would lead to polycrystalline deposit is not strictly valid.

Phase transition and polymorphism

Polymorphism is often observed in the case of thin films even though the same material does not show morphism in the bulk form. Finch, Wilman and Yang in 1947 observed both f.c.c. and h.c.p. forms of nickel formed by electro-deposition. Rubidium bromide which has normally NaCl type of structure was found to have CsCl type of structure when deposited on silver substrate (Schulz, 1951a), the misfit being zero. He also observed that cesium and thallium halides in the thin film form often possessed NaCl type of structure (Schulz 1951b). During the study of Cr, Ni, Be, Co etc. by electron diffraction Bublik (1952) observed that the change of structure occurs due to the difference of thickness of the film also. A new b.c.c. form was also reported when nickel was evaporated on rocksalt under suitable conditions (Finch, Sinha and Goswami, 1955). During the study on the reaction of sulphur vapour on copper single crystals, Trehan and Goswami (1959) observed polymorphism in Cu_2S. Even from the cubic forms of ZnS and CdS Aggarwal and Goswami (1963a) obtained the corresponding hexagonal phase when the materials were evaporated in vacuo.

In the recent years immense interest has been shown on the selenides and tellurides of metals especially in thin film form because of their semiconducting properties. As these properties are considerably dependent upon the structures and crystal growth process, a detailed study on the crystal

growth process, their phase change, development of orientations, epitaxial growth etc. has been made on the selenides and tellurides of mercury, thallium and indium and also on some intermetallic compounds like indium antimonide which are known to be semiconductors.

--

C H A P T E R - II

EXPERIMENTAL TECHNIQUE

(a) Preparation of substrates

In the present study the substrates used for deposition were both amorphous and crystalline materials, the amorphous substrates consisted of collodion films and glasses whereas the latter consisted of single crystal substrates such as (100), (110) and (111) faces of rocksalt and the cleavage face of mica i.e. (0001) face.

The (100) face of rocksalt was prepared by cleaving a rocksalt crystal with a sharp and clean knife under slight pressure. The other faces, such as (110) and (111) were prepared by grinding the rocksalt crystals at appropriate angles with different grades of emery papers down to 0000. These faces were etched by dipping momentarily in distilled water and then quickly pressed with filter papers. Faces prepared in this way were examined by electron diffraction technique. Crystals were reground and reetched, if necessary, to get the appropriate faces. For the cleavage faces of rocksalt etching was not necessary. Fresh crystal surfaces were always used for every fresh deposition to avoid contamination.

Collodion films were prepared by putting a drop of collodion solution in amyl acetate on the surface of distilled

water in a petri dish (diameter about 10 cms). Amyl acetate evaporated quickly and a thin uniform collodion film was left over the surface of water. This collodion film was then picked up on a clean and fine wire gauge. The films thus prepared were dried in a dessicator.

Glass substrates were made by cutting microscope slides to sizes about 1 x 2 cm^2 . Their sharp edges were ground and the slides were washed with nitric acid, running tap water and then dipped in acetone and dried in an oven at about 80°C.

For mica (0001) face, a freshly cleaved mica was used, the size of the mica pieces used for deposition being the same as those of the glass pieces.

The substrates used were always handled by tweezers to avoid possible grease contamination.

(b) Method of deposition

The method of deposition of films over the substrates as mentioned before was from vapour phase. The evaporation was carried out in a pyrex glass tube about 50 cms. in length and 6 cms. in diameter. The filament terminals were made of copper rods (about 1/8" diameter), which were put through a rubber stopper fitted tightly with the glass tube. The other end of the tube was closed with a similar rubber stopper fitted with a tube, which was connected to the pump for evacuation. The stoppers used were initially boiled in NaOH solution for a few hours to remove sulphur and other

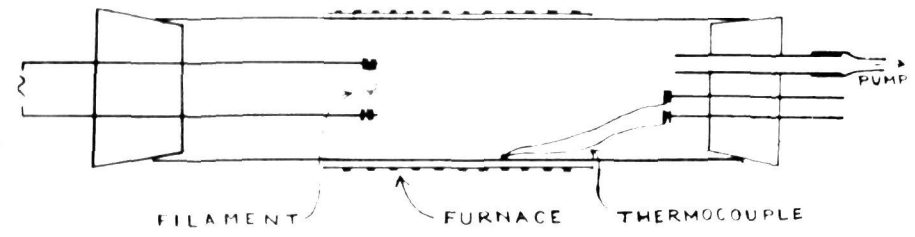

Fig. 1. Evaporation Assembly

impurities. Tungsten, nichrome or kanthal wires were used as filaments, from which the compounds were evaporated. The selection of the filament was made according to the melting point of the compounds to be evaporated. Evaporation was carried out by passing a current through the filament, the current being controlled by a dimmerstat and a step-down transformer (25 volts-10 amps.). The substrates were usually put 4 to 5 cms. away from the filament. In some cases they were put just below or far away from the filament, depending upon the nature of experiments. The system was continuously evacuated by an Edwards' two stage rotary pump. Oil diffusion pump was used when higher vacuum was necessary. Fig.1 shows the evaporation assembly used.

(c) Heating of the substrates

The deposition was carried out at different substrate temperatures, ranging from room temperature to a maximum of about 400°C. The temperature of the substrates was maintained by a tubular furnace made by winding resistance wire on a silica tube. The diameter of this silica tube was slightly bigger than the outer diameter of the pyrex tube used as vacuum chamber, so that it could be slided over the vacuum chamber. The length of the furnace was $\sim$15 cms. The furnace was designed to reach a maximum temperature of about 450°C. The heating of the furnace was controlled by a variac. Before deposition the substrates were put inside the chamber in such a way that the crystal faces would receive the deposit at an

inclined angle. The chamber was then evacuated for a long time and the furnace was made on and kept at the desired temperature for about an hour and a half. The temperature inside the vacuum chamber was measured with a thermocouple put inside the chamber.

(d) Removal of the deposit films from the substrates

To study the surface structure by reflection method the substrates along with the deposits were put directly in the electron diffraction camera, after cooling them down to the room temperature in vacuo and the electron beam was allowed to graze on the deposit films. When the film was to be studied by transmission method, it was removed from the surface in the following way.

Distilled water was taken in a petri dish and the crystal was held gently by a tweezer in such a way that the film surface would be nearly horizontal. The crystal was slowly dipped in the dish of water allowing the rocksalt to dissolve and the film to float on the surface of water. Usually a bigger petri dish was used with sufficient water to avoid sodium chloride contamination. These films were then picked up over the nickel wire gauge over which a thin film of collodion was previously placed and dried as described before in paragraph (a). These films were then dried in vacuo in the diffraction camera.

(e) Examination of the specimen

The electron diffraction camera used in the present investigation was of cold-cathode type (Finch and Wilman, 1937). The accelerating voltage used was of the order of 50-60 KV. The camera lengths were 50 and 25 cms. The deposits were generally first studied by reflection and subsequently by transmission after removing the films from the substrates as described before. Deposits on glass and mica were always studied by reflection only whilst on collodion by transmission.

The bulk materials after preparation were first studied by X-ray powder method to know their bulk structures and then evaporated from the filaments as described before in paragraph (b).

(f) Interpretation of electron diffraction patterns

The electron diffraction patterns obtained can usually be classified in the following categories.

(1) Single crystal or two-degree (2-d) oriented patterns which mostly consist of spots. The disposition of these spots changes considerably when the azimuthal direction of the beam changes with respect to the deposit axes.

(2) Ring patterns which do not change with the change of beam direction are no doubt due to the polycrystalline nature of the deposit.

(3) One-degree (1-d) oriented patterns (generally of discontinuous arc-type) are also due to polycrystalline deposits, but with a preferred orientation (fibre axis).

Quite often the observed patterns, however, consist of a mixture of the above.

The method of interpretation of the electron diffraction patterns from the crystalline deposits as adopted in the present investigation was described by Finch and Wilman (1937), Thomson and Cochrane (1939), Wilman (1948 a,b; 1949, 1952), Pinsker (1953), Cowley (1953, 1956), Raether (1951) and hence not discussed here.

--

C H A P T E R - III

STRUCTURE AND CRYSTAL GROWTH OF SELENIDE AND TELLURIDE OF MERCURY

A. INTRODUCTION

Out of $A^{II} B^{VI}$ type of compounds, namely, selenides and tellurides of Zn, Cd and Hg, the compounds HgSe and HgTe have the highest mobility as well as very low activation energy. As a result these two compounds have great possibilities for uses in various electronic and optical devices, such as Hall generator, magnetometer, infrared detector etc. The effect on electrical resistance of selenium due to the contact with metallic mercury was observed by many workers (Moss, 1877; Brown, 1913; Tisdale, 1918). Zachariasen (1925, 1926) investigated the structure of HgSe and HgTe and reported that these two compounds crystallised with zinc-blende type of structure. The lattice parameter of HgSe was found to be $a_o = 6.080 \pm 0.004$ Å with calculated density 8.266 gm/cm^3. de Jong (1926) reported the lattice parameters of tiemannite (HgSe) and coloradaite (HgTe) to be as 6.069 ± 0.006 Å and 6.43 Å respectively with space group $F\bar{4}3$ m. The effect of mercury vapour on selenium rectifier (Williams and Thompson, 1941) and the decrease of thermoelectric power in the presence of mercury vapour were reported

(Henisch and Francois 1950, 1951). An elaborate study was made on the above reported phenomena by Henisch and Saker (1952). Selenium rods were kept in contact with mercury vapour or liquid mercury for long time and the scrap material from the surface of selenium was examined by the X-ray powder method. It was found that the material thus formed had zinc-blende type of structure with the lattice parameter $a_o = 6.04$ Å which was similar to that for HgSe reported by Wyckoff (1931, $a_o = 6.07$ Å).

While studying Se and Te films condensed on collodion supports by electron diffraction, Zorll (1964) observed that mercury vapour from the diffusion pump in the vacuum system reacted with the films. The lattice constant of the crystalline films were determined. The values were

HgSe cubic, B3 type, $a_o = 6.074 \pm 0.006$ Å,

HgTe cubic, B3 type, $a_o = 6.429 \pm 0.006$ Å.

From the X-ray powder patterns the value of a_o was determined for HgSe and was found to be equal to 6.085 Å (Swanson, Gilfrich and Cook, 1957). The methods of the preparation of HgTe polycrystalline samples and the study of their electrical and optical properties were described by Carlson (1958), Lagrenaudie (1958) and Furmeron-Rodot and Rodot (1959). Elpat'evskaya (1958) prepared layers of HgSe-HgTe on glass and mica substrates and studied electrical properties at different temperatures. Black, Ku and Minden (1958) reported the preparation of single crystal of HgTe and the study of

Hall coefficient and resistivity as a function of temperature and magnetic field. Solid solutions of various compositions of CdTe-HgTe were prepared (Lawson et al. 1959) and their electrical and optical properties were studied. CdTe-HgTe, CdTe-ZnTe and HgTe-ZnTe systems were prepared for all compositions and their lattice parameters were determined (Woolley and Ray, 1960). Thermoelectric properties were measured for HgSe-HgTe systems by Branch, Zhdanova and Lev (1961). It was noticed that the electrical conductivity had a maximum for a 50-50% mixture. Measurements were made of the photo emission spectrum, current-voltage characteristics and optical absorption by Sorokin (1961) for HgTe. Long wave-length photo effect was reported by Blue et al. (1961) for HgSe and it was found to respond from visible to 15 μ. Single crystals of HgSe were prepared and their electrical properties measured between 90° to 500°K (Gobrecht et al. 1961). It was found to possess ZnS type of structure and split into (100) planes.

A phase transition was noticed (at 15,000 Kg/cm^2 pressure) for HgTe when studying electrical resistivity at high pressure (Blair and Smith, 1961). However, no information about the structure to which HgTe changed was given. A detailed analysis of Hall coefficient data obtained between 77° and 350°K for HgSe containing excess donor concentrations was reported by Harman and Strauss (1961). Solid solutions $HgTe_{1-x}Se_x$ were prepared with x varying from 0 to 1 and their

electrical properties were studied between 77° to 400°K (Rodot, Rodot and Triboulet, 1961). HgTe-CdTe solid solutions were prepared and conductivity measurements were carried out (Shneider and Gavrishchak, 1961).

Phase change for HgSe at pressure about 7.5 K bars was reported by Kafalas et al. (1962). It was found that below 170°K temperature the pressure phase was retained at atmospheric pressure. X-ray diffraction showed hexagonal type of structure with a = 4.32 Å, c = 9.62 Å, with calculated density 8.95 gm/cm^3. Kruse et al. (1962) reported long wave-length photo effect in HgSe, HgTe and HgTe-CdTe. The method of preparation of very pure p- and n-type HgTe was described and electrical measurements between 20° and 300°K temperatures were tabulated by Rodot and Triboulet (1962).

HgSe and HgTe were examined under high pressure by X-ray and it was found that ZnS type of structure transformed to distorted NaCl type (Mariano and Warekois, 1963). The lattice parameters were reported as,

HgSe at 15 K bars B3 6.09 to B9 4.32 Å, 9.68 Å;
HgTe at 20 K bars B3 6.44 to B9 4.46 Å, 9.17 Å.

Porowski and Galzaska (1964) reported phase transition within the pressure range 6 to 9 x 10^3 atmospheres for HgSe. Measurements on electrical properties were reported for single crystals of HgSe (Giriat, 1964). Single crystals of HgSe and HgTe were grown from vapour phase (Krucheanu,

Nikulesku and Vanku, 1965) and X-ray measurements were carried out for both powder and single crystal specimens. Lattice parameters determined from powder photographs were 6.08 Å and 6.445 ± 0.003 Å for HgSe and HgTe respectively. The authors concluded that hexagonal forms of the wurtzite type, characterising a number of $A^{II} B^{VI}$ compounds were not found in the present cases. Cruceanu et al. (1965) grew single crystals of HgTe and determined the lattice period as 6.466 ± 0.002 Å. Electrical measurements were carried out for these crystals.

Solid solutions of system $Zn_xHg_{1-x}Te$ were prepared and electrical measurements were carried out by Cruceanu et al. (1966) for different compositions. Kolosov and Sharavskii (1966) reported the measurements of thermoelectric power between 140° to 340°K and thermal conductivity between 90° to 430°K for p-type HgTe.

From the above survey of literature it appears that even though some work has been carried out on crystal structure and more on electrical properties, no attempt has been made to study the crystal growth process, phase transformation with evaporation condition, etc. for the vapour phase deposits of HgSe and HgTe. Since both the compounds have got great prospects for application in many devices and also that the electrical and optical properties etc. are so much dependent on the structure, defects etc. a thorough knowledge of crystal growth process on amorphous as well as

single crystal substrates is of great importance. With this view in mind a detailed study on crystal growth process at different substrate temperatures from vapour phase has been undertaken.

b. EXPERIMENTAL

Preparation of selenide and telluride of mercury

The selenide and telluride of mercury were prepared by the reaction of the component elements in vacuo, at temperatures above the melting point of the individual elements and the compounds. For this selenium (99.99%) or tellurium (99.99%) and mercury (distilled were taken according to the stoichiometric proportions (1:1 atomic proportion) in a silica tube of diameter about one cm. and sealed in vacuo ($\sim 10^{-5}$ mm of Hg). The sealed tube containing Hg and Se then slowly heated in an electric furnace upto $\sim 250^{\circ}C$ and kept at this temperature for about two hours, so that selenium would react slowly with mercury. The temperature of the furnace was then raised step by step (by about $50^{\circ}C$ per hour) to about 360°-$370^{\circ}C$, above the boiling point of mercury ($356.9^{\circ}C$) and kept for about two hours, so that the reaction would be completed at this temperature only. To get a homogeneous product of HgSe the temperature of the furnace was further raised slowly to about $700^{\circ}C$ and kept at that temperature for about 6 hours. The furnace temperature was then lowered to about $500^{\circ}C$ and the tube was suddenly immersed into cold water.

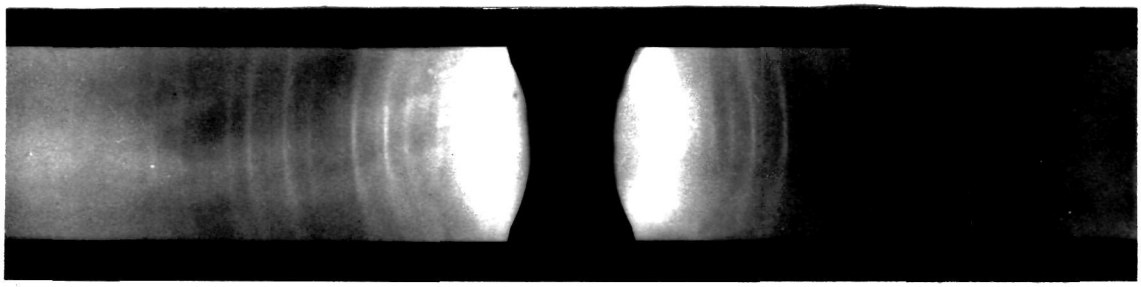

Fig. 2. X-ray powder pattern of HgSe

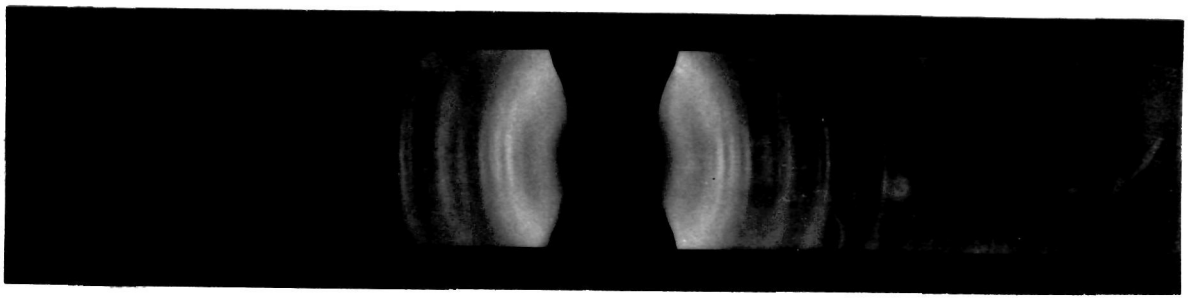

Fig. 3. X-ray powder pattern of HgTe

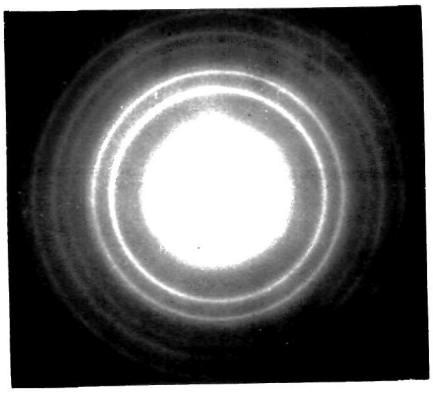

Fig. 4. HgSe on collodion film deposited at R.T.

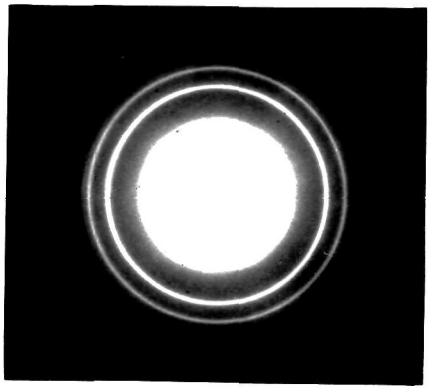

Fig. 5. same as fig. 4 when deposited at ~100°

T A B L E - I

Analysis of the pattern (fig.5)

I/I_o	d Å	hkl	a_o Å
vs	3.51	111	6.08
w	3.04	200	6.08
s	2.15	220	6.08
ms	1.83	311	6.07
m	1.75	222	6.07
w	1.52	400	6.08
m	1.40	331	6.09
m	1.24	422	6.08
w	1.17	333, 115	6.08
w	1.03	531	6.08
		Mean a_o =	6.08 Å

vs - very strong
s - strong
ms - medium strong
w - weak

For the preparation of HgTe almost the same heating cycle was carried out, with the exception that the final temperature was kept at about 600°C. Above 450°C much slower heating rate was maintained, since above that temperature strong interaction between tellurium and mercury takes place (Delves and Lewis, 1963). For cooling also almost the same rate was maintained and when the temperature was about 300°C the tube was plunged into cold water as before.

The compounds thus prepared were examined by X-ray powder method (figs. 2 & 3, HgSe and HgTe respectively) to know their bulk structures. The disposition of various reflections and their d-values agreed with the zinc-blende type of structure of the compounds. These compounds were then evaporated in vacuo and deposited on various substrates i.e. rocksalt, collodion etc. and their surfaces were studied by electron diffraction technique as mentioned in chapter-II.

C. RESULTS

(a) Mercury selenide deposits

(1) On collodion support

HgSe vapour condensed on collodion support at room temperature in vacuo yielded polycrystalline patterns (fig.4) when studied by transmission methods. The patterns consisted of rings, the disposition of which showed that they were due to cubic type of structure. The presence of only all odd and all even hkl reflections suggests that the film had the face centred cubic structure. Further, it is

seen that there are some reflections, such as 200, 420 etc. which are very weak or sometime absent. This suggests the zinc-blende type of structure of HgSe. When the film was tilted about an axis perpendicular to the beam direction neither the intensity of the individual ring changed nor the ring broke into arcs, suggesting thereby the polycrystalline nature of the deposits without any preferred orientation. The lattice parameter was measured by taking $11\bar{2}0$ of graphite ring ($d_{11\bar{2}0} = 1.230$ Å) as standard. When the deposition was made at substrate temperature about 100°C, the transmission patterns became sharper than before (fig.5), no doubt, due to an increase in crystal size, whilst the intensities of different reflections remained unaltered. Table-I shows the analysis of the pattern.

Intensities of hkl reflections in the case of electron diffraction pattern in kinematical cases for polycrystalline materials are given by the relation

$$I \propto F_e^2 \, d^2 \, p$$

where

$$F_e^2 = \left[\sum f_e \cos 2\pi (hu + kv + lw)\right]^2 + \left[\sum f_e \sin 2\pi (hu + kv + lw)\right]^2$$

Here F_e is the crystal structure factor for electrons d and p are the spacing and multiplicity factor respectively, f_e is

the electron scattering factor for an atom with coordinate u,v,w and h,k,l the indices of reflections. HgSe has a zinc-blende type of structure. The values of F_e with different h k l indices are given by the following conditions.

(a) h k l mixed $F_e = 0$

(b) h k l all odd or all even

(i) $h+k+l = 4n+2$ $F_e = 4(f_{Hg} - f_{Se})$

(ii) $h+k+l = 4n$ $F_e = 4(f_{Hg} + f_{Se})$

(iii) $h+k+l = 4n-1$ $F_e = 4(f_{Hg}^2 + f_{Se}^2)^{\frac{1}{2}}$

An examination of the above conditions reveals that quantitatively structure factors for 200, 420, 600 etc. given by condition b(i) will be small compared to the structure factor for 220, 400, 440 etc. [by b(ii)] and 111, 311, 333 etc. [by b(iii)] . These conditions will be further modified by the actual value of f_e for each atom, in this case for Hg and Se and also on the value of $(\sin\theta)/\lambda$, since electron scattering factor falls monotonically with $(\sin\theta)/\lambda$. Considering all these conditions, as well as the values of d and p, it may be said that in the case of HgSe reflections satisfying b(i) will be of weak intensity whereas those given by b(ii) and b(iii) will be of high intensity provided $(\sin\theta)/\lambda$ was very close. The visual estimation of the intensities conforms to the above. Thus it appears that on neutral collodion support HgSe films retain the normal zinc-blende type of structure.

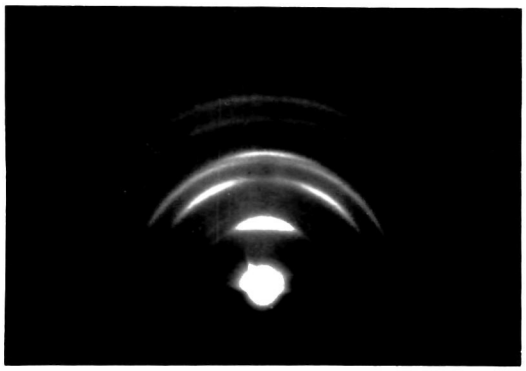

Fig. 6 Thicker deposits of HgSe on glass support at R.T.

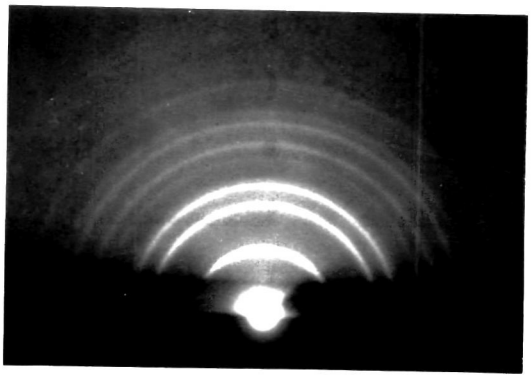

Fig. 7. Thinner deposits of HgSe on glass at ~ 100°C

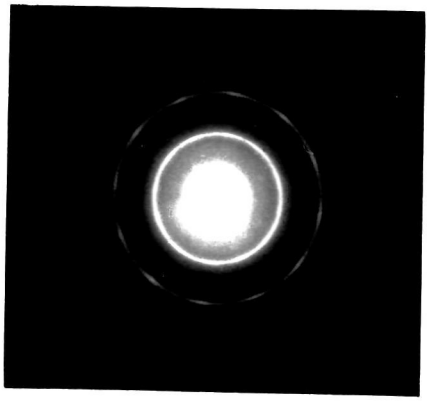

Fig. 8. HgSe on (100) NaCl deposited at R.T.

(2) On amorphous glass substrates

Deposits formed on glass at room temperature yielded patterns (fig.6) consisting of arcs symmetrically distributed with reflections having unusual intensities lying in the plane of incidence. The d-values of the arcs showed that these reflections were due to HgSe having normal zinc-blende structure. Further the presence of 111 and its higher order of reflections (with unusual intensity distribution) in the plane of incidence suggests that the deposits developed 1-d $\{111\}$ orientation. When the deposition was carried out at higher substrate temperature (100°-150°C) for thinner deposits patterns (fig.7) due to unoriented crystallites were obtained. If the deposits were thick enough, however, 1-d $\{111\}$ oriented patterns were obtained.

(3) On rocksalt substrates

On (100) face of rocksalt

HgSe deposited on cleavage face of rocksalt at room temperature did not show any clear pattern by reflection. The same film when put for transmission yielded patterns (fig.8) consisted of rings and spots, no doubt, due to the formation of both poly and single crystal deposits. It is interesting to note that there were a few extra weak reflections which could not be accounted for with the normal structure alone. However, the presence of these weak

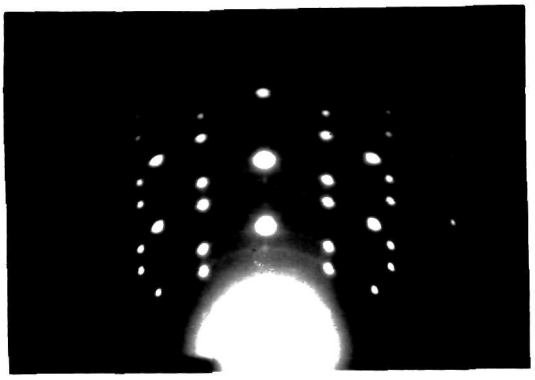

Fig. 9. HgSe on (100) NaCl at ~ 80°C. 2-d {111} orientation Beam along ⟨110⟩ of NaCl

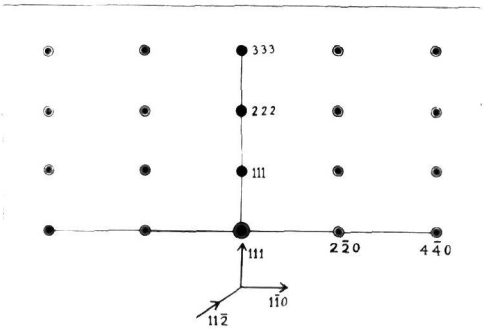

Fig. 10. Theoretical pattern for 2-d {111} crystals (f.c.c.) Beam along ⟨11$\bar{2}$⟩.

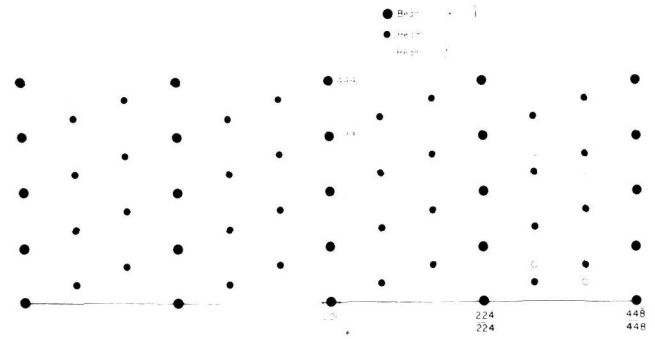

Fig. 11. Theoretical pattern for 2-d {111} oriented crystals

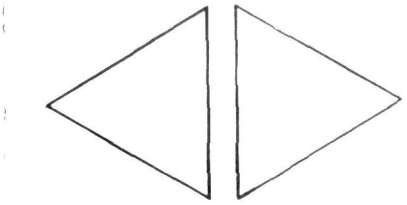

Fig. 12. Disposition of normal and anti 2-d {111} oriented crystals

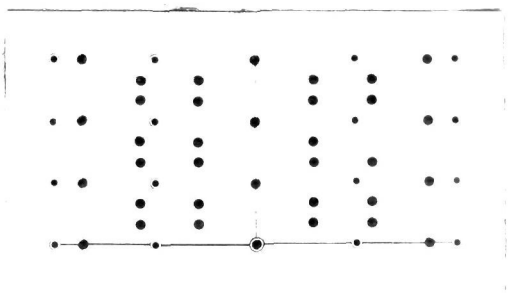

Fig. 13. Theoretical pattern for 2-d {111} crystals beam along [1$\bar{1}$0] + [$\bar{1}$10] + [11$\bar{2}$].

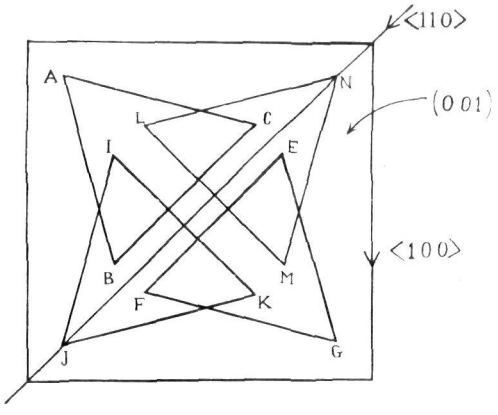

Fig. 14. Disposition of normal and anti 2-d {111} oriented crystals on (001) face of NaCl

reflections could be explained as due to the formation of a new hexagonal phase.

Deposits formed at substrate temperature about 80°C yielded patterns by reflection consisting mostly of spots, occasionally with faint rings passing through them. It was noticed that when the beam direction was along the cube-edge direction of the rocksalt crystal, the reflection pattern of the deposit did neither show any symmetrical pattern nor it was easily interpretable. But when the beam direction was changed by about 15° off the cube-edge direction the pattern was found to be symmetrical. The same pattern was repeated for every azimuthal rotation of 30° with respect to this direction i.e. along $\langle 110 \rangle$ direction of the rocksalt crystal and 30° to it. The symmetrical pattern is shown in fig.9. It was also seen that with the change of beam direction, with respect to the rocksalt crystal, the pattern changed considerably, whilst the spot rows in the plane of incidence remained unchanged. The presence of 111 reflection and its higher orders in the plane of incidence and the fact that the spot pattern changed considerably with azimuthal change of beam direction suggests that HgSe crystallites developed 2-d $\{111\}$ orientation. A detailed consideration of the disposition of spots (reflections) showed that they were arranged in two different rectangular networks with their sides in the ratio of $\sqrt{3} : \sqrt{24}$ and $\sqrt{3} : \sqrt{8}$.

Theoretical considerations show that 2-d $\{111\}$ oriented crystallites by reflection will yield $\sqrt{3} : \sqrt{8}$ type rectangular arrangement of spots when the electron beam is along $\langle 211 \rangle$ direction of the crystallites (fig.10). When the beam direction is changed by 30° which corresponds to the $\langle 110 \rangle$ direction of the deposits, the pattern should be asymmetrical. This pattern should repeat for every further rotation of 60° of the specimen with respect to the beam direction. The reflection pattern will, however, be symmetrical with sides of the rectangular network in the ratio of $\sqrt{3} : \sqrt{24}$, even for 110 direction of the beam when the crystal developed both the normal and anti 2-d $\{111\}$ orientation (fig.11). The disposition of the crystallites for normal and anti 2-d $\{111\}$ orientation is shown in fig.12. This suggests that 2-d $\{111\}$ oriented crystallites of HgSe grew epitaxially on rocksalt cleavage face in such a way that $\langle 110 \rangle$ direction of one type of crystals corresponded to the $\langle 211 \rangle$ direction of the other which were also similarly oriented. As the rectangular arrangement of spots with sides $\sqrt{3} : \sqrt{24}$ and $\sqrt{3} : \sqrt{8}$ appeared simultaneously and the pattern was also symmetrical, the beam direction for the crystallites was simultaneously $\langle 1\bar{1}0 \rangle$ $\langle \bar{1}10 \rangle$ $\langle 11\bar{2} \rangle$. Theoretical pattern for the above beam directions is shown in fig.13. The disposition of 2-d $\{111\}$ oriented crystallites on rocksalt cleavage face is shown in fig.14. It can be seen that when the beam is grazing along $\langle 110 \rangle$ direction

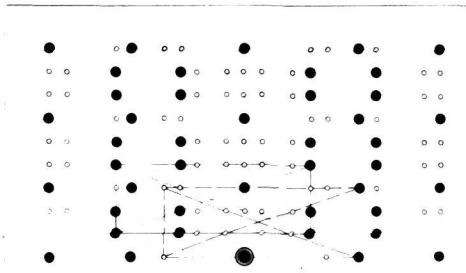

Fig. 15. Same as fig. 13 along with reflections due to dynamical scattering

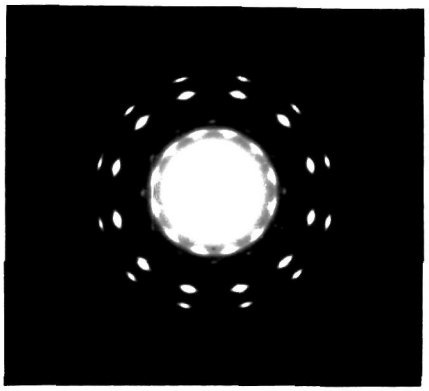

Fig. 16. Transmission pattern for these deposits on (100) NaCl at ~ 80°C

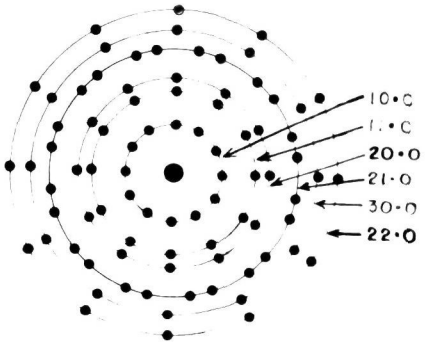

Fig. 17. Theoretical pattern for 2-d $\{00.1\}_H$ crystals rotated by 50°

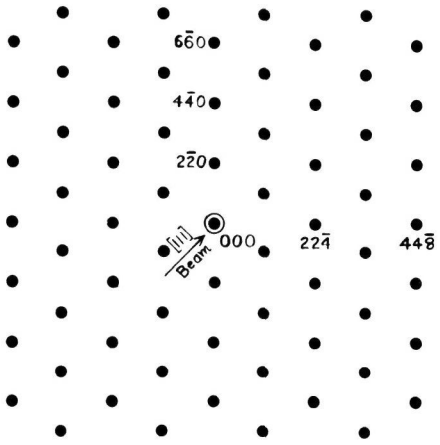

Fig. 18. Theoratical pattern for 2-d {111} crystals (f.c.c.)

T A B L E - II

Analysis of the pattern (fig.16)

d Å	hkl (cubic)	hk.l (hex.)
3.74	-	10.0
3.51	111	00.2
3.05	200	-
2.16	220	11$\bar{2}$0
2.00	-	10.3
1.84	311	20.0
1.76	222	00.4
1.52	400	-
1.40	331	21.1
1.24	422	-
1.17	511, 333	00.6
1.08	440	22.0

$a_H = 4.30$ Å, $c_H = 7.02$ Å

of the rocksalt crystal for the pair of crystallites LMN and IJK the beam direction is $\langle 211 \rangle$, whilst for the other pair ABC and GEF the beam direction becomes $\bar{1}10$ and $1\bar{1}0$. When the azimuthal beam direction is changed by 30°, the new directions for the first pair of crystallites become 110 $\bar{1}\bar{1}0$ whilst for the latter pair it corresponds to $\langle 211 \rangle$. This arrangement of 2-d $\{111\}$ oriented crystallites over (100) face of rocksalt explains the simultaneous appearance of rectangles of sides in the ratio of $\sqrt{3} : \sqrt{24}$ and $\sqrt{3} : \sqrt{8}$. Further it can be pointed out here that symmetrical patterns are possible for beam directions $\langle 110 \rangle$ and 15° to $\langle 100 \rangle$ of the substrate. This is also in agreement with our observations.

In addition to the reflections discussed above it was seen that there were few extra spots, though very faint, at distances 1/3, 2/3 in between the reflections 111, 222 etc. and also at other places symmetrically disposed. These extra reflections appear to have fractional indices. These spots can be well explained if we consider the effect of dynamical scattering where a beam once diffracted can again interact with the object as a primary beam and rediffracted giving rise to secondary reflections. The appearance of these reflections due to such secondary scattering is shown in fig.15, where filled circles are due to the usual kinematical scattering, whilst small unfilled circles are due to the dynamical scattering. Considering this effect the appearance

of all the weak reflections can be well explained. Similar cases of dynamical scattering were observed by Goswami (1957). Trehan and Goswami (1958) from Fe deposits and Cu_2O surfaces respectively.

When the same film was examined by transmission method, patterns as shown in fig.16 were obtained. These consist of many more reflections other than those due to the cubic form of HgSe. The analysis of the pattern is given in table-II. The innermost reflection consists of 12 equidistant spots, followed by an equal number of reflections, though slightly spread over, lying on a faint ring. The innermost reflection is due to $10\bar{1}0$ of hexagonal modification, whereas the subsequent reflections are corresponding to 111, 200, 220 (or $11\bar{2}0$ of hexagonal), $10\bar{1}3$ of hexagonal, 311 (or $20\bar{2}0$ of hexagonal) 222 and 400 etc. reflections of cubic phase. It can be seen that the reflections such as 200, 220, 020 and undiffracted beam form a rectangular array. This suggests that the deposit-film developed 2-d $\{100\}$ orientation. Further 12 equidistant spots on the reflections mentioned before suggest that the 2-d $\{100\}$ orientation was rotated by 30°. The presence of 12 equidistant spots lying on $10\bar{1}0$ and $11\bar{2}0$ reflections and so on can be explained on the basis of the development of 2-d $\{00.1\}$ orientation of the hexagonal modification of HgSe crystallites azimuthally rotated by 30°. The theoretical pattern for 2-d $\{00.1\}$ orientation of hexagonal crystallites

rotated by 30° is shown in fig.17. The above interpretation, however, cannot explain the appearance of reflections such as 111, 222 etc. Since 2-d $\{111\}$ orientation for HgSe crystallites was observed by the reflection method, for transmission 111 and its higher order reflections should be absent. The theoretical transmission pattern for 2-d $\{111\}$ oriented crystallites is shown in fig.18 where reflections other than 111, 222 etc. appeared. On the other hand the appearance of reflections 111, 222 etc. can be explained if the crystallites develop 2-d $\{211\}$ orientation. The presence of 12 equidistant reflections suggest that 2-d $\{211\}$ oriented crystallites were rotated by 30°. A theoretical pattern for 2-d $\{211\}$ orientation of f.c.c. crystallites rotated by 30° is shown in fig.19. This type of orientation was also observed by Aggarwal and Goswami (1963a). Thus HgSe deposits formed on (100) face of NaCl at substrate temperature 80°C showed both the normal and anti 2-d $\{111\}$ orientation when examined by reflection method, but 2-d $\{100\}$ $\{211\}$ of cubic form and 2-d $\{00.1\}$ orientation of the hexagonal modification by transmission. This suggests that though the surface layers developed 2-d $\{111\}$ orientation the layers below them up to those in contact with the substrate had features different from the surface layers. These features are, no doubt, characteristic of the growth of the deposit crystals.

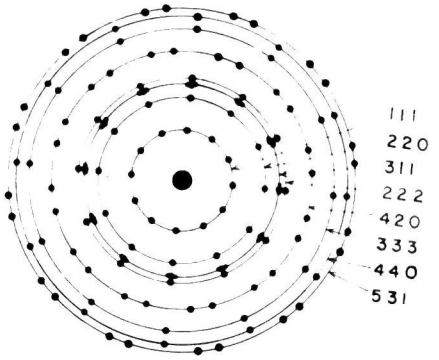

Fig. 19. Theoratical pattern for 2-d {211} crystals rotated by 90°.

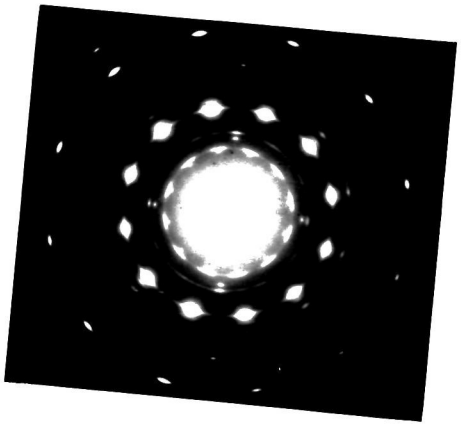

Fig. 20. HgSe on (100) NaCl deposited at. ~ 100°C

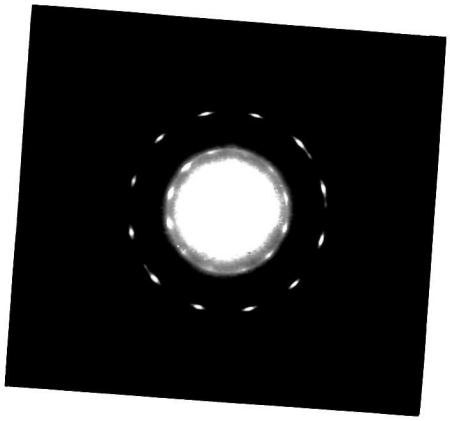

Fig. 21. HgSe on (100) NaCl at. ~ 150°C

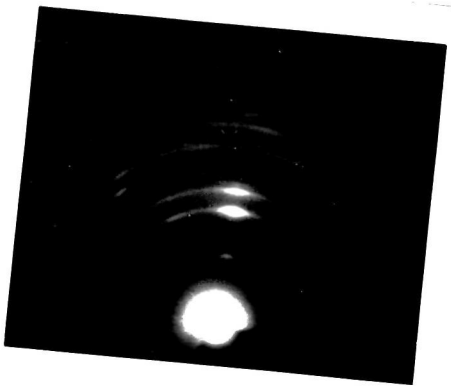

Fig. 22. Refln pattern from the deposits of HgSe on (110) NaCl at. ~ 100°C
Beam along <100> of NaCl

The reflection patterns obtained from the deposits formed at $\sim 100^{\circ}C$ of substrate temperature were similar to those obtained at $\sim 80^{\circ}C$. The transmission patterns (fig.20) from these films were slightly different. It is seen that unlike the 12 reflections of 200 in the previous cases there were only four spots with its higher orders. This indicates the development of 2-d $\{100\}$ orientation, but there were no rotations of the crystallites. Other reflections were exactly similar to those obtained in the previous cases. It was further observed that the hexagonal reflections become more prominent in these cases. The sharp ring just beyond 200 reflection of HgSe is due to 200 reflection of NaCl. Thus it appears that when the deposition of HgSe was carried out on rocksalt cleavage face at temperature about $100^{\circ}C$ additional 2-d $\{100\}$ orientation was also observed by transmission along with the others as mentioned before. At about $150^{\circ}C$ substrate temperature reflection patterns showed 2-d $\{111\}$ orientation as discussed previously. The transmission patterns (fig.21) were similar to those of the deposits at $80^{\circ}C$ with the exception that the deposit had more tendency to develop the hexagonal phase at this temperature.

On (110) face of rocksalt

Thin deposits of HgSe on (110) faces of rocksalt at about 80° and $100^{\circ}C$ did not yield good reflection patterns. The pattern showed in fig.22 was obtained when beam direction

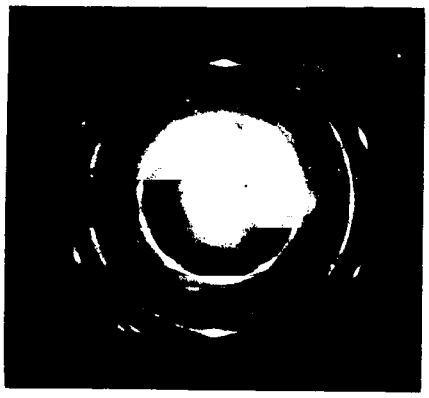

Fig. 23. Hg Se on (110) NaCl deposited at ~ 100°C

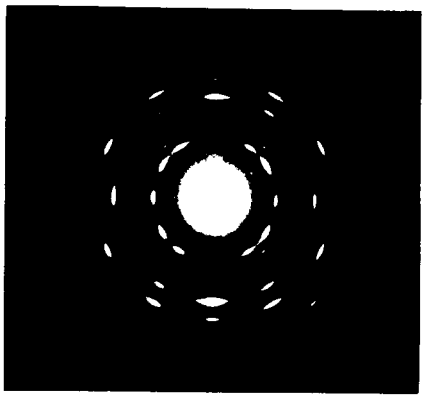

Fig. 24. same as fig. 23 deposited at ~ 150°C

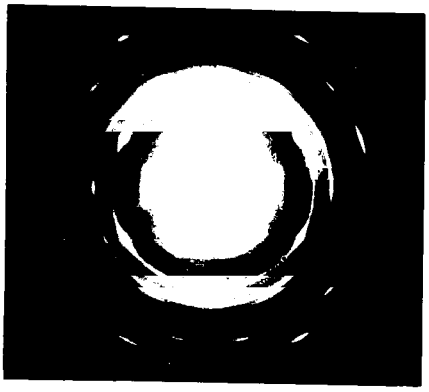

Fig. 25. Hg Se on (111) NaCl at ~ 150°C

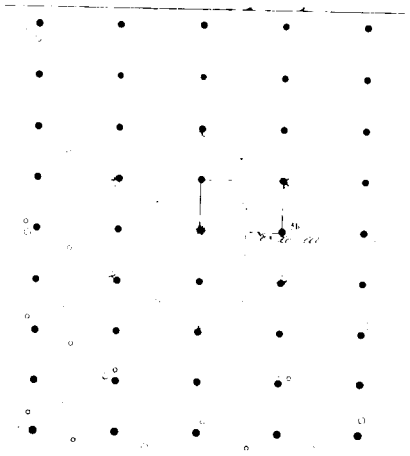

Fig 26. Theoretical pattern for 2-d {211} oriented crystals rotated by 60°

was along $\langle 100 \rangle$ of the rocksalt face. Though the orientation is not that clear, it can be seen that there is 220 reflection in the plane of incidence which forms square type of arrangement along with 400, $2\bar{2}0$ and the undeflected spot. When the beam direction was changed, this arrangement of spot also changed considerably suggesting the development of 2-d $\{110\}$ orientation along with other orientations. Fig.23 shows the transmission pattern from the same film. This pattern consisted of rings as well as spots lying on the rings. The disposition of these reflections shows that the deposit developed predominantly cubic type of structure, though there is some evidence for the presence of hexagonal modification, the amount of which was very small. The spots 220, 222 and 002 along with the undeflected spot form a rectangular array with 111 reflection at the centre and the ratio of the sides of the rectangle is $1 : \sqrt{2}$. This clearly shows that the deposits of mercury selenide developed 2-d $\{110\}$ orientation. Further from the disposition of the spot pattern with respect to the cube-edge of the substrate crystal, which was parallel to the film-edge it was concluded that 2-d $\{110\}$ oriented film grew epitaxially on (110) in such a way that $\langle 110 \rangle$ of HgSe was parallel to $\langle 100 \rangle$ of NaCl.

In the temperature range about 130°-150°C the deposit yielded patterns (fig.24) consisted of spots and rings. An analysis of the pattern shows that there is a square network

of pattern formed with 200, 220, 020 along with the undeflected spot suggesting thereby the development of 2-d $\{100\}$ orientation of the crystallites of HgSe. It can further be seen that very faint 200 reflection along with 222, 022 and the undeflected spot form rectangles with 111 reflection at the centre showing thereby that 2-d $\{110\}$ orientation of crystallites has also developed. Another arrangement of spots seen on the same pattern with 111, 311, 220 and the undeflected spot forming a rectangular array, no doubt, characteristic of 2-d $\{211\}$ orientation of the deposits. The above three types of orientations namely 2-d $\{100\} + \{110\} + \{211\}$ of cubic crystallites of HgSe can explain the appearance of most of the spots.

On (111) face of rocksalt

HgSe deposited on rocksalt (111) face at 100°-130°C yielded patterns (fig.25) consisted of rings as well as spots. It will be seen that there are six strong spots (reflections) lying on 111, 220 and 311 rings forming a hexagonal network. In addition there are six more spots (very weak) lying on 220 and 311 rings. The hexagonal arrangement apparently suggests that the orientation may be due to 2-d $\{111\}$ of the cubic HgSe. The closest spot to the undeflected beam forming the hexagonal network is 220. The d_{hkl} value measured from the diffraction pattern, however, showed that the closest spot is due to 111 reflection. For 2-d $\{111\}$ orientation of

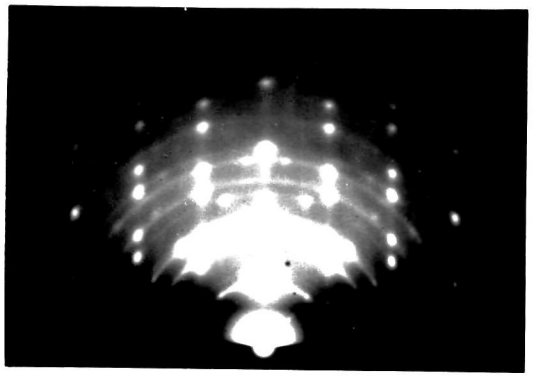

Fig. 27. Hg se on mica (0001) face deposited at ~ 150°C. 2-d {111} + {115} orientations

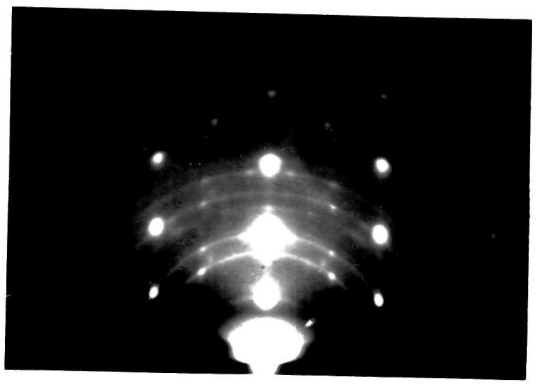

Fig. 28. Same as fig. 27. when beam direction was changed by 30° w.r.t. the previous dirn.

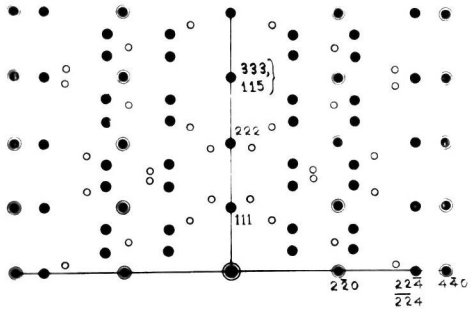

Fig. 29. Theoretical pattern showing reflections due to 2-d {111} + {115} oriented crystals.

a cubic crystal by transmission the nearest spot cannot be 111. Further consideration, however, shows that the development of 2-d $\{211\}$ orientation would give rise to 111 reflection. If the crystals are mutually rotated by 60° they will give rise to hexagonal arrangement of spot as shown in fig.26. Additional faint spots may be due to mutual rotation of 30° of the 2-d $\{211\}$ oriented crystallites. The deposits at $\sim 150^{\circ}C$ also showed same type of orientation. In this case the patterns became sharper and the hexagonal modification became more prominent.

(4) On mica cleavage face

Deposits of HgSe on cleavage face of mica i.e. (0001) face, at substrate temperature between 100°-$150^{\circ}C$ yielded pattern as shown in fig.27. This pattern consisted of sharp spots lying over faint rings. Due to the appearance of large number of spots the pattern appears to be complex. When the azimuthal direction of the electron beam was changed the pattern also changed considerably, while the row of spots in the plane of incidence remained unaltered. The fact that 111 and its higher order of reflections were in the plane of incidence and the pattern changed considerably due to the change of beam direction suggested that the HgSe crystallites developed 2-d $\{111\}$ orientation. A closer examination of the pattern revealed that the strong spots were mainly arranged in a rectangular array of sides $\sqrt{3} : \sqrt{24}$ with spots at distances 1/3, 2/3 along the diagonals. This suggests that

the deposits developed both normal and anti 2-d $\{111\}$ orient ation as described in the case of reflection pattern from the deposits on (100) face of rocksalt. When the azimuthal beam direction was changed by 30° another symmetrical pattern (fig.28) was obtained. It can be seen here that the strong spots were arranged in a rectangular network with sides in the ratio of $\sqrt{2} : \sqrt{8}$. This showed that the beam direction for the deposit 2-d $\{111\}$ oriented crystallites was $\langle 211 \rangle$ The theoretical patterns (figs.10,11) also confirm this view. It can be pointed out here that even in fig.27 there are faint spots which are also arranged in a rectangular array with sides in the ratio of $\sqrt{3} : \sqrt{8}$ and in fig.28 faint spots arranged in rectangular array with sides $\sqrt{3} : \sqrt{24}$ This shows that even though for most of the crystals the beam was along $\langle 110 \rangle$ direction, there were a few for which the beam direction corresponded to $\langle 211 \rangle$. Thus the deposits grew epitaxially with both the normal and anti 2-d $\{111\}$ orientation, with a few crystallites rotated by 30°.

The above interpretation though explains most of the spots, there were a few extra spots such as 111 at 40°, 200 at 15°, 220 at 75°, 311 at 10° and 40°, and 422 at 52° from the plane of incidence which cannot be explained on the basis of the above orientations. On the other hand if the deposits developed 2-d $\{115\}$ orientation all these spots can be well explained, which are shown in the theoretical diagram (fig.29). The appearance of 2-d $\{115\}$ orientation

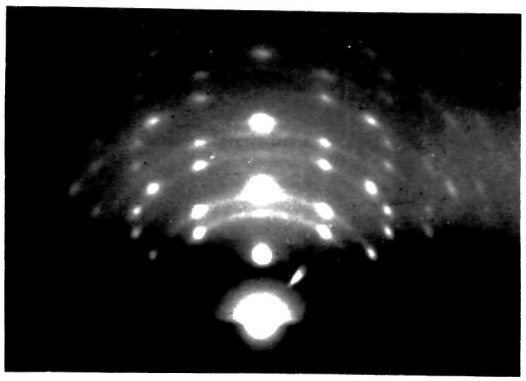

Fig. 30. For thicker deposits of HgSe on mica (0001) face.

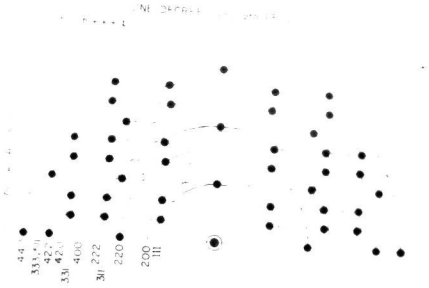

Fig. 31. Theoretical pattern for 1-d {111} oriented crystals.

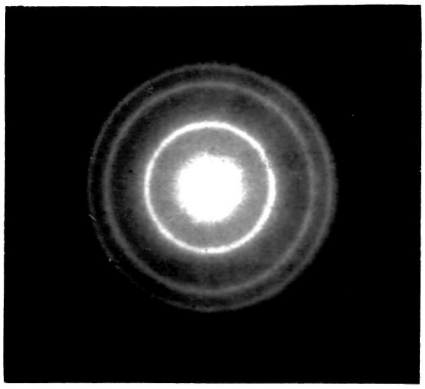

Fig. 32. HgTe on collodion film deposited at R.T.

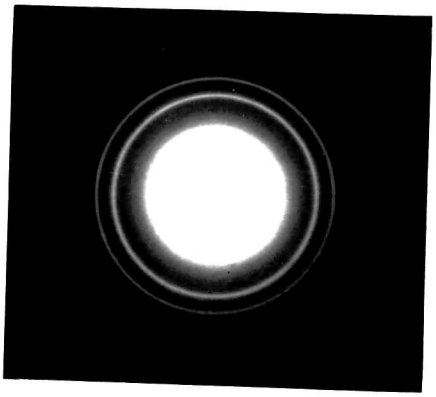

Fig. 33. Same as fig. 32 when deposited at ~100°C

T A B L E - III

Analysis of the pattern (fig.33)

I/I_o	d Å	hkl	a_o Å
s	3.72	111	6.44
ms	3.22	200	6.44
ms	2.27	220	6.43
m	1.95	311	6.46
w	1.86	222	6.45
w	1.61	400	6.44
m	1.48	331	6.45
m	1.32	422	6.45
w	1.24	511, 333	6.44
w	1.09	531	6.45
		Mean a_o =	6.45 Å

s - strong
ms - medium strong
m - medium
w - weak

and 2-d $\{111\}$ orientation seems to be due to twinned structure and the reason for them will be discussed later on.

If the deposit was thicker, particularly within the temperature range 80°-100°C on mica (0001) face, the pattern obtained was of the type shown in fig.30. This pattern looks apparently similar to normal and anti 2-d $\{111\}$ orientation of crystallites. On closer examination, however, it is found that there are extra pairs of reflections such as on 331 and 420 etc. These cannot appear when the f.c.c. crystallites developed normal and anti 2-d $\{111\}$ orientation. If the crystallites develop perfect 1-d $\{111\}$ orientation the presence of these reflections can be well explained. A theoretical pattern (fig.31) explains all the reflections observed in the present case. Thus the deposits when thicker developed nearly perfect 1-d $\{111\}$ orientation at higher temperature.

(b) Mercury telluride deposits

(1) On collodion support

HgTe deposits on neutral collodion support at room temperature in vacuo yielded patterns showed in fig.32. Neither the ring pattern obtained from these films broke into arcs on tilting of the specimen about an axis perpendicular to the electron beam nor there was any change of intensity of the individual ring. This suggested that the polycrystalline deposits of HgTe on collodion support did not develop any

Fig. 34. HgTe deposits on glass support at R.T.

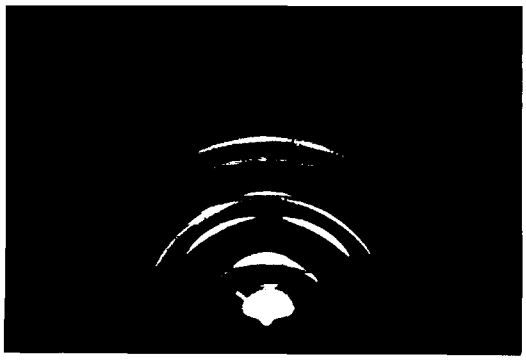

Fig. 35. HgTe deposits on glass support at ~ 100°C

preferred orientation. All the reflections had either all even or all odd hkl indices suggesting that the film had an f.c.c. type of structure. The films deposited at higher substrate temperature yielded sharper rings (fig.33). The consideration of the intensity distribution of different reflections as was done in the case of HgSe patterns suggests that HgTe also had zinc-blende type of structure. An analysis of the pattern is given in table-III. It is also seen that there are a few extra reflections which are due to the presence of free tellurium along with HgTe.

(2) On glass substrate

HgTe deposited on glass substrate at room temperature showed half rings, the disposition of which showed that the reflections were due to mercury telluride deposits (fig.34). The deposits at higher substrate temperature such as 100°-$130^{\circ}C$ showed sharper patterns (fig.35). It was seen that the reflections 111 and 222 and their higher orders were in the plane of incidence and the fact that the pattern did not change even with the change of beam direction suggested that the crystallites developed 1-d $\{111\}$ orientation as was found in the case of HgSe deposits.

(3) On rocksalt substrates

On (100) face of rocksalt

HgTe deposited from vapour phase in vacuo on the cleavage face of rocksalt at substrate temperature $\sim 80^{\circ}C$

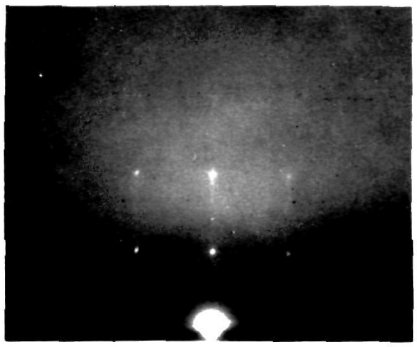

Fig. 56. HgTe on (100) NaCl at ~ 80°C. Beam ⟨100⟩ NaCl

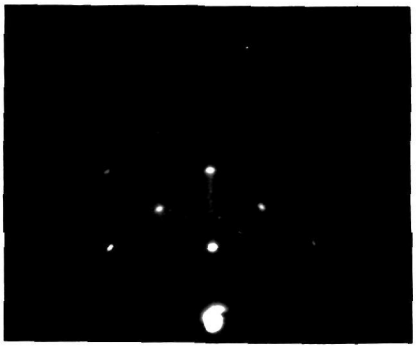

Fig. 57. HgTe on (100) NaCl when beam dir^{n} ⟨110⟩ NaCl

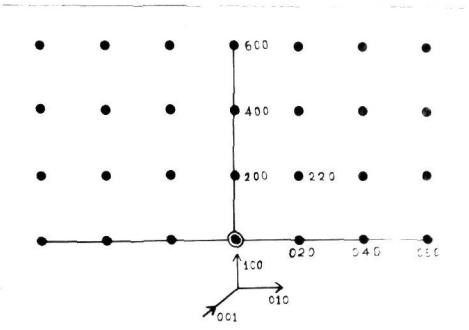

Fig. 58. Theoretical pattern for 2-d {100} crystals Beam ⟨001⟩ of deposits

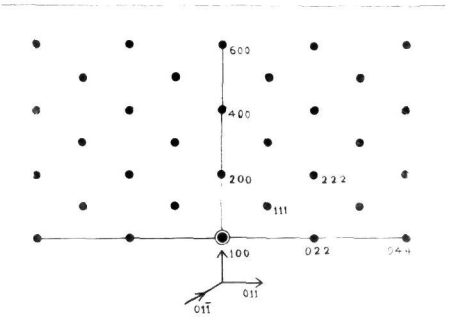

Fig. 59. Same as fig 58 when beam direction is along ⟨01$\bar{1}$⟩

yielded patterns (fig.36) by reflection, when the beam direction was along the cube-edge of the rocksalt crystal. The patterns consisted of reflections (spots) arranged in a square network where 200, 400 etc. reflections were in the plane of incidence. When the beam direction was changed to $\langle 110 \rangle$ of the rocksalt crystal, the pattern (fig.37) also changed to centred $\sqrt{2}$ type rectangles while the reflections 200, 400 etc. were still in the plane of incidence. This clearly showed that the deposits developed 2-d $\{100\}$ orientation. The theoretical patterns for 2-d $\{100\}$ orientation of f.c.c. crystallites for $\langle 001 \rangle$ and $\langle 01\bar{1} \rangle$ beam directions are shown in figs.38,39 respectively. It was also noticed that the spot rows were elongated towards the shadow edge forming discrete lines, no doubt, due to the refraction effect caused by the highly smooth as well as wavy nature of the deposit surface. Since the film was very thin, they broke into small pieces while removing from the substrate. Hence no transmission pattern could be taken.

If, however, the deposits were a little thicker the reflection patterns were completely different as shown in fig.40 with the beam direction along $\langle 110 \rangle$ of NaCl substrate. Similar patterns were also obtained at about 100°C. The patterns showed that 111 and its higher orders of reflection were in the plane of incidence. When the azimuthal beam direction was $\langle 110 \rangle$ to the substrate crystal, the symmetrical

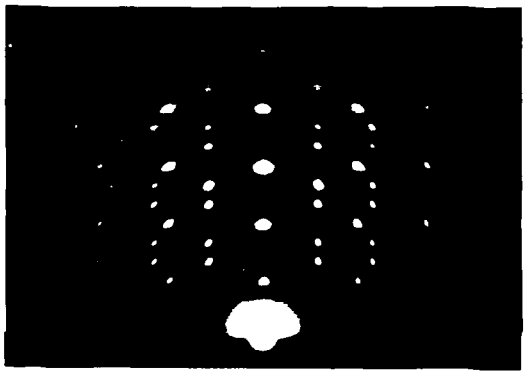

Fig. 40. Thicker deposits of HgTe on (100) NaCl deposited at ~100°C
Beam ⟨110⟩ of NaCl

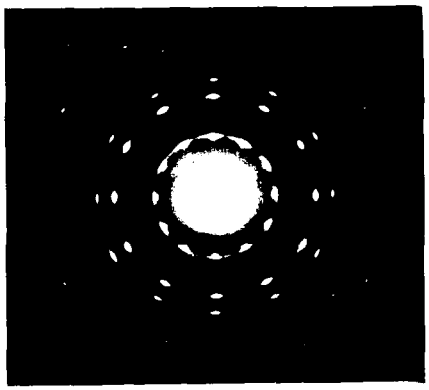

Fig. 41. Transmission pattern from the same film showing pattern fig. 40 by reflection.

T A B L E - IV

Analysis of the pattern (fig.41)

d Å	hkl (cubic)	hk.l (hex.)
3.92	-	10.0
3.72	111	00.2
3.22	200	-
2.27	220	11.0
2.12	-	10.3
1.95	311	20.0
1.86	222	00.4
1.61	400	-
1.48	331	21.1
1.33	422	-
1.24	511, 333	-
1.14	440	22.0

$a_H = 4.56$ Å, $c_H = 7.45$ Å

pattern was obtained which, however, repeated after every rotation of 30° of the crystal with respect to the beam direction. This symmetrical pattern consisted of reflections (spots) arranged in two rectangular networks one of sides in the ratio of $\sqrt{3} : \sqrt{24}$ with spots at 1/3, 2/3 of its diagonals while the other rectangular arrangement with sides in the ratio of $\sqrt{3} : \sqrt{8}$ as was discussed in the case of HgSe. Thus mercury telluride grew epitaxially with normal and anti 2-d $\{111\}$ orientation rotated by 30°.

Transmission patterns for the same film shown in fig.41 consisted of reflections due to the f.c.c. and hexagonal modification of HgTe. The innermost reflection consisting of 12 equidistant spots was due to 10.0 reflection of the h.c.p. structure. The 12 equidistant spots lying on the 10.0, 11.0 and 20.0 reflections of hexagonal phase and the fact that 000, 10.0, 11.0 and 20.0 reflections (spots) formed a centred rectangular array with sides in the ratio of $1.633 : \sqrt{8}$ suggest the development of 2-d $\{00.1\}$ orientation of the hexagonal crystallites rotated by 30°. The theoretical pattern for 2-d $\{00.1\}$ orientation rotated by 30° is shown in fig.17. Further closer examination of the patterns reveales that there are 12 equidistant spots lying on 111 reflection as well as on 222. These again suggest the development of 2-d $\{211\}$ orientation rotated by 30° as was mentioned in the case of HgSe. An analysis of the pattern (fig.41) is given in table-IV.

Fig. 42. HgTe on (110) NaCl deposited at. ~ 80°C
Beam along <001>

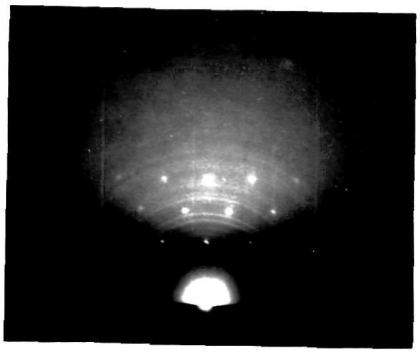

Fig. 43. Same as fig 42
Beam along <1$\bar{1}$0>

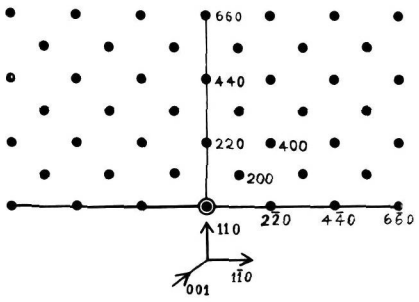

Fig. 44. Theoretical pattern for 2-d {110} oriented crystals beam along <001>

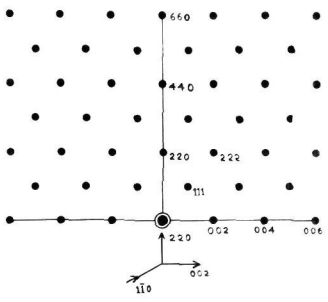

Fig. 45. Theoretical pattern for 2-d {110} oriented crystals beam along <1$\bar{1}$0>

Deposits at 130°C substrate temperature by transmission showed similar patterns as obtained for the deposits at ~100°C. The lattice parameters for hexagonal modification of HgTe are a_H = 4.56 Å, c_H = 7.45 Å.

On rocksalt (110) face

Deposits of HgTe at room temperature on (110) face of rocksalt showed ring patterns characteristics of zinc-blende type of structure. When the deposition was carried out at substrate temperature ~ 80°C the deposit yielded patterns (fig.42) consisted of spots and rings when the beam direction was along 100 of the substrate. It was observed that 220 and its higher order reflections were in the plane of incidence and 000, 220, 400 and $2\bar{2}0$ reflections formed the square network with 200 reflection at the centre. When the beam direction was changed to ⟨110⟩ of the rocksalt crystal the pattern shown in fig.43 was obtained, whilst the rows of spots in the plane of incidence remained unchanged. This pattern consisted of reflections (spots) forming centred $\sqrt{2}$ type of rectangles with 000, 220, 222 and 002 reflections at the corners, while 111 reflection (spot) was at the centre. This clearly suggests that the f.c.c. type of HgTe crystallites developed 2-d {110} orientation on the rocksalt (110) face. The theoretical patterns for 2-d {110} orientation for the beam directions ⟨100⟩ and ⟨110⟩ are shown in figs. 44 & 45 respectively. This 2-d {110} orientation was found to be such that ⟨110⟩

Fig. 46. HgTe on (110) NaCl deposited at ~100°C

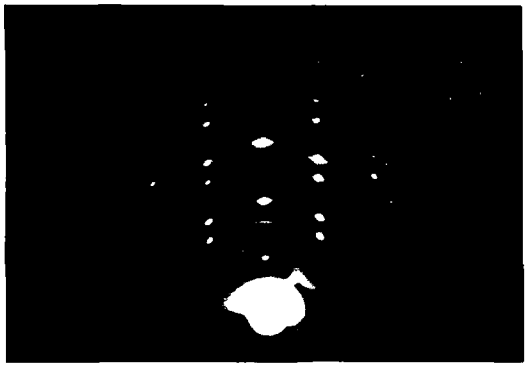

Fig. 47. HgTe on (111) NaCl deposited at ~ 100°C. Beam along ⟨110⟩ of rock salt face.

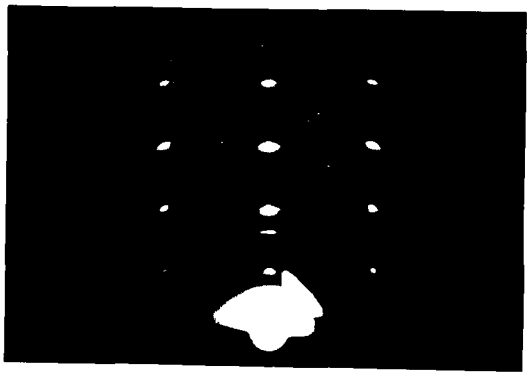

Fig. 48. Same as fig. 47. when beam along ⟨211⟩ of rock salt face.

of the deposit crystal parallel to $\langle 110 \rangle$ of the substrate. The same conclusion was drawn when the film examined by transmission methods. The extra rings observed in the pattern are due to free tellurium.

For the films with thicker deposits at substrate temperature $\sim 100^{\circ}C$ patterns similar to fig.46 were obtained. These patterns consisted of strong arcs which did not change even with the change of beam direction. Here it is seen that 111, 220 etc. reflections (arcs) were in the plane of incidence. The above facts suggest the development of 1-d $\{111\} + \{110\}$ orientations of HgTe crystallites. The transmission patterns obtained from these films were polycrystalline in nature and similar to those obtained from th deposits on collodion supports.

On rocksalt (111) face

Deposits of HgTe on rocksalt (111) face at substrate temperature $\sim 100^{\circ}C$ showed patterns (fig.47) by reflection when the beam direction was $\langle 110 \rangle$ for the substrate. These patterns are very much similar to those obtained for HgSe and HgTe on (100) face of rocksalt at higher substrate temperature. The pattern consisted of 111 and its higher order in the plane of incidence and changed considerably with the change of azimuthal direction of the beam. This suggests 2-d $\{111\}$ orientation of HgTe crystallites over (111) face of rocksalt. The reflections are arranged in a rectangular

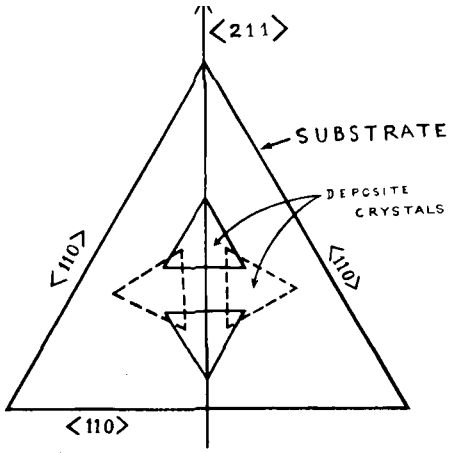

Fig. 49. Disposition of 2-d {111} oriented crystals on (111) face of NaCl

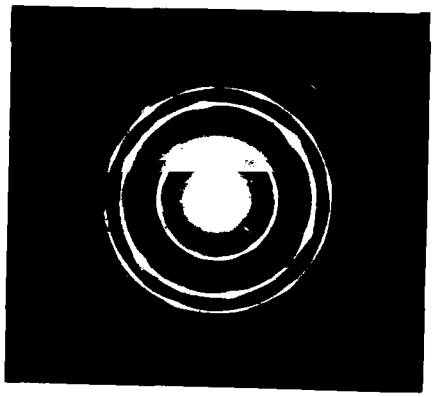

Fig. 50. Transmission pattern from the film showing patterns fig. 47-48.

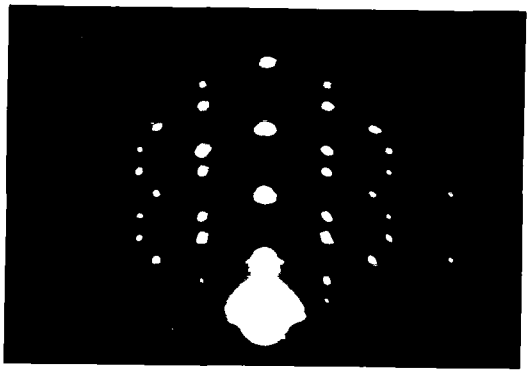

Fig. 51. HgTe on mica (0001) face at ~ 100°C. 1-d {111} orientation

network with sides in the ratio of $\sqrt{3}$: $\sqrt{24}$ with spots at distances 1/3, 2/3 of the diagonals. Very faint spots arranged in rectangles with sides in the ratio of $\sqrt{3}$: $\sqrt{8}$ was also observed in this case. On changing the beam direction to $\langle 211 \rangle$ of the substrate, the latter type of rectangles i.e. with sides $\sqrt{3}$: $\sqrt{8}$ became prominent whilst with sides in the ratio of $\sqrt{3}$: $\sqrt{24}$ became faint (fig.48). This suggests that there are traces of 2-d $\{111\}$ oriented crystallites rotated by 30°. The disposition of 2-d $\{111\}$ oriented crystallites over rocksalt (111) face is shown in fig.49.

Transmission pattern for the same deposit is shown in fig.50. The disposition of spots on 111 and other reflections suggests the possible development of 2-d $\{211\}$ orientation rotated by 30° which was discussed in the case of the deposits of HgSe on (111) face at higher substrate temperature.

(4) <u>On cleavage face of mica</u>

HgTe deposited on mica cleavage face in vacuum at substrate temperature $\sim 100^{\circ}$C showed patterns (fig.51). These patterns consist of strong spots and weak rings over them. A closer examination of the pattern reveals that there are pairs of spots on 331 and 420 reflections at angles $\sim 8^{\circ}$ and 15° with the shadow edge (undeflected spot being taken as centre) which cannot be accounted for with the 2-d $\{111\}$ oriented pattern. However, when the pattern is compared with 1-d $\{111\}$ oriented pattern (fig.31) drawn theoretically it is seen that the pairs of spots observed are well explained. Thus it can be

assumed that HgTe crystallites developed nearly perfect 1-d $\{111\}$ orientation on mica cleavage face.

D. DISCUSSION

Zachariasen (1925, 1926) reported that both tiemannite (HgSe) and coloradaite (HgTe) had zinc-blende type of structure with lattice parameters 6.08 Å and 6.43 Å respectively. Compounds prepared in this laboratory from the pure elements with stoichiometric proportions of Hg, Te and Se were examined by the X-ray powder method. It was found that both the compounds mentioned above had zinc-blende type of structure, though a few weak extra reflections were also present. Vacuum deposited films obtained on different substrates at various substrate temperatures showed patterns due to the zinc-blende type of structure and often mixed with the hexagonal (C.P.) modification. In the bulk form, however, according to Krucheanu, Nikulesku and Vanku (1965) these compounds have cubic structure only. The above observations of ours showed the presence of both cubic and h.c.p. modifications similar to those reported by Aggarwal and Goswami (1963 a,b) for thin films of sulfides of Zn, Cd and Hg. The hexagonal modifications of HgSe and HgTe conform to the close-packed type, as will be discussed later on.

Orientations of the deposits of selenide & telluride of mercury

The two compounds usually have zinc-blende type of structures even though the depositions were carried out on

various substrates at different temperatures. Selenide and telluride of mercury deposited on the (100) face of rocksalt at higher substrate temperatures developed a mixture of 2-d $\{100\}$ and 2-d $\{211\}$ orientations of the cubic phase together with 2-d $\{00.1\}$ of hexagonal modification, all rotated by 30°. In some cases at higher substrate temperature 2-d $\{100\}$ orientation not rotated by 30° was observed. The above observations were made for the films examined by the transmission method. Surface layers on the other hand as examined by reflection method showed the development of normal and anti 2-d $\{111\}$ orientation rotated by 30°. For a very thin film of HgTe on (100) face of NaCl, a 2-d $\{100\}$ orientation of the crystallites at the surface layers was observed. These observations showed that thinner films developed parallel orientation namely 2-d $\{100\}$ and thicker films developed 2-d $\{111\}$ orientation when examined by reflection method. The observations of 2-d $\{100\}$, $\{211\}$ and $\{00.1\}$ orientations by transmission method suggest that during the crystal growth process the film grew with parallel orientation and as the film thickness increased another 2-d $\{111\}$ orientation also developed possibly through the intermediate 2-d $\{211\}$ orientation. The appearance of extensive $\{111\}$ twinned structure along with the above observations showed that the development of 2-d $\{211\}$ of cubic and $\{00.1\}$ of hexagonal orientations were, no doubt due to the growth defect such as twinning and stacking fault as will be discussed later on.

On the (110) face of rocksalt both HgSe and HgTe films grew epitaxially at higher substrate temperature with parallel orientation. For very thin films of HgTe 2-d $\{110\}$ orientation developed whilst at higher substrate temperature and also for thicker films 2-d $\{100\}$, $\{110\}$ and $\{211\}$ orientations of the deposited films were observed. On the octahedral face of rocksalt HgTe developed both normal and anti 2-d $\{111\}$ orientation while by transmission method 2-d $\{211\}$ orientation rotated by 30° was observed for both the compounds.

On mica cleavage face, for HgSe deposits at higher substrate temperature both normal and anti 2-d $\{111\}$ orientation was observed with an additional 2-d $\{115\}$ orientation. For thicker films, sometimes 1-d $\{111\}$ orientation was also observed. In the case of HgTe deposits on cleavage face of mica at higher substrate temperature almost perfect 1-d $\{111\}$ orientation was obtained. On amorphous glass substrate both the compounds developed 1-d $\{111\}$ orientation. The development of different orientations of the two phases namely cubic and hexagonal (C.P.) can, however, be explained by the crystal growth process, phase change and the orientation relation between different phases as will be discussed in the subsequent paragraphs.

Twinning and change of orientation

It has been pointed out above that for a single phase deposits normally more than one orientation of the crystallites

were observed. Though the substrates used were usually the simple planes such as (100), (110), (111) of rocksalt and mica cleavage faces, yet it was observed that the deposits developed high indexed planes over these substrates. The high indexed orientations can, however, be explained on the basis of single or multiple twinning phenomena.

Crystals are called twinned when they consist of portions that are joined together with a definite mutual orientation (Barret, 1952) and the orientation of the twinned crystals is such that one is a mirror image of the other on a certain plane. Such a plane is called twinning plane. The twinned growth can be induced by interfacial stress developed between the deposit and the substrate or by any other disturbances created during the normal growth process. As a result, new planes of the deposit crystal become parallel to the initially grown epitaxial layer. These planes are usually high indexed planes and hence complicated diffraction patterns appear from the surface layers. Patterns from twinned crystallites become more complicated when single twinned crystals retwin (the case of double and multiple twinning). The crystallography of twinning has been discussed by many workers (Menzer, 1938 a,b,c; Hall, 1954; Jawson and Dove, 1954). Goswami (1954) has shown how single and multitwinning affect the diffraction patterns. Trehan and Goswami (1959) have calculated the different planes

which would appear for different epitaxial layers (orientations) depending on the twinning plane as well as on the nature of twinning. In the case of cubic crystallites (f.c.c.) hhl type of twinning is more common. The geometry for such a twinned pattern is related by

$$\theta = 2 \tan^{-1} \frac{l}{h\sqrt{2}}$$

where θ is the angle by which the twinned pattern has to be rotated around the undeflected spot to coincide with the pattern due to the untwinned crystal (Elleman and Wilman, 1948). Most commonly diamond and f.c.c. type crystals twin on $\{111\}$ planes and the body centred cubic crystals twin on their $\{112\}$ planes (Hall, 1964).

If (hkl), (uvw) and (HKL) are the initial, twinning and final planes (parallel to hkl planes) then the following relation is satisfied,

$$\cos\theta = \frac{hu + kv + lw}{\sqrt{u^2} \cdot \sqrt{h^2}} = \frac{uH + vK + wL}{\sqrt{H^2} \cdot \sqrt{u^2}}$$

$$\begin{vmatrix} H & K & L \\ u & v & w \\ h & k & l \end{vmatrix} = 0$$

From the above two relations it is possible to find out the indices (HKL). When the initial plane is (100) and twinning occurs on (111) plane then $(\bar{1}22)$ plane of the twinned

crystallites become parallel to the initial plane i.e. to (100) plane of the substrate. If the twinned crystal further twins on $(\bar{1}11)$ plane it can be seen that $(\bar{7}44)$ plane of the second twinned crystals (referred to the parent crystal) becomes parallel to (100) surfaces. As $(\bar{7}44)$ plane is a very odd plane its nearest simpler plane $\{\bar{2}11\}$ only differing about $3^{o}24'$ would lie very close to the initial orientation $\{100\}$ and hence give diffraction pattern. Thus 2-d $\{211\}$ orientation arises in the following way :

$$(100) \xrightarrow{T(111)} (\bar{1}22) \xrightarrow{T(\bar{1}11)} (\bar{7}44) \simeq (\bar{2}11)$$

On the (100) face both 2-d $\{100\}$ and $\{111\}$ orientations were often observed by reflection method whereas the additional 2-d $\{211\}$ and $\{00.1\}$ orientations were observed by transmission. It is easy to see how 2-d $\{211\}$ orientation is derived from the initially grown 2-d $\{100\}$ oriented crystallites due to double twinning phenomena on $\{111\}$ planes. The development of hexagonal phase with 2-d $\{00.1\}$ orientation is due to the growth fault which will be discussed in the subsequent paragraphs.

The appearance of $\{115\}$ orientation in the case of HgSe deposits on cleavage face of mica at higher substrate temperature and for thinner films can be explained on the basis of twinning. By a single twinning on $(11\bar{1})$ plane of 2-d $\{111\}$ oriented crystals would bring $(\bar{1}\bar{1}\bar{5})$ plane of the twinned crystal exactly parallel to the initial (111) face.

This explains the simultaneous appearance of $\{111\}$ and $\{115\}$ orientations (Goswami, 1962). In the case of $\{110\}$ oriented surface layers such twinning would bring $\{114\}$ orientation.

Transformation from face centred cubic to hexagonal (close-packed)modification

It is well-known that the crystals belonging to f.c.c. and the hexagonal (C.P.) structure have the closest packing of atoms (or ions) in the unit cell. If atoms (or ions) can be represented by spheres then their arrangement in $\{111\}$ plane of f.c.c. and $\{00.1\}$ plane of hexagonal crystals, which are equivalent to each other, can be shown in the following way.

The sequence of atoms (or ions) in the $\{00.1\}$ plane of hexagonal crystals consists of two layers of atoms A and B. In the first layer there are six atoms arranged around a central atom forming a hexagonal network as shown by the filled circles in fig.52. The second layer B consisting also of six atoms regularly arranged in a hexagonal array will occupy position above or below the layer A, but displaced slightly laterally occupying the hollow positions over the layer A as shown by hatched circles. The third layer of atoms above or below the B layer can occupy two alternative positions viz. (i) vertically above or below A layer but at the same disposition or (ii) at positions C having the same arrangement as A or B but further shifted as shown by

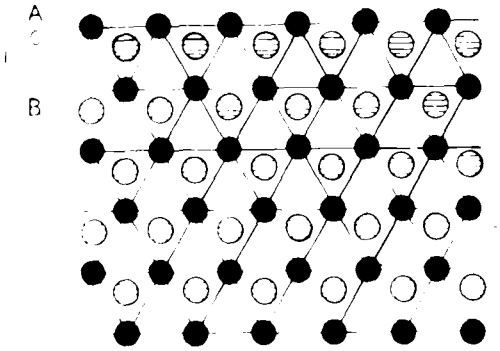

Fig. 52. Hexagonal close-packing on (0001) plane

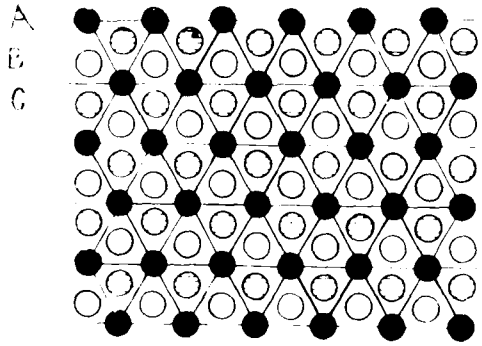

Fig. 53. Close packing on (111) plane of f.c.c. crystals.

the unfilled circles in the fig.53. Both these two alternatives will give rise to the closest packing of atoms. In the former case where the layers consist of the sequence of atoms such ABABAB.....etc. is called the hexagonal close-packing arrangement, whereas in the second case where there is a third layer indicated by the unfilled circles with a sequence of layer ABCABC.....etc. will give rise to f.c.c. structure.

In the ideal condition of crystal growth process the sequence of layers on $\{111\}$ plane of f.c.c. crystal will be ABCABC.....etc. as mentioned before. If, however, the growth process is somehow disturbed the sequence of atoms changes and the following cases may occur.

(a) Regular reversal of stacking sequence of atoms viz.

ABCABCABACBACBA.....etc.

(b) Regular omission of some layers such as,

ABCABABACAC.....etc.

(c) Irregular omission of layers

ABCABACBC.....etc.

Due to the above defects in the sequence layers new reflections or spots other than those due to the normal $\{111\}$ orientation will appear in the diffraction patterns. The reversal of the sequence as in (a) will result in the phenomena of twinning on $\{111\}$ plane. In the case of the regular omission of layers as mentioned in (b) the sequence of the atoms will be

similar to hexagonal close-packing and reflections due to hexagonal modification will also appear. The irregular omission of layers of atoms as in the case (c) will give rise to streaks passing through the diffraction spots. Often in diffraction patterns all these three effects were seen. Since $\{111\}$ plane of f.c.c. crystal is equivalent to $\{00.1\}$ plane of hexagonal (C.P.), the simultaneous development of both the orientations, no doubt due to the growth fault, can easily be understood. As already mentioned, the development of 2-d $\{211\}$ orientation was caused by double twinning phenomenon due to the faults in stacking layers on $\{111\}$ type of plane.

Crystal growth process in vapour phase deposits

It has already been mentioned for both the active and inactive substrates that the deposits of HgSe and HgTe were either epitaxial or polycrystalline with or without orientation depending on evaporation conditions as well as the nature of the substrates. The crystal growth process resulting from vapour phase deposits can be visualised in the following way.

The deposits when condensed on the substrate will naturally be influenced by it and hence will try to rearrange themselves and form nuclei of the crystal conforming with the substrate surface. The temperature

of the substrate gives mobility to the deposit-atoms, thus helping them to occupy the minimum potential energy sites. Substrates like glass and collodion are amorphous and hence have no special orientating effect. The deposit-atoms thus forming nuclei will be randomly disposed over the substrate surface resulting in polycrystalline films. As the deposit thickness increases with the time of deposition, the evaporation conditions such as rate of deposition, temperature of the substrate etc. would exert considerable influence of their own leading to the development of 1-d oriented crystallites. In the present cases 1-d $\{111\}$ oriented crystallites are observed for thicker deposits on glass at appropriate temperatures. Similar observations were made in the case of cathodic (Finch, Wilman and Yang, 1947) and chemical growth processes (Trehan and Goswami, 1959).

If, however, the substrate is active i.e. of single crystal type, the deposit-atoms would take up sites conforming to the substrate structure and develop 2-d orientation leading to an epitaxial growth. This epitaxial growth will also be favoured if the substrate temperature is high, since it will give enough mobility to the deposit-atoms to take appropriate minimum potential sites. Further with the higher substrate temperature the thickness of the epitaxial layer will also be more compared to the deposits formed at the lower substrate temperature. As lower temperature will considerably reduce the mobility of the atoms on the surface,

the epitaxial layer formed at this temperature can be as low as 1-2 Å thickness and hence may not even be observable by the electron diffraction technique. This explains why at room temperature no epitaxial layer could be detected on rocksalt or mica substrates even by reflection method.

As epitaxial layers grow in thickness, defects are often introduced into the crystal structure due to the non-ideal condition of the deposition. These defects are mainly stacking faults, twinning etc., some of which have been observed in our experiments. As the thickness grows further the orientating influence of the substrates and also of the previously deposited layers decreases and a stage is reached when the deposits are no longer affected by the substrate surface, thus resulting in polycrystalline deposits. This explains the formation of polycrystalline films even on single crystal substrates as observed in many cases.

With the further increase of thickness the growth of the deposits is modified by the evaporation conditions alone, hence resulting in 1-d orientation as discussed in the case of deposits on glass. The reason for the appearance of 1-d $\{111\}$ orientation on cleavage face of mica is thus understood. It was also found that whether the substrate was single crystal or amorphous, in almost all the cases when the deposit was considerably thick the surface layers developed 1-d orientation.

C H A P T E R - IV

STRUCTURE AND CRYSTAL GROWTH OF TELLURIDES AND SELENIDE OF INDIUM

A. INTRODUCTION

Group III-VI compounds especially selenides and tellurides of indium have relatively been less explored, both from the fundamental as well as practical point of view, even though these compounds are potential semiconductors. It is only in recent times that some interest have been shown on the structural and physical properties of these compounds. Some of these compounds also form solid solutions with other semiconducting compounds. Hahn and Klingler (1949a) made an X-ray analysis of the compound In_2Te_3 and reported zinc-blende structure with the following data : $a_o = 6.158 \pm 0.005$ Å, $U = 233.5$ Å^3, $D_m = 5.75$ gm/cm^3, $D_x = 5.80$ gm/cm^3. Inuzuka and Sugaike (1954) had grown single crystal of In_2Te_3. X-ray powder photograph with CuK radiation gave the cell edge as 18.40 ± 0.04 Å, whilst by Weissenberg photographs it was found to be 18.6 Å. The space group determined to be as F $\bar{4}$3 m. Grigore'va (1958) prepared seven different compositions in Ga_2Te_3-In_2Te_3 systems. X-ray measurements showed the solutions to be homogeneous with zinc-blende type of structure and the

lattice parameters were found to vary linearly with the composition. InAs-In_2Te_3 forms continuous solid solutions with ZnS structure (Goryunova and Radautsan, 1958), the lattice parameter varying continuously with the composition.

Woolley and Pamplin (1959) investigated the oriented structure of In_2Te_3 by X-ray powder method to determine the details of the atomic arrangement in the ordered structure.

Solid solutions of InSb-In_2Te_3 (Woolley, Gillett and Evans, 1960), In_2Te_3-CdTe, In_2Te_3-ZnTe and In_2Te_3-HgTe (Woolley and Ray, 1960) were prepared and the variation of lattice parameters with the composition and electrical properties were measured. Various electrical properties and absorption spectrum for In_2Te_3 were reported by Zuze et al. (1960). The influence of pressure on electrical conductivity, thermal e.m.f., the impurity effects etc. for vacuum annealed polycrystalline In_2Te_3 were investigated by Averkin, Sergeeva and Shelykh (1960).

A systematic study on the phase compositions of In_2Te_3 was made by Zaslavskii and Sergeeva (1961). Polycrystalline specimens were prepared under different conditions of synthesis and heat treatment. The results of X-ray analysis showed two phases of the compound In_2Te_3 and named as α-In_2Te_3 and β-In_2Te_3. The transformation of α-$In_2Te_3 \rightleftarrows \beta$-$In_2Te_3$ is accompanied by a change of density 5.73 gm/cm^3 to 5.79 gm/cm^3 at 620°C and 520°C. The high temperature form (β)

was of zinc-blende type with a_β = 6.14 Å space group F $\bar{4}3$ m, z = 4/3 In_2Te_3 molecule and of density 5.73 gm/cm^3. The low temperature form (α) was with a_α = 18.50 Å, z = 36 In_2Te_3 molecules and with space group F $\bar{4}3$ m. The absorption spectra and the photoconductivity response spectra of α and β modifications of In_2Te_3 were studied (Petrusevich and Sergeeva, 1961). Thermal conductivity of β -In_2Te_3 was found to be very small and practically independent of temperature (Zaslavskii, Sergeeva and Smirnov, 1961). For α -In_2Te_3 thermal conductivity rose with the increase of ordering of the lattice rising considerably on lowering the temperature. Thermal conductivity measurements indicated a reversible transition of β to α form. The rate of the formation of α-modification during annealing depended strongly on the dimensions of crystallites, the larger the crystallites the lower the rate. α -In_2Te_3 was prepared by slow cooling of the melt to room temperature whilst β -In_2Te_3 prepared by slowly cooling the ampoules to 600°-580°C and then quenching in an ice-bath. Woolley and Pamplin (1961) measured the various physical parameters of the compound In_2Te_3. It was shown that the activation energy at 470°C was not associated with a change in the structure. Striking electrical characteristics were observed for solid solutions of Sb_2Te_3-In_2Te_3 and Bi_2Te_3-In_2Te_3 (Rosenberg and Strauss, 1961). These solid solutions were virtually independent of the Hall coefficient with respect to indium concentration. Zhuze, Sergeera and

Shelykh (1961) reported the measurements of electrical conductivity, thermoelectric power and Hall effect of In_2Te_3, which contained a large number of cation vacancies.

An infrared microscopic study was made on In-Te system (Holmes et al. 1962) and a revised phase diagram was proposed in the region of In_2Te_3. Chizhevskaya and Glazov (1962) noticed that electrical conductivity of all compositions increased noticeably with temperature. In_2Te_3 was confirmed to be a very stable compound at liquid form after melting and did not become partially dissociated until high temperatures were reached. Solid-solutions of HgTe or CdTe and In_2Te_3 or Ga_2Te_3 were prepared, their lattice parameters determined, electrical properties and optical absorption etc. were studied by Spencer, Pamplin and Wright (1962). Thermodynamic properties of In_2Te_5, In_2Te_3, In_2Te and InTe were determined between the temperatures 380° and 425°C (Gerasimov, Abbasev and Nikol'skaya, 1962).

Amorphous structures of In_2Te_3 were studied by electron diffraction (Andrievskii et al., 1963) and reported that the compound did not possess a constant structure in the whole range of existence of amorphous phase. Thermal conductivity and temperature gradient were measured for In_2Te_3 and the results were explained by the effect of defects in the structure (Aliyev and Dzhangirov, 1963).

The phase diagram for the binary system In-Te had been clarified and corrected particularly in the region near the composition In_2Te_3 by Grochowski et al. (1964). During this study two new phases, namely In_2Te_4 and In_3Te_5 were identified. Some of the semiconducting properties of the alloy HgTe-In_2Te_3 (Spencer 1964) and the superconductivity in metallic indium antimonide with Sn and In_2Te_3 were studied (Tittman et al., 1964).

Investigations on the effects of deviations from stoichiometric ratios in $A_2^{III} B_3^{VI}$ type of compounds in particular In_2Te_3 were made by Palatnik et al. (1965). Phase diagram was illustrated and identified for In_2Te_3 and the reasons for deviations were considered. Aliev and Dzhangirov (1965) reported the measurements of thermal and electrical conductivity, thermo e.m.f. and Hall effect in InSb-In_2Te_3 alloys. The change in electrical conductivity and thermo-electric power of In_2Te_3 on melting were studied by Zhuze and Shelykh (1965). Wright (1965) observed that the energy gap increased linearly with lattice parameter as the In content of HgTe-In_2Te_3 alloys increased.

Polycrystalline specimens for InSe, In_2Se and In_2Se_3 were prepared by direct fusion (Brice, Newsman and Wright, 1958) and their electrical and physical measurements were made. A phase change for In_2Se_3 at 196°C was observed. In_2Se_3 has got at least four modifications (Semiletov, 1961 a,b,c) two

hexagonal, one cubic and one monoclinic. α -In_2Se_3 at room temperature is a double layer hexagonal packing of Se-atoms a = 16.00 Å, c = 19.24 Å space group C_6^6 — C 6_3, z = 32, β-In_2Se_3 stable over 200°C with a = 7.11 Å, c = 19.30 Å with space group C_6^3 — C 6_5, z = 6.

Schubert, Dorre and Gunzel (1954) in a brief communication reported the lattice parameters of InSe, In_2Se and In_2Te, without any further details. According to these authors InSe had a rhombohedral lattice with parameters a = 4.023 Å and c = 25.05 Å, while In_2Se and In_2Te both of orthorhombic type with lattice parameters a = 4.073 Å, b = 12.62 Å, c = 15.62 Å and a = 4.46 Å, b = 12.62 Å, c = 15.36 Å respectively. Optical and electrical properties of InSe were reported by Damon and Redington (1954) and the structure by electron diffraction by Semiletov (1958).

Slavnova, Luzhnaya and Medvedeva (1963) determined the melting points of the compounds as InSe = 660 ± 10°C, In_2Se_3 = 900 ± 10°C and In_2Se = 540 ± 10°C (heating under decomposition). X-ray analysis of In-Se alloy was made and found to be consisted of InSe, In_2Se and In in the InSe-In_2Se region (Slavnova and Yeliseyev, 1963). Both n- and p-type In_2Se single crystals were grown from a melt by the method of extraction (Stakhira, 1963). It was shown that In_2Se was probably formed by the reaction $In + InSe \rightleftharpoons In_2Se$. The melting point was found to be 578°C and the rhombic system

of In_2Se crystals was confirmed. Optical properties of In_2Se were reported by Borets and Stakh'yra (1964).

An electron diffraction study was made on the structure of In_2Se (Man and Semiletov, 1965). In_2Se films were prepared by sublimating the compound onto rocksalt cleavage face kept at room temperature and then heated upto 200°-300°C for 2-3 hours or evaporated directly on hot rocksalt crystals at 200°-300°C and then annealed for about 1.5 hours. The lattice parameters determined were as a = 15.24 Å, b = 12.32 Å and c = 4.075 Å. It was concluded that In and Se atoms of two elements were in general position 4(g): xyo, $\bar{x}\bar{y}o$; $\frac{1}{2}+x$, $\frac{1}{2}-y$, $\frac{1}{2}$; $\frac{1}{2}-x$, $\frac{1}{2}+y$, $\frac{1}{2}$; which suggested that the atoms were disposed in pairs only in the two planes (xyo) and (xy$\frac{1}{2}$). Space group was found to be D_{2h}^{12} — P_{nnm}. Electrical properties of the semiconductor In_2Se were studied by Zhad'ko et al. (1965). Guliev and Medvedeva (1965) described the conditions for the production of poly- and single-crystalline In_5Se_6. X-ray study revealed monoclinic type of lattice for In_5Se_6 with lattice parameters a = 17.48 Å, b = 4.09 Å, c = 9.37 Å and β = 101° specific density at 20°C = 5.66 gm/cm^3.

It is clear from the above survey of the literature that though considerable work has been done on physical properties and also on bulk structures of the above compounds, very little attention has been paid to the structures of these compounds in thin film form, their growth process,

phase transformation under different evaporation conditions etc. Since the properties of thin film are structure sensitive, a detail study has been made on the thin films of selenide and tellurides of indium.

B. EXPERIMENTAL

Preparation of selenide & telluride of indium (In_2Se, In_2Te, In_2Te_3)

The methods of preparation of the compounds In_2Se, In_2Te and In_2Te_3 were similar to those described in the previous cases. Stoichiometric proportions of the elements indium (99.99%), selenium or tellurium were taken, in the case of In_2Se and In_2Te in the ratio of 2:1 (atomic proportions) and in the case of In_2Te_3 in the ratio of 2:3 (atomic proportions), in silica tubes. These tubes were evacuated ($\sim 10^{-5}$ mm of Hg) and sealed in vacuum. The sealed tubes were heated in an electric furnace and the temperature was raised to about 200°C so that indium melts (m.p. = 155°C) and a slow reaction would proceed. The temperature was kept at this stage for about two hours and then raised just above the temperature of the melting point of tellurium or selenium (as the case might be), and kept at the same temperature for about 2 hours. The final temperature was then raised to about 700°C and kept overnight at this temperature. The temperature of the furnace was then lowered down to $\sim$ 300°C and the tubes were immersed in cold water. Compounds thus

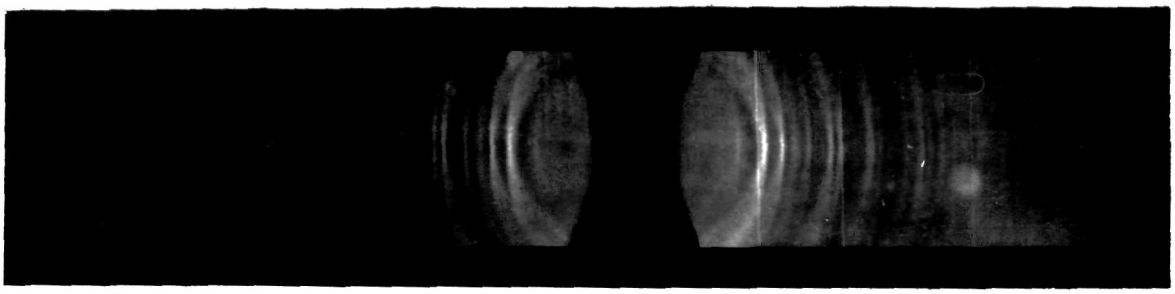

Fig. 54. X-ray powder pattern of In_2Se

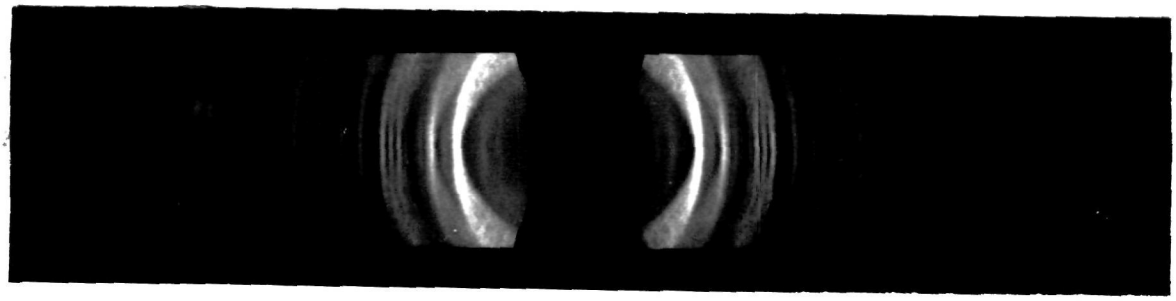

Fig. 55. X-ray powder pattern of In_2Te

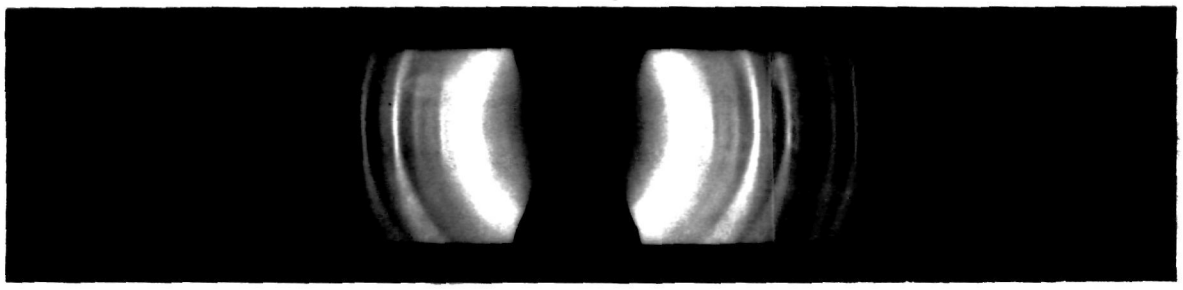

Fig. 56. X-ray powder pattern of In_2Te_3

formed were tested for homogeneous composition by X-ray powder method (figs. 54, 55, 56).

In the case of In_2Te_3 it was noticed that during evaporation decomposition took place and Te deposition was observed for the first few evaporations. However, at higher substrate temperatures these excess of tellurium deposited just outside the enclosure of the furnace. To avoid tellurium deposition always a small piece of In_2Te_3 was taken on a filament and the deposition was carried out at higher substrate temperature. It was noticed that though at the first evaporation slight trace of tellurium was observed during the next successive evaporations In_2Te_3 deposition was obtained.

C. RESULTS

(a) Indium telluride (In_2Te_3) deposits

(1) On collodion support

In_2Te_3 was deposited on neutral collodion supports within the temperature range between room temperature to about 150°C showed halos which might be due to the growth of very fine crystallites. Several trials were made but the same sort of results were obtained in all the cases.

(2) On amorphous glass substrate

Deposits of In_2Te_3 on amorphous glass substrate at temperatures ranging from room temperature to $\sim$ 250°C did

Fig. 57. In_2Te_3 on glass support deposited at ~ 300°C

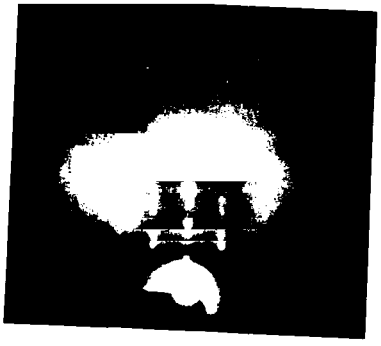

Fig. 58. In_2Te_3 on (100) NaCl deposited at ~300°C

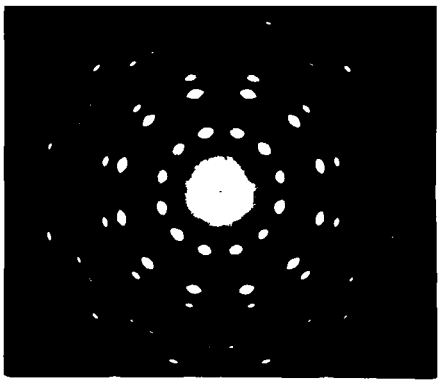

Fig. 59. Same film (showing pattern fig. 58) by transmission.

T A B L E - V

Analysis of the pattern (fig.59)

d Å	hkl (cubic)	hk.l (hex.)
3.77	-	10.0
3.64	111	00.2
3.07	200	-
2.18	220	11.0
2.01	-	10.3
1.87	311	20.0
1.54	400	-
1.38	420	21.1
1.25	422	-
1.18	333, 115	00.6
1.08	440	22.0
1.04	531	-

$a_H = 4.35$ Å, $c_H = 7.13$ Å

not show any clear pattern. When the deposition was carried out at substrate temperature $\sim 300^{\circ}C$ it yielded patterns shown in fig.57. These patterns consisted of half rings which did not show any change in the intensity of the individual ring with the change of beam direction. This shows that the crystallites were randomly disposed. The disposition of the reflections showed that the deposits developed f.c.c. type of structure.

(3) On rocksalt faces

On (100) face of rocksalt

Deposits of In_2Te_3 on rocksalt cleavage face up to substrate temperature $\sim 200^{\circ}C$ showed very poor patterns. The deposits at substrate temperature about 250°-$300^{\circ}C$ yielded pattern as showed in fig.58. These patterns are similar to those obtained in the case of HgSe and HgTe deposits over (100) rocksalt face. Here 111 and its higher order reflections were in the plane of incidence and the ratio of the sides of the rectangular arrays were $\sqrt{3} : \sqrt{24}$ and $\sqrt{3} : \sqrt{8}$ when the beam direction was $\langle 110 \rangle$ and 30° to it for the rocksalt substrate. This suggests that In_2Te_3 crystallites on rocksalt (100) face developed both normal and anti 2-d $\{111\}$ orientation rotated by 30° as discussed before in the case of HgSe and HgTe. The disposition of the crystallites on rocksalt (100) face is the same as shown in fig.14 for the case of HgSe.

Transmission pattern (fig.59) from the same film is of much interest. The pattern consisted of intense reflections (spots) lying on faint rings. It can also be seen that there were fine streaks joining the intense spots which were no doubt due to the crystal defects, such as stacking faults or due to the curvature of the film which arose when the film was placed over the wire gauge. The inner most reflections consisted of two faint rings (can be seen on close examination) and spots over them. The first reflection consisted of 12 equidistant spots which were due to 10.0 reflection of a new hexagonal phase of In_2Te_3. Twelve spots over 10.0, 11.0 and 20.0 reflections along with the undeflected spot formed a hexagonal network which is rotated by 30° suggesting thereby that 2-d $\{00.1\}$ orientation of the hexagonal crystallites developed as discussed in the case of HgSe and HgTe. Twelve equidistant spots on 111 reflection of the cubic crystallites along with 311 and 220 forming a rectangular array showing that 2-d $\{211\}$ orientation of the cubic crystallites also developed which was rotated by 30°. The theoretical pattern for 2-d $\{00.1\}$ of hexagonal crystallites rotated by 30° and 2-d $\{211\}$ orientation of cubic crystallites rotated by 30° are shown in the figs. 17 & 19 respectively. Further it can be seen that the reflection at the crossing point of the streaks which was 200 reflection of the cubic phase and its higher order reflection 400 could be seen in

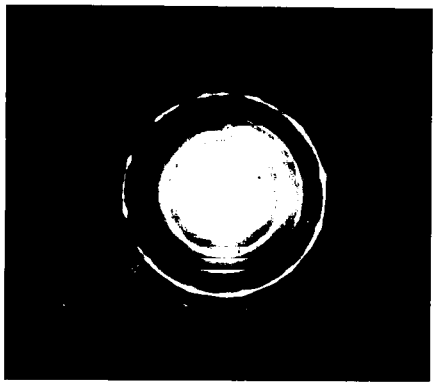

Fig. 60. Transmission pattern from thicker deposits of In_2Te_3 on (100) NaCl at ~ 300°C

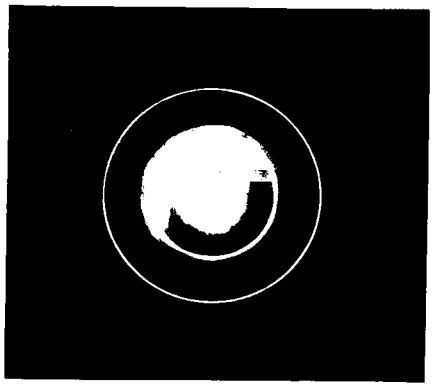

Fig. 61. In_2Te_3 on (110) NaCl deposited at ~ 500°C

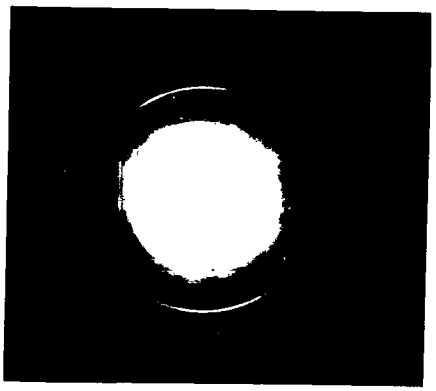

Fig. 62. Tilted pattern of fig. 61.

between 311 and 420. It can be seen that there were twelve such weak reflections suggesting the development of 2-d $\{100$ orientation of the cubic crystallites. Thus it can be summed up that In_2Te_3 grew epitaxially on rocksalt cleavage face when evaporated at substrate temperature 250°-300°C developed 2-d $\{211\}$ and $\{100\}$ orientations of the cubic phase while there was strong development of 2-d $\{00.1\}$ orientation of the hexagonal phase, all the oriented crystallites being rotated by 30°. An analysis of the above pattern is given in table-V.

It can be mentioned here that when the film was thicker predominantly hexagonal form of crystallites grew on (100) face of rocksalt (fig.60). Here the innermost two reflections were very clearly resolved and twelve weak reflections (spots) on 10.0, 11.0 and 20.0 along with the undeflected beam showed the development of 2-d $\{00.1\}$ orientation of the hexagonal phase of In_2Te_3. The 'a' and 'c' values calculated from hexagonal (C.P.) relation agreed well with the observed values of reflections.

On (110) and (111) faces of rocksalt

Deposits of In_2Te_3 on rocksalt (110) and (111) faces within the temperature range 200°-300°C showed very poor patterns by reflection. When the films were put for transmission ring patterns (fig.61) were obtained for (110) face. These patterns consisted of reflections due to both hexagonal

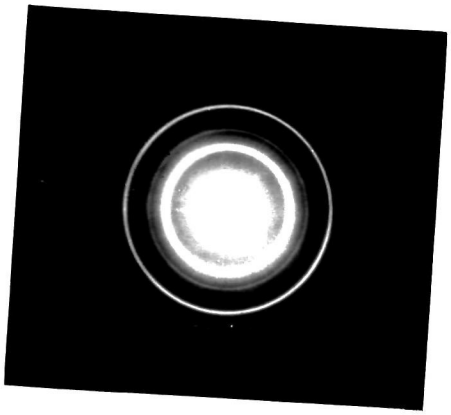

Fig. 63. In_2Te_3 deposits on (111) NaCl at ~ 300°C

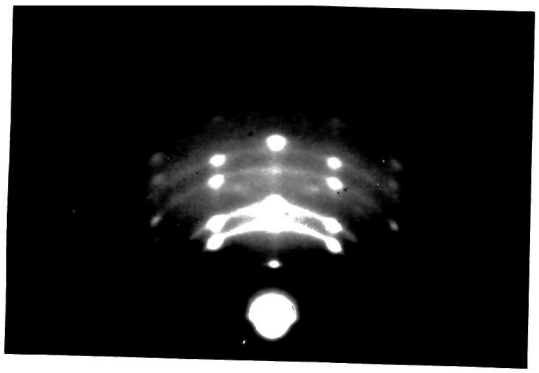

Fig. 64. In_2Te_3 on mica (0001) face deposited at ~ 300°C

Fig. 65. same as fig. 64 when beam direction was changed by 30° w.r.t. latter fig. i.e. 64.

TABLE - VI

Analysis of the pattern (fig.68)

I/I_o	d Å	hkl	a_o Å
s	3.65	111	6.15
m	2.84	200 of NaCl	-
s	2.18	220	6.16
m	2.00	10.3 (hex.)	-
ms	1.86	311	6.16
w	1.78	222	6.15
vw	1.61	-	-
w	1.53	400	6.12
m	1.38	420	6.16
m	1.26	422	6.17
		Mean a_o =	6.15 Å

s - strong
m - medium
ms - medium strong
w - weak
vw - very weak

and cubic phases. When the films were tilted about an axis perpendicular to the beam direction the intensity of the individual ring changed considerably and the rings broke into arcs suggesting the development of 1-d orientation of the crystallites (fig.62). For the deposits of (111) face by transmission ring patterns (fig.63) were observed. These deposits were, however, polycrystalline in nature without any preferred orientation. In spite of several trials single crystal films could not be obtained on these two faces of rocksalt. An analysis of the pattern is given in table-VI.

(4) On mica cleavage face

Deposits of In_2Te_3 on mica (0001) face did not show any clear pattern up to 250°C, however, at substrate temperature $\sim$ 300°C epitaxial growth of In_2Te_3 crystallites over mica cleavage face was observed. These patterns (fig.64) showed strong reflections (spots) which were similar to those obtained for HgSe and HgTe on rocksalt (100) and mica cleavage face. It can be seen that 111 and its higher order reflections are in the plane of incidence and the pattern changed from $\sqrt{3} : \sqrt{24}$ type of rectangular arrangement to $\sqrt{3} : \sqrt{8}$ type of rectangles (fig.65) due to a change of beam direction by 30° suggesting normal and anti 2-d $\{111\}$ orientation of the crystallites. However, in this case the oriented crystallites were not rotated by 30°.

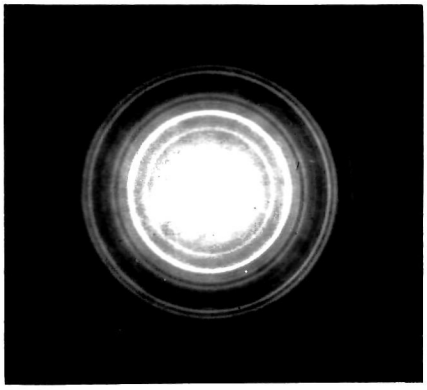

Fig. 66. In_2Se on collodion film deposited at ~100°C

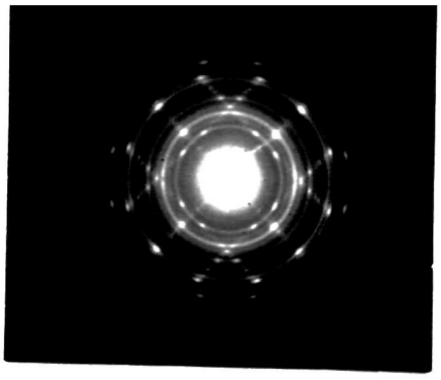

Fig. 67. In_2Se on (100) NaCl deposited at ~250°C

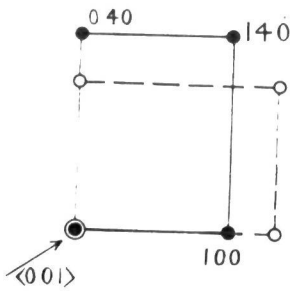

Fig. 68. 2-d {001} oriented pattern rotated by 90°

T A B L E - VII

Analysis of the pattern (fig.66)

I/I_o	d Å	hkl
m	3.86	110
s	3.10	122
w	2.85	042
m	2.69	132
m	2.62	406
m	2.51	140
w	2.30	-
w	2.12	036
s	2.04	200
s	1.94	220
w	1.82	-
w	1.71	240

T A B L E - VIII

Analysis of the pattern (fig.67)

d Å	hkl	d Å	hkl
9.406	-	2.630	406
6.261	020	2.501	140
4.769	013	2.434	-
4.076	100	2.296	-
3.859	110	2.210	-
3.634	-	2.120	036
3.406	-	2.038	200
3.140	040	1.938	220
3.061	-	1.803	-
2.846	042	1.705	240
2.712	132	1.644	-

(b) Indium selenide (In_2Se) deposits

(1) On collodion support

In_2Se deposited on collodion supports at room temperature yielded poor patterns. When the deposition was carried out at substrate temperature between 100°-150°C the patterns (fig.66) became sharper. Table-VII show the d_{hkl} values obtained by comparing with graphite $11\bar{2}0$ reflection as standard. These agreed well with values calculated from the lattice parameters of In_2Se given by Man and Semiletov (1965). On rotation of the film about an axis perpendicular to the beam direction there was no change of intensity of the rings and they did not break into arcs suggesting thereby that the deposit crystallites were randomly disposed over the substrate.

(2) On rocksalt substrates

On (100) face of rocksalt

Deposits of In_2Se on rocksalt cleavage face at substrate temperatures below 100°C yielded patterns by transmission similar to those obtained in the case of deposits on collodion supports. When the deposition was carried out at substrate temperature between 200°-300°C by transmission method spot patterns (fig.67) were obtained. These patterns mainly consisted of rings along with rows of spots, the latter forming square network. Due to the appearance of a range number of

spots and rings and the streaks passing through them, the patterns appeared to be very complicated. An analysis of the pattern is given in table-VIII. A closer examination reveals that most of the reflections can be explained on the basis of the orthorhombic structure of In_2Se with a_o = 4.075 Å, b_o = 12.32 Å, c_o = 15.24 Å. The perpendicular distance between the rows of spots gives the value of one parameter namely a_o (= 4.075 Å). Thus it can be seen that the 100 reflection (spot) is very faint whilst 200 is much stronger. The spots 100, 140 and 040 formed a rectangular arrangement along with the undeflected spot. This sort of arrangement can explain most of the reflections observed in the pattern. It can further be seen that the same sort of arrangement can be made in the other perpendicular direction. Thus it is clear that the spot patterns mainly consist of reflections which can be arranged at the corners of two types of rectangles with sides a_o and $b_o/4$, the rectangles being rotated by 90° (fig.68). This suggests that In_2Se crystals developed 2-d $\{001\}$ orientation on rocksalt cleavage face and were rotated by 90° Besides this arrangement there are many more spots lying on faint rings which could not be accounted for by the said arrangements. These spots may be due to the crossing of continuous streaks over the rings which enhanced the intensity of reflections at these points. It can be pointed out that the observed orientation namely 2-d $\{001\}$ was such that $\langle 110 \rangle$ direction of the rocksalt (100) face was parallel to either

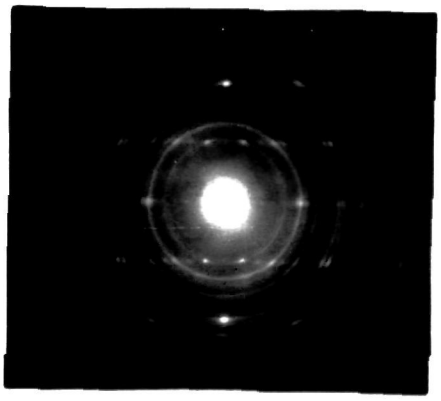

Fig. 69. In_2Se on (110) Nacl deposited at. ~300°C

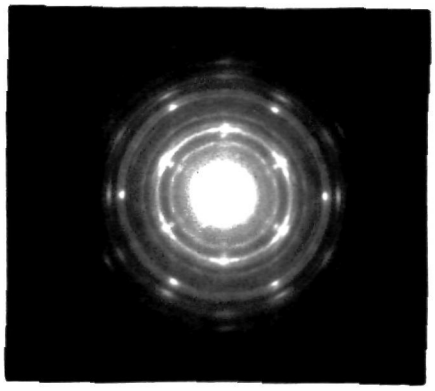

Fig. 70. In_2Se deposits on (111) Nacl at. ~300°C

$\langle 100 \rangle$ or $\langle 010 \rangle$ direction of the deposit crystallites.

On (110) face of rocksalt

Deposits of In_2Se on (110) face of rocksalt showed ring patterns up to about 150°C substrate temperature. When the deposition was carried out at substrate temperature ~200°C In_2Se showed patterns (fig.69) which consisted of reflections forming rows. Most of the reflections were lying at the corners of a rectangular array of sides a_o and $b_o/4$. This suggests the development of 2-d $\{001\}$ orientation of In_2Se crystallites on the (110) face of rocksalt. The same sort of arrangement was also observed in the case of deposits formed over the cleavage face of rocksalt which was rotated by 90°. In this case it is seen that the In_2Se crystallites developed 2-d $\{001\}$ orientation but there was no rotation of the crystallites. It was further noticed that the deposits grew with $\{001\}$ orientation in such a way that $\langle 110 \rangle$ direction of the rocksalt surface was parallel to $\langle 100 \rangle$ direction of the deposit crystallites.

On (111) face of rocksalt

In_2Se deposits on rocksalt (111) faces at temperatures between room temperature and 250°C yielded polycrystalline patterns very similar to those obtained in the cases of deposits on collodion support. At substrate temperature about 300°C the patterns obtained (fig.70) were much interesting and at the same time complicated. These patterns

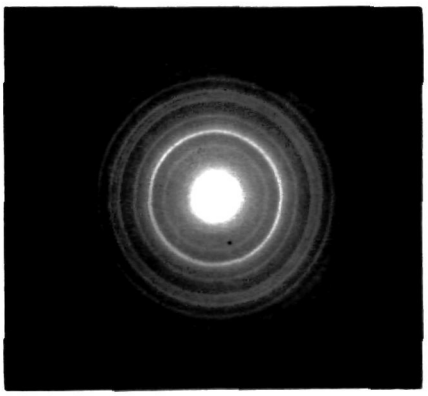

Fig. 71. In_2Te deposits on collodion film at ~ 100°C

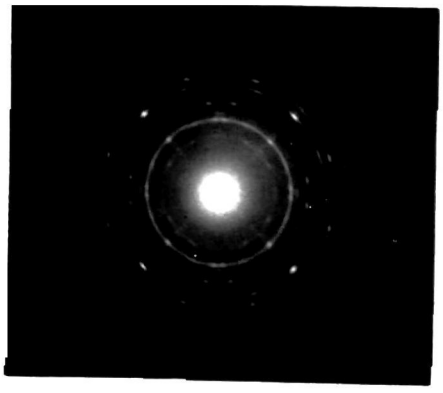

Fig. 72. In_2Te deposits on (100) NaCl at ~ 250°C.

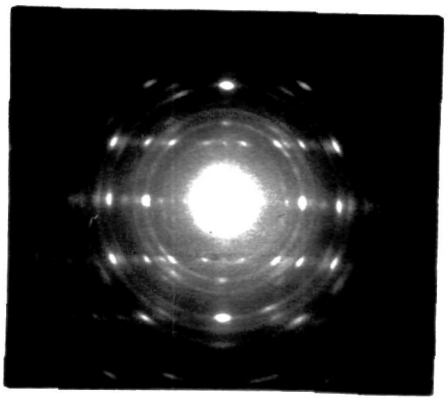

Fig. 73. In_2Te on (110) NaCl deposited at ~ 250°C.

TABLE - IA

Analysis of the pattern (fig.72)

I/I_o	d Å	hkl
vw	4.44	100
vw	4.05	111
s	3.24	040
m	2.96	042
m	2.82	-
ms	2.64	140
m	2.62	-
w	2.40	044
s	2.22	200
m	2.11	202
m	2.03	222
w	1.84	280

s - strong
ms - medium strong
m - medium
w - weak
vw - very weak

(2) On rocksalt faces

On (100) face of rocksalt

In_2Te deposited on rocksalt cleavage face at substrate temperature below 250°C yielded ring patterns similar to those obtained on collodion substrates. The deposits at substrate temperature 200°-250°C yielded patterns (fig.72) consisting of rings and spots. These spots are arranged to form a square-net pattern similar to that of In_2Se films obtained on (100) face of the rocksalt crystal at higher substrate temperature. The appearance of most of the spots can be explained on the basis of the orthorhombic lattice of In_2Te, the orientation of the crystallites being such that 'ab' plane of the cell was parallel to the support while 'c' axis perpendicular to it. Thus In_2Te crystallites developed 2-d $\{001\}$ orientation rotated by 90°. An analysis of the pattern is given in table-I. a_o and b_o values are determined from the arrangement of the spots and found to be a_o = 4.44 Å. b_o = 12.96 Å.

On (110) face of rocksalt

Deposits formed on (110) face of rocksalt crystal from room temperature to about 150°C yielded polycrystalline patterns. When the deposition was carried out at substrate temperature 200°-300°C, patterns as shown in fig.73 were obtained. These patterns consisted of rings and spots, the

spots being arranged in rows forming layer lines. Due to the appearance of a large number of reflections such patterns are usually complex. The arrangement of spots can, however, be explained in the same way as done in the case of In_2Se. The layer lines are at distance equal to a^* of the orthorhombic cell and thus it can be assumed that most of the crystallites were lying in parallel rows. Unlike the patterns on (100) face of rocksalt the crystals were not rotated through 90°. However, in between the rows there are few extra spots which along with other spots form rectangular arrangements with sides corresponding to a and b/4, showing thereby that a few crystallites were rotated by 90° with respect to the others. Thus the crystallite developed 2-d $\{001\}$ orientation on (110) face of rocksalt, the orientation being such that $\langle 110 \rangle$ direction lying on the rocksalt (110) face was parallel to $\langle 100 \rangle$ direction of the In_2Te crystallites.

On (111) face of rocksalt

In_2Te deposits on octahedral face of rocksalt yielded always polycrystalline patterns very similar to those obtained for deposits on collodion supports. These patterns were found to be due to randomly disposed crystallites as it was evident from the fact that there were no changes in the patterns on tilting the specimens about an axis perpendicular to the beam direction.

D. DISCUSSION

Indium forms different compounds and solid solutions with selenium and tellurium giving rise to phases, such as In_2Se, In_2Te; InSe, InTe; In_2Se_3, In_2Te_3 and possibly also a few others of different compositions. Because of the easy solubility of selenium and tellurium in various proportions with indium, different phases were observed. In many cases the structure of these phases has not been fully established (Pearson, 1958). Of the compounds studied in the present case In_2Te_3 has a cubic structure (zinc-blende type), whereas In_2Se and In_2Te have orthorhombic structure as reported by Schubert, Dorre and Gunzel, (1954).

In_2Te_3 has also two modifications namely α and β forms. The β -form is a high temperature form with lattice a_β = 6.14 Å whilst α-form has lattice parameter a_α = 18.4 Å. During our experiments β -In_2Te_3 films were always obtained. The lattice parameter also agreed well with the known value. Epitaxially grown films were obtained only on the cleavage face of rocksalt whilst on other faces polycrystalline deposits were observed. On all the faces a new hexagonal modification of In_2Te_3 not previously reported was observed.

On cleavage face of rocksalt by reflection 2-d $\{111\}$ orientation was obtained while by transmission always 2-d $\{211\}$ orientation of cubic and 2-d $\{00.1\}$ orientation of hexagonal modification were found. The explanation of such growth was

given in the case of HgSe and HgTe. It was noticed that the spots were connected with fine streaks, no doubt, due to the defect structure of In_2Te_3.

It was pointed out before in the results that In_2Se deposits grew epitaxially on (100), (110) and (111) faces of rocksalt at higher substrate temperatures while the deposits formed at substrate temperature below 200°C yielded ring patterns, the orientation for the crystallites at higher substrate temperature being 2-d $\{001\}$. It is quite interesting to note that the deposits on (100) face of rocksalt grew in such a way that 110 direction of the substrate was always parallel to either $\langle 100 \rangle$ or $\langle 010 \rangle$ direction of the orthorhombic crystallites the third axis being perpendicular to the surface of the substrate. Since there are two $\langle 110 \rangle$ directions lying on (100) face of rocksalt perpendicular to each other, there are two possibilities of crystal orientations thus giving rise to the observed 2-d $\{001\}$ orientation rotated by 90°. In the case of the deposits on (110) face of rocksalt the same was observed. It was noticed that $\langle 100 \rangle$ direction of the deposit crystallites was parallel to $\langle 110 \rangle$ of the rocksalt face, thus suggesting that In_2Se grew epitaxially on (110) face of rocksalt in such a way that $\langle 100 \rangle$ direction of the deposits was parallel to $\langle 110 \rangle$ direction of rocksalt face. In this case the orientation observed was 2-d $\{001\}$ but not rotated by 90°. In the case of the deposits on (111) face of rocksalt also showed 2-d $\{001\}$ orientation which

was rotated by 60°. It can be pointed out that on (111) face of rocksalt there are three ⟨110⟩ directions which are at 60° to each other. Hence it can be suggested that in this case also the orthorhombic crystallites developed 2-d {001} orientation, the disposition of the crystallites being such that ⟨100⟩ direction of the deposit-crystals was parallel to ⟨110⟩ directions of the substrate surface. This will give rise to a pattern of 2-d {001} oriented crystallites rotated by 60°.

A consideration of the atomic distances on the three faces of rocksalt namely (100), (110) and (111) has shown that the distance between atoms along ⟨110⟩ direction of the substrate is about 4.00 Å which is nearly equal to a_o of In_2Se unit cell (4.075 Å). This clearly showed why ⟨100⟩ direction of the orthorhombic crystallites grew along ⟨110⟩ direction of the rocksalt face in all the observed cases.

For the deposits of In_2Te on (100) face of rocksalt at higher substrate temperature 2-d {001} orientation rotated by 90° was observed which was similar to those observed for In_2Se deposits on (100) face of rocksalt. Similar 2-d {001} orientation was also observed for the deposits on the (110) face of rocksalt. Deposits on the (111) face of rocksalt crystals, however, yielded ring patterns.

Thus In_2Te deposits also grew epitaxially on (100) and (110) faces of rocksalt with 2-d {001} orientation at appropriate substrate temperature.

C H A P T E R - V

STRUCTURE AND CRYSTAL GROWTH OF SELENIDE AND TELLURIDE OF THALLIUM (Tl_2Se, Tl_2Te)

A. INTRODUCTION

Thallium chalcogenides has great possibility of uses in a wide group of vitreous semiconductors which are of large practical importance for their high conductivity and large thermal e.m.f. and as photoconducting materials. Hahn and Klingler (1949b) prepared the compound of Tl-Se by heating pure thallium and selenium in bombs of jena-glass in vacuum in a bunsen flame and annealed for 25 hours at 200°-300°C. Powder patterns showed that there existed two phases, namely TlSe and Tl_2Se, but no unit cell dimension etc. was given.

Stasova and Vainshtein (1958) have reported an electron diffraction determination of the structure of Tl_2Se. It has got a tetragonal cell with lattice parameters $a = 8.52 \pm 0.02$ Å and $c = 12.68 \pm 0.03$ Å, $n = 10$, with space group C_{4h}^3 - P4/n. The structure consists of thallium tetrahedra united by layers of selenium atoms. On the vertical $0\frac{1}{2}z$, $\frac{1}{2}0z$ layers alternate with linear Tl_2Se groups. Selenium ions may enter into these groups forming phases of variable composition. The diffusion of component elements

in Tl_2Se was studied by means of marked atoms (Tl^{204} and Se^{75}) (Akhundov and Abdullayev, 1958).

The excess of noise of two amorphous semiconductors Tl_2Te-As_2Te_3 and Tl_2Se-As_2Te_3 was found to be smaller than could be measured (Kornfel'd and Sochava, 1959). It was suggested that the lack of excess noise might be connected with the absence of certain macroscopic heterogeneties, such as grain boundaries normally found in crystalline semiconductors.

The dependence of photoelectric properties of Se semiconductors coated with an artificial layer of either Tl_2Se or InSe on X-radiation was determined by Bakhyshov and Abdullaev (1960). Photo e.m.f. generated was plotted against the current of the X-ray tube at different applied voltages. The short circuit current was found to be a linear function of the X-ray intensity. For glasses of As_2Se_3-Tl_2Se system a complex structure was characterised by absorption in the short wave-length spectral region (Kolomiets and Pavlov, 1960). As % of Tl_2Se increased the formation of absorption bands first observed to increase and then fall off with variation in composition. Rabenau, Stegherr and Eckerlin (1960) reported a new compound Tl_2Te_3 in the system Tl-Te. Single crystals of TlSe were prepared using 99.989% pure thallium and 99.99% pure selenium by heating in evacuated quartz ampoules at 500°C (vacuum 10^{-4} torr) for six hours (Akhundov, Abdullayev and Guseynov, 1960).

X-ray analysis gave the lattice parameters as, a = 8.02 Å and c = 7.00 Å of tetragonal cell. Investigations were carried out on materials of the $Tl_2Se.As_2(Se,Te)_3$ system which has got high electrical conductivity (Kolomiets and Nazarova, 1960). Hall voltage measurements were carried out covering the range from 0.2 to 3000 μV, the maximum magnetic field intensity during measurements reaching 1800 Oe. Solid solutions of different compositions of As_2Te_3 and Tl_2Se with Sb_2Te_3, Bi_2Te_3 or Sb_2Se_3 were prepared and tested by Uphoff and Healy (1963). It was found that some samples were amorphous whereas others were diphasal including both amorphous and crystalline phases. Electrical properties such as resistivity, Seebeck coefficient and thermal conductivity were measured for these compositions. Terpilowski and Zaleska (1963) studied the thermodynamic properties of liquid Tl-Te system by measuring the electromotive forces. The dependence of excess thermodynamic functions of mixing on the composition of the liquid solutions was discussed. A description was given of the results of a study of the photoelectret state in thin amorphous layers of $Tl_2Se.As_2Se_3$ prepared by evaporation in vacuo by Lyubin and Fomina (1964). Measurements of the electrical conductivity and Hall constant of p-type TlSe for 80°-573°K were reported by Guseinov and Akhundov (1964). It was stated that the energy gap value for the various crystallographic directions were consistent with the previous data.

Kolomiets, Mamontova and Stepanov (1965) have established the existence of impurity and induced photoconductivity in glassy semiconductors based on metal chalcogenides. The kinetics of impurity photoconductivity and its spectral dependence were investigated for $Tl_2Se.As_2Te_3$, a compound with sufficiently high conductivity at room temperature (10^{-3} ohm^{-1} cm^{-1}). Experiments were carried out to measure the electrical conductivity of Tl_2Te in the solid and liquid state by Katilene and Regel (1965). The conductivity measurements were carried out on an alloy consisting of 23.8 wt. % Te + 76.2 wt. % Tl, corresponding to the compound Tl_2Te. It was concluded that Tl_2Te like thallium sulfide behaved like a normal semiconductor in regard to the temperature dependence of electrical conductivity.

Thus from the above survey of literature it is evident that the two compounds Tl_2Se and Tl_2Te though have been studied in details for their electrical properties but very little attention has been paid to their film structures and crystal growth process. The structure of Tl_2Te has not yet been determined. In the following, the crystal growth process from vapour phase for the above two cases has been undertaken.

b. EXPERIMENTAL

Preparation of selenide and telluride of thallium (Tl_2Se, Tl_2Te)

Selenide and telluride of thallium were prepared by a similar method as discussed previously for the other compounds. Stoichiometric proportions of thallium and selenium (or tellurium) were taken (Proportion 2:1 atomic) in silica tubes which were then sealed in vacuo ($\sim 10^{-5}$ mm of Hg) and subsequently heated in an electric furnace at temperature about 600°C. The temperature of the furnace was raised slowly from room temperature to about 350°C (melting point of thallium = 303.5°C) and kept at this temperature for about two hours so that most of the reaction would be completed at the lower temperature. The temperature of the furnace was then raised above the melting point of tellurium (or selenium) and kept at that temperature for about an hour and then the temperature was slowly increased to about 600°C and kept overnight at this temperature. The temperatures of the tubes were lowered down to about 300°-400°C and then suddenly immersed in cold water.

X-ray powder patterns for Tl_2Se and Tl_2Te were taken with Mo target but they were of very poor quality.

Tl_2Se and Tl_2Te (bulk) thus prepared were evaporated in vacuo from kanthal filaments as mentioned in chapter-II.

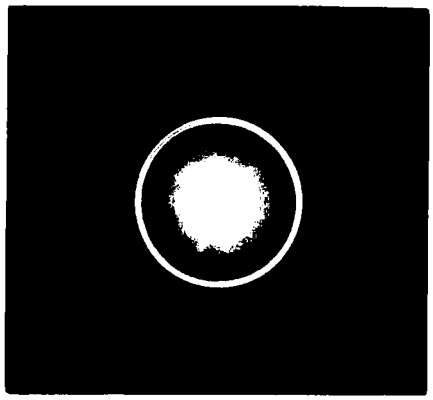

Fig. 74. Tl_2Se deposits on collodion film at R.T.

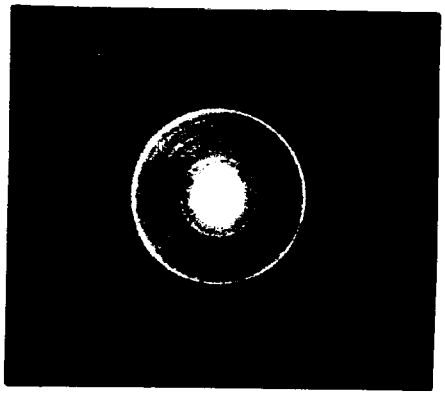

Fig. 75. Tl_2Se on collodion film at R.T. after heating in vacuo at ~ 100°c

Fig. 76. Tl_2Se on (100) NaCl deposited at ~200°c. Beam along ⟨100⟩ of NaCl

T A B L E - X

Analysis of the pattern (fig.74)

I/I_o	d Å	hkl
m	6.02	110
w	4.25	200
m	3.64	211
w	3.25	212
m	3.01	220
s	2.78	301
s	2.68	310
w	2.49	312
vw	2.34	321, 115
w	2.13	400
w	2.02	330
m	1.91	420

$a = 8.52$ Å, $c = 12.68$ Å

Deposits on rocksalt crystals were examined by reflection method. To study the films by transmission method when the substrates were dissolved unlike the other films they did not detach and very often they sink or break into pieces. To avoid these difficulties and to get continuous films after dipping the rocksalt in water the films were gently removed with the help of a needle and placed over the collodion coated wire gauze. Removal of the films was much more difficult and hence many trials had to be made to get proper films with their edges intact.

C. RESULTS AND DISCUSSION

(a) Thallium selenide (Tl_2Se)

(1) Deposits on collodion support

Tl_2Se deposits on collodion support at room temperature yielded ring patterns (fig.74). When the film was tilted about an axis perpendicular to the beam direction it was observed that there was neither any change of intensity nor any discontinuity in the rings showing thereby that the film was due to polycrystalline deposit without any preferred orientation of the crystallites. When the same film was heated in vacuo for about an hour at about 100°C and cooled down to room temperature patterns similar to fig.75 were obtained. The d_{hkl} values measured for different reflections agreed well with the tetragonal structure of Tl_2Se (table-X).

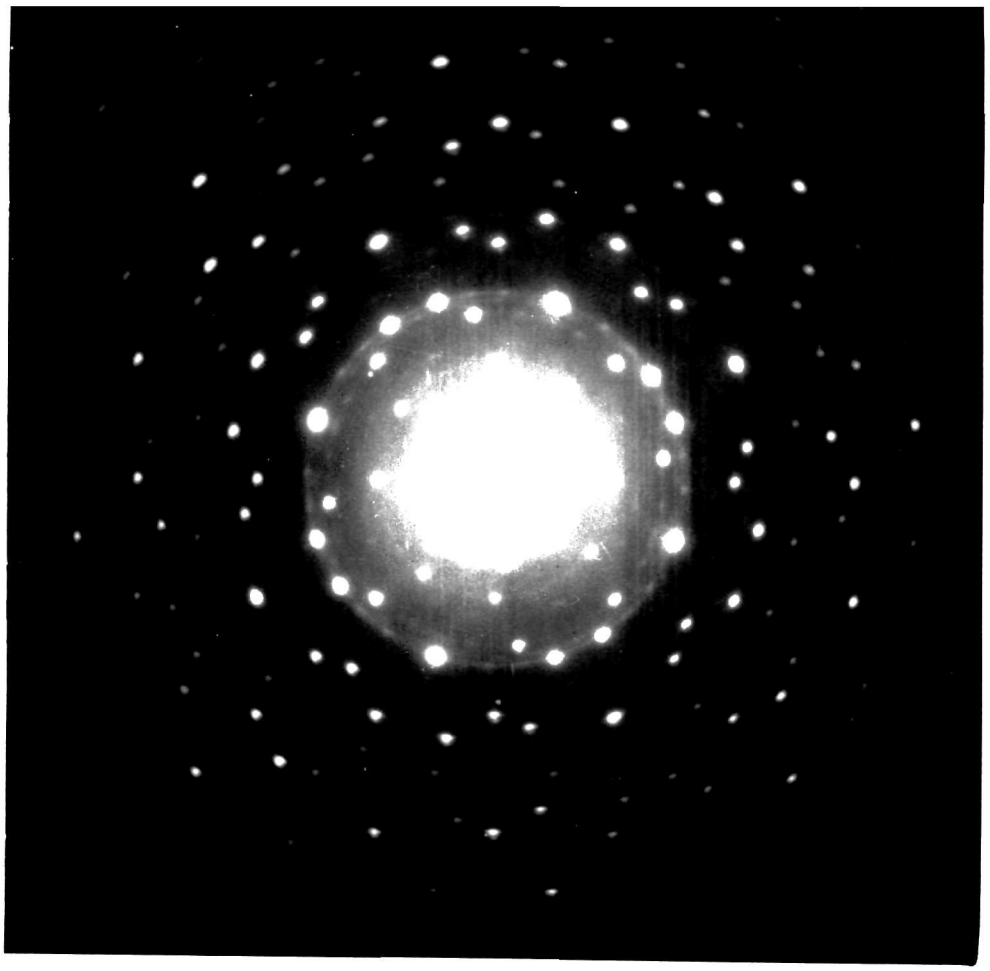

Fig. 77. Transmission pattern for Tl_2Se deposits on (100) NaCl at ~200°C.

T A B L E - XI

Analysis of the pattern (fig.77)

d Å	hkl	a_o Å
6.02	110	8.51
4.27	200	8.54
3.01	220	8.51
2.70	310	8.54
2.13	400	8.52
2.01	330	8.51
1.91	420	8.55
1.67	510	8.51
1.50	440	8.50
1.46	530	8.51
1.42	600	8.52
1.35	620	8.54
	Mean a_o =	8.52 Å

(2) On rocksalt surfaces

On (100) face of rocksalt

Deposits of Tl_2Se on the cleavage face of a rocksalt crystal at substrate temperature below 150°C yielded patterns similar to those obtained on collodion films. Deposits formed at the substrate temperature range between 200°-250°C yielded patterns (fig.76) by reflection when the electron beam was grazing along the cube-edge direction of the rocksalt crystal. This pattern consisted of reflections which were arranged in a rectangular network with their sides in the ratio of 1:1.41. On an azimuthal rotation of the beam direction the pattern changed considerably whilst the row of reflections in the plane of incidence remained unchanged. The symmetrical patterns consisted of reflections 001 and its higher orders in the plane of incidence, while 001, $1\bar{1}1$, $1\bar{1}0$ and 000 at the corners of the rectangle. The above facts suggest that Tl_2Se crystallites developed 2-d $\{001\}$ orientation on the cleavage face of rocksalt. There were a few extra spots in the pattern which could not be accounted for easily.

The same film when examined by the transmission method yielded interesting but apparently complicated patterns (fig.77) Table-XI shows the analysis of the pattern. The innermost reflection consisting of eight spots was due to 110 reflection

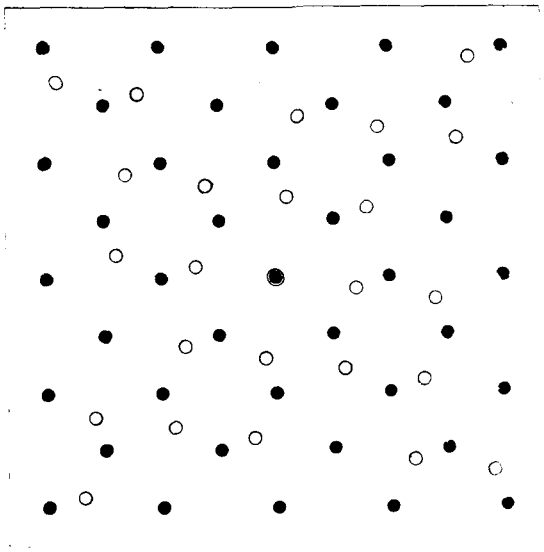

Fig. 78. Theoretical pattern for fig. 77

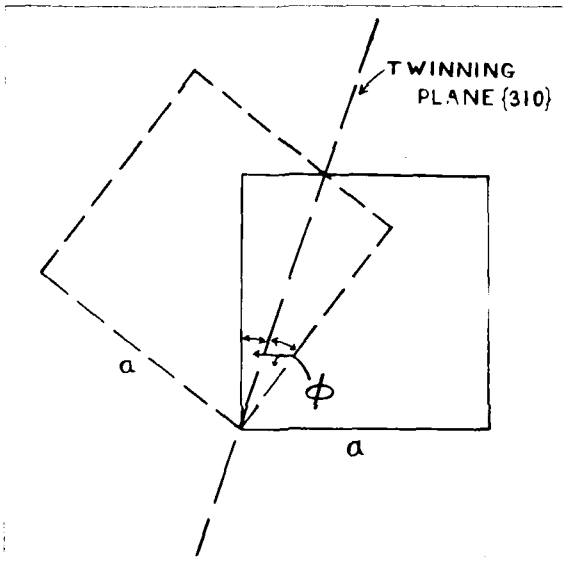

Fig. 80. Twinning of crystals on {310} plane.

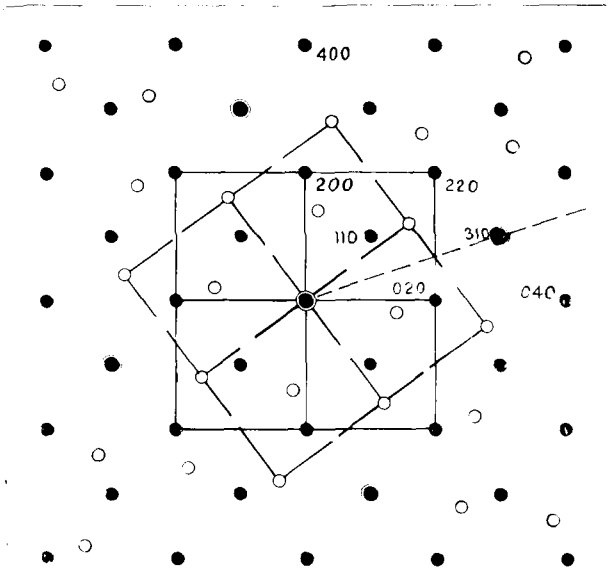

Fig. 79. Indexed pattern of fig 77 & 78.

of the tetragonal lattice of Tl_2Se. Though the patterns appeared to be very complex a closer examination of these patterns revealed that all the reflections were due to two types of centred square networks of patterns mutually rotated by about 37°. These square-nets of patterns are shown by filled and unfilled spots in the fig.78 and correspond exactly with all the reflections observed in the diffraction patterns. The indexed diagram is shown in fig.79. It can be seen that four spots on 310 reflection are more intense than the rest of the spots lying over the same ring. This increase of intensity of some spots suggests that they were due to the superimposition of reflections from the two mutually rotated patterns about the undeflected beam. These are shown in the diagram with centred filled circles. It may here be pointed out that even after repeated evaporations exactly similar patterns with the same angle of rotation was observed in all the cases without fail. This constant angle of rotation could neither be due to any minor variation of the evaporation condition nor it could be due to any arbitrary rotation as was observed in the case of evaporated films of tin sulphide (-ous) (Badachhape and Goswami, 1964). Such a fixed rotation of one pattern with respect to the other seems to be due to the growth of twinned crystallites of Tl_2Se. According to Dana a lattice is twinned when 'one or more parts, regularly arranged, are in reverse position with reference to the other part or parts'

This means that the twinned and untwinned parts of a crystal are mirror reflections of each other in a certain plane of the crystal. The plane of reflection is called as twinning plane. This has already been discussed in chapter-III (D).

In the present case of the transmission patterns the reflections observed were all *hko* type for both the twinned and untwinned crystals when the original crystal has 001 orientation. The appearance of reflections arising both from the twinned and untwinned crystallites when the beam was along $\langle 001 \rangle$ direction suggested that the twinning plane was $\{hko\}$ type. It can be mentioned here that the reflections due to twinned structure of f.c.c. crystallites with $\{111\}$ as twinning plane can only be observed when the beam direction is $\langle 110 \rangle$, which is one of the important axis lying on $\{111\}$ plane. Thus for hko twinning plane for tetragonal structure when the beam is grazing along $\langle 001 \rangle$ the reflections due to twinned and untwinned crystallites will appear simultaneously.

An examination of the patterns shows that one pattern becomes mirror image of the other when reflected about a plane along $\langle 310 \rangle$ and perpendicular to the plane of the paper. It is also seen that if the original pattern i.e. the centred square network is rotated about an axis joining 310 reflection and the undeflected spot (shown by broken line in the fig.79) by 180° the other pattern is obtained.

All these suggest that the twinning plane was $\{310\}$. It is possible to calculate the angle between the twinned plane and the original plane from the relation

$$\cos\phi = \frac{Hh + Kk + a^2/c^2 \cdot L\ell}{(H^2 + K^2 + a^2/c^2 \cdot L^2)^{\frac{1}{2}} \cdot (h^2 + k^2 + a^2/c^2 \cdot \ell^2)^{\frac{1}{2}}}$$

where ϕ is the angle between the planes hkl (original) and HKL (twinning plane), 'a' and 'c' being the lattice parameters for the tetragonal system. Taking the initial plane $\{100\}$ and the twinning plane $\{310\}$ the angle ϕ is calculated and found to be $18^{\circ}28'$. Fig.80 shows the twinned and untwinned crystals, the twinning plane being perpendicular to the plane of the figure. The reflections from such crystals will be given by the corners of the squares, since the beam direction is perpendicular to the plane of the diagram. Thus the angle between the observed reflections will be $2\phi = 36^{\circ}56'$ which is very close to the observed angle of rotation of the two patterns.

In the case of tetragonal crystals the usual twinning planes are of $\{110\}$ (Dana and Dana, 1951), $\{301\}$ and $\{101\}$ type (Hall, 1954). The above results and discussions show that in the case of Tl_2Se which has a tetragonal structure the observed twinning plane for evaporated films was of $\{310\}$ type. This is the first time when such a twinning plane has been observed for Tl_2Se and in fact for any tetragonal structure.

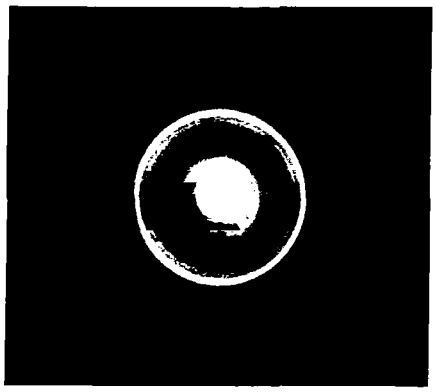

Fig. 81. Tl_2Te on collodion film deposited at ~ 100°C.

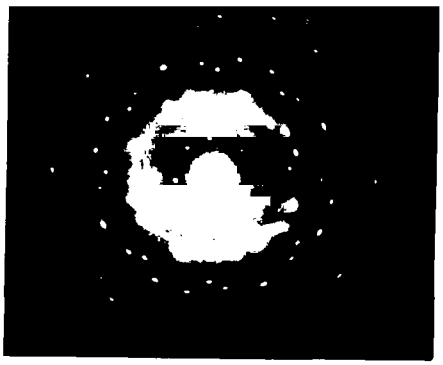

Fig. 82. 2-d {001} orientation of Tl_2Te rotated by ~ 37° deposited on (100) NaCl at ~ 200°C.

TABLE - XII

Analysis of the pattern (fig.82)

d Å	hko	a Å
6.29	110	8.90
4.44	200	8.88
3.15	220	8.90
2.81	310	8.88
2.22	400	8.88
2.10	330	8.90
1.99	420	8.88
1.74	510	8.87
1.54	440	8.89
1.53	530	8.90
1.48	600	8.88
1.40	620	8.88

Mean a = 8.88 Å

T A B L E - XIII

Analysis of the pattern (fig.81)

I/I_o	d Å	hkl
m	6.29	110
w	4.43	200
w	3.81	211
m	3.14	220
s	2.89	301
s	2.81	310
m	2.585	312
w	2.43	321
m	2.22	400
m	2.09	106
m	1.99	403
m	1.90	422
w	1.84	-
w	1.75	510
m	1.68	512

$a = 8.88$ Å, $c = 13.20$ Å

s - strong
m - medium
w - weak

On (110) & (111) faces of rocksalt

Tl_2Se deposited on rocksalt (110) and (111) faces within substrate temperatures ranging from room temperature to about 250°C yielded always polycrystalline patterns similar to those obtained for deposits on (100) face of rocksalt.

(b) Thallium telluride (Tl_2Te) deposits

(1) On collodion support

Deposits of thallium telluride (Tl_2Te) on neutral collodion supports in vacuo within the substrate temperature ranging from room temperature to about 150°C yielded polycrystalline patterns as shown in fig.81. On rotation of the specimen about an axis perpendicular to the beam direction neither the intensity of the individual rings changed nor the rings broke into arcs showing thereby that Tl_2Te crystallites were randomly disposed over collodion support. As there are no data available so far about the lattice parameters of Tl_2Te the identification of the reflections has been carried out by the method discussed below using both single crystal and polycrystalline patterns.

(2) On (100) face of rocksalt

Tl_2Te deposits on cleavage face of rocksalt within the temperature range from room temperature to about 150°C

yielded polycrystalline deposits similar to that obtained for deposits on collodion films. When the deposition was carried out at substrate temperature about 200°-250°C and the films examined by transmission method yielded patterns (fig.82) similar to those obtained for the compound Tl_2Se. These patterns also consisted of spots arranged in circles which appear to be due to two types of centred square type of patterns mutually rotated about the undeflected spot by about 37° as observed in the case of Tl_2Se. These patterns were also indexed in a similar way as was done for Tl_2Se assuming a similar sort of structure for Tl_2Te. Table-XII shows the analysis of the pattern from which the parameter a_o is calculated. Since Se and Te belong to the same group of the periodic table it is reasonable to assume that the chemical bond of Tl_2Se and Tl_2Te will also be of similar nature and hence the structure should be also of similar type. This consideration though reasonable may not always be correct as in many compounds formed by elements belonging to the same group of the periodic table may have different structures. The single crystal patterns from both Tl_2Se and Tl_2Te, however, show similar dispositions and can therefore be presumed to belong to the same crystal class. The a_o was calculated from the spot pattern assuming the beam direction to be $\langle 001 \rangle$ by comparing the $(11\bar{2}0)$ of graphite reflection and found to be equal to 8.88 Å. Since

the third parameter c cannot appear in the transmission pattern for 2-d $\{001\}$ oriented crystallites to determine its value, the reflections from the polycrystalline samples were compared with the tetragonal chart with varying c/a value. It was found that for c/a $\fallingdotseq$ 1.45 almost all the lines from polycrystalline patterns correspond very well with positions of the reflection in the chart. All the reflections were then given provisional indices and c was calculated for the observed hkl reflections using the formula,

$$\frac{1}{d^2_{hkl}} = \frac{(h^2+k^2)}{a^2} + \frac{l^2}{c^2}$$

The average value of c calculated from 211, 301 and 312 reflections was found to be ~ 13.20 Å. Assuming the lattice parameters as correct, the different d_{hkl} values are calculated and found to be in good agreement with the observed values. Table-XIII shows the analysis of the polycrystalline pattern.

It may be mentioned here that compared to Tl_2Se the lattice parameters of Tl_2Te are slightly larger. This can also be understood easily from the consideration of ionic radii of the elements. The ionic radii for the elements Se^{2-}, Te^{2-} and Tl are 1.98 Å, 2.21 Å and 1.44 Å respectively.

Since ionic radii of Te is larger than Se and since the structure of Tl_2Te and Tl_2Se are of similar type, the lattice parameters of Tl_2Te will also be larger than Tl_2Se. It may be mentioned here that the number of reflections observed for Tl_2Te was not enough and hence it was not possible to determine its space group.

--

C H A P T E R - VI

STRUCTURE AND CRYSTAL GROWTH OF INDIUM ANTIMONIDE

A. INTRODUCTION

In recent years especially after the last war search for newer materials with better and desirable semiconducting properties has been going on. It has soon been found that many alloys and intermetallic compounds especially of indium and antimony could be potential sources for semiconducting materials. Studies on indium antimonide have shown promising results. In the last decade various techniques were used to prepare InSb films particularly on glass substrates. Most of the workers used their own techniques of preparation of the films and different results were reported for their electrical properties etc.

X-ray powder patterns were taken for the compound prepared by heating stoichiometric proportions of the elements (Gorjunova and Fedorova, 1955). This showed the zinc-blende type of structure with lattice parameter $a_o = 6.465 \pm 0.003$ Å. An electron diffraction study on sublimated layers showed ZnS type of structure with $a_o = 6.465$ Å (Konozenko and Mikhnovs'kyĭ, 1956). Kurov (1957) showed by experiments of

his own and from the patterns obtained by Konozenko and Mikhnovs'kyi that the latter authors were dealing with the films of antimony only though InSb was used for evaporation. Kurov pointed out that InSb films could be obtained by the simultaneous evaporation of both the elements. Haasen (1957) studied the crystallography of growth twins in InSb single crystals. It was observed that the twin orientations were related by 60° rotation about $\langle 111 \rangle$ and the boundary plane was $\{111\}$. Semiletov and Rozsibal (1957) discovered a hexagonal structure other than the previously known ZnS type. The lattice parameter of the ZnS type was 6.46 Å and the corresponding hexagonal (C.P.) were a_H = 4.56 Å, c_H = 7.46 Å. Paparditis (1957) prepared InSb films over glass and mica substrates by evaporating the compound in vacuum and electrical properties were measured for the annealed films. Photoconducting properties of InSb detectors were described by Avery et al. (1957). A pure single crystal slice was used in a magnetic field of 10,000 Gauss and studied its infrared sensitivity.

By electron optical investigation on InSb films evaporated at different substrate temperatures it was found that at about 400°C substrate temperature reasonably large crystals were developed (Reimer, 1958). Kurov and Pinsker (1958) studied the layers of In-Sb of changing composition. An electron diffraction study showed the presence of amorphous Sb at the one end, hexagonal and cubic InSb at the centre and metallic In at the other end. Electrical properties of

InSb films, prepared by vacuum deposition were measured by Gunther (1958), Kurov and Pinsker (1958). Current-voltage characteristics of n-and p-type InSb single crystals at 90° and 78°K were reported by Kanai (1958 a,b). Rodot (1958) reviewed the semiconducting properties, the theory of thermoelectric and thermomagnetic effects for InSb and the experimental results were presented.

The preparation of barrier layer photovoltaic cells was discussed by Galavanov and Erokhina (1959). The theory of operation and construction of infrared detector, based on photoelectromagnetic effect of InSb was reported by Kurse (1959). Electrical conductivity and Hall coefficient were measured by Putley (1959) for InSb between 2°K and 300°K.

Literatures on the preparation of InSb, optical, electrical and photo effects and its applications were reviewed by Moss (1960). Large area self-supporting films (10 μ thickness) of InSb were prepared by sudden squashing of a drop of molten InSb between two optical flats and their optical and electrical properties were measured (Bate and Taylor, 1960).

Thermal and electrical properties for single crystal InSb between 195° and 715°K were reported by Busch and Steigmeier (1961). The design, fabrication and electrical characteristics of an n-p-n InSb transistor which operates

at 77°K was discussed by Henneke (1961). The spectral dependence of transmission and the possibility of use of InSb as optical media was discussed by Belashov and Belashova (1961).

Substrate temperature effect for sputtered InSb films were observed by Monlton (1962). Dale and Senecal (1962) found by electron diffraction that when flash evaporated films were annealed at 130°C no free In or Sb existed in InSb films. X-ray investigation was made for the lattice parameter for different compositions of In and Sb other than stoichiometric composition. It was found that a_o for stoichiometric composition as 6.47965 Å, while for 50% excess of Sb and In as 6.47961 Å and 6.47962 Å respectively (Ozolinsh et al. 1963). Agalarzade and Semiletov (1963) prepared InSb films by flash evaporation, electron diffraction showed both cubic and hexagonal crystallites. A b.c. tetragonal structure with $a = 5.79 \pm 0.05$ Å and $c = 3.11 \pm 0.05$ Å was discovered at room temperature under 23 Kilobars of pressure (Banus et al. 1963). Flash evaporated InSb films on Ge, GaAs and CaF_2 single crystals were studied by Richards, Hart and Gallone (1963). It was observed that within 250°-300°C substrate temperature twinned films and within 300°-400°C single crystal films growth took place. Over 400°C Sb evaporates leaving In on the surface. X-ray powder pattern for 70 wt. % in In-Sb showed a simple cubic lattice with $a_o = 3.05$ Å which was a

metastable phase. High pressure phase of InSb was confirmed which had a tetragonal white tin structure with lattice $a_o = 5.92$ Å, $c_o = 3.06$ Å (Smith and Martin, 1963).

Well oriented InSb films were grown on mica at substrate temperature about 340°C. Electrical properties were measured as a function of temperature for these films (Juhasz and Anderson, 1964). Temperature dependence of photoconductivity of InSb films between 100°-350°K (Kasyan, 1964) and electrical properties of n-type InSb at 77° and 20°K temperatures in high electric fields were studied (Bok and Guthmann, 1964). Kasper and Brandhorst (1964) discovered in the vicinity of ~ 30 Kilobars pressure an orthorhombic structure of InSb other than β-Sn type.

Various electrical measurements on InSb, either in bulk or thin film form at different temperatures were reported (Buchsbaum et al., 1965; Shalyt and Tamarin, 1965; Bausch et al., 1965; Ferry et al., 1965). A method of measuring weak magnetic field using magnetoresistance effect on InSb was described by von Broke, Martens and Weiss (1965). Straumanis and Kim (1965) redetermined the lattice parameter of InSb prepared from 99.999% pure elements and found to be $a_o = 6.47937 \pm 0.00003$ Å at 25°C including refraction correction. Experimental density determined as 5.7747 ± 0.0004 gm/cm^3 and the expansion coefficient as $5.37 \pm 0.50 \times 10^{-6}$ °C^{-1}. Actual number of molecule per unit cell was very close to 4.0000 indicating the structure of InSb to be perfect.

A method of the preparation of InSb films and the effect of annealing on electrical properties were described by Williamson (1966). A strong resistance anomaly and negative magneto resistance between 0.1 and 4.2°K were observed in n-type InSb by Katayama and Tanaka (1966). Vodopyanov and Kurdiani (1966) irradiated InSb by neutrons at 77°K and found that a change of conductivity type occur for p-type materials, while for n-type samples only change in the magnitude of their conductivity was observed. Baev (1966) observed negative resistance and the associated generation of oscillations at point contacts in p-type InSb.

From the above survey of literature it is seen that though much work has already been done on electrical properties and the way of preparation of InSb films whilst the study of the growth process of the films on single crystal as well as neutral faces is lacking. A systematic study on the growth process of InSb on different faces of rocksalt crystals, mica and neutral surfaces has been undertaken with a view to know more about the crystal growth process from vapour phase with substrate temperature.

L. EXPERIMENTAL

Preparation of InSb

InSb was prepared by taking stoichiometric proportions (1:1 atomic proportion) of the elements indium (99.99%) and

antimony (99.9%) in a silica tube which was then sealed in vacuum ($\sim 10^{-5}$ mm of Hg.). The silica tube was then inserted in an electric furnace and heated from room temperature to about 200°C so that indium would melt (m.p. of indium = 155°C) and slow reaction would proceed. The tube was kept at this temperature for about two hours and then the temperature of the furnace was raised slowly step by step (about 100°C per hour) to about 650°C (m.p. of Sb = 630°C). The furnace was kept at this temperature for about two hours and finally it was raised to 700°C and kept overnight at this temperature. The temperature of the furnace was then lowered down to 400°C and the silica tube was put into cold water suddenly. InSb thus prepared had a bright shining appearance.

X-ray powder pattern (fig.83) taken with Mo target consisted of reflections due to InSb. However, a few extra reflections were also observed.

InSb was deposited by evaporating a piece of compound in vacuo on different faces of rocksalt, mica glass and collodion as described in chapter-II. It was, however, noticed that in the first evaporation the patterns observed were due to antimony only. During successive evaporations amount of antimony was reduced and the films showed reflections characteristic of InSb + Sb. When evaporation was carried out at higher substrate temperature about 200°C and above, the deposits except for the first one or two evaporations consisted entirely of InSb.

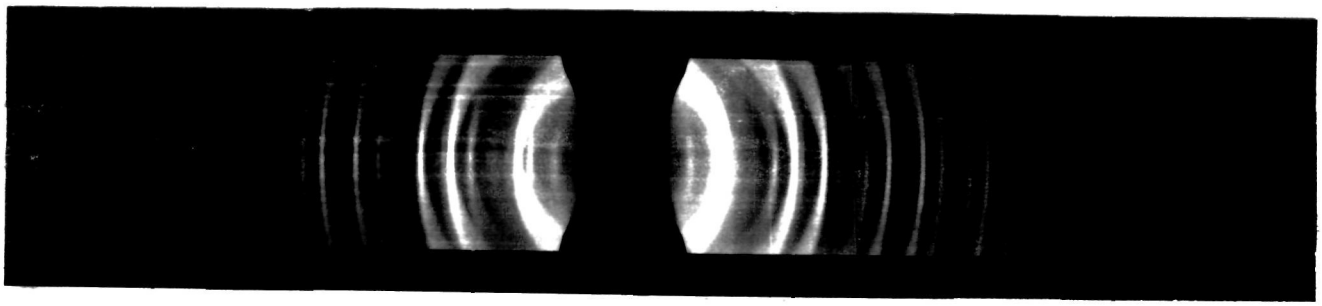

Fig. 83. X-ray powder pattern of InSb.

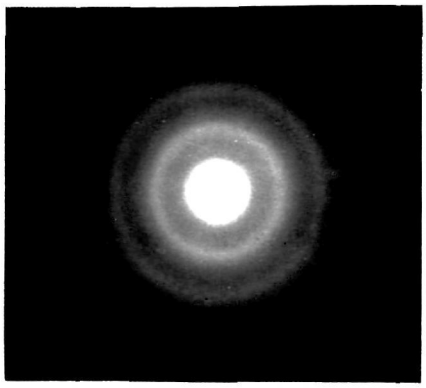

Fig. 84. InSb on collodion film at ~ 100°C.

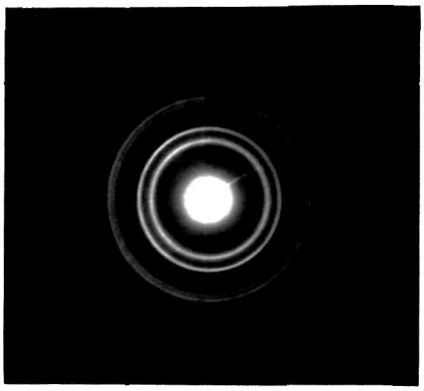

Fig. 85. same as fig. 84. but deposited at ~ 150°C.

C. RESULTS

Indium antimonide deposits

(1) On collodion support

The films obtained on collodion supports at room temperature showed patterns due to crystalline antimony only. Successive evaporations were carried out from the same piece of the compound but no crystalline InSb film was obtained even on annealing at $\sim 100^{\circ}C$ in vacuo. When the evaporations were carried out at $100^{\circ}C$ substrate temperature halo type of patterns (fig.84) was obtained.

At $\sim 150^{\circ}C$ substrate temperature ring patterns due to crystalline InSb+Sb were obtained (fig.85). The intensity of the reflections did not change due to the tiltation of the specimen about an axis perpendicular to the beam direction showing that the deposits were due to randomly disposed crystallites of InSb.

(2) On glass substrate

Deposition of indium antimonide on glass surface did not yield any clear pattern up to about $300^{\circ}C$. At substrate temperature $\sim 350^{\circ}C$ weak patterns due to f.c.c. type of crystallites were observed. It was noticed that the reflections did not change with the change of beam direction and were always of continuous nature suggesting the deposit of InSb to be polycrystalline.

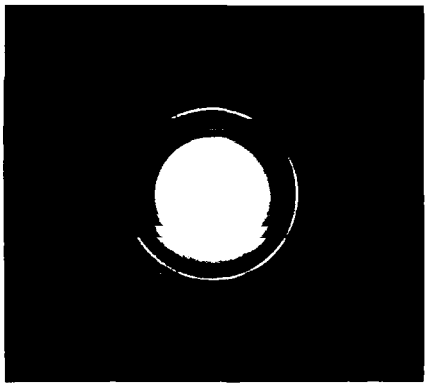

Fig. 86. In Sb on (100) NaCl deposited at ~ 200°c.

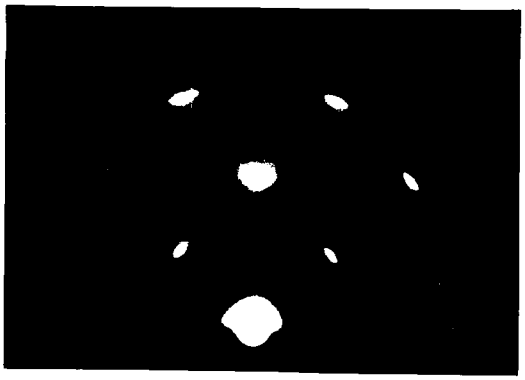

Fig. 87. 2-d {100} orientation of In Sb on NaCl (100) at 300°c Beam along <100> of NaCl

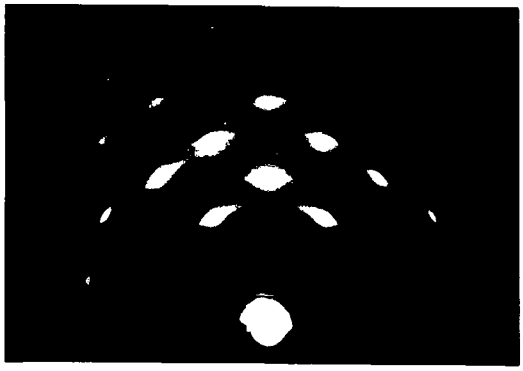

Fig. 88. Same as fig. 87. but beam along <110> of NaCl

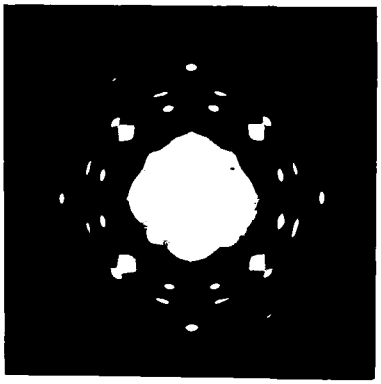

Fig. 89. Transmission pattern from the same film as fig. 87, 88.

TABLE - XIV 14

Analysis of the pattern (fig.86)

I/I_o	d Å	hkl (cubic)	hk.l (hex.)
vs	3.72	111	00.2
w	3.11	-	-
w	2.83	-	-
s	2.28	220	11.0
w	2.17	-	10.3
s	1.95	311	-
vvw	1.87	222	00.4
vw	1.62	400	-
w	1.48	331	21.1
w	1.32	422	-
w	1.25	511, 333	00.6
vvw	1.14	440	22.0
w	1.09	531	-

$a_{cubic} = 6.47$ Å; $a_H = 4.57$ Å

$c_H = 7.47$ Å

vs - very strong
s - strong
w - weak
vw - very weak
vvw - very very weak

(3) On rocksalt surfaces

On (100) face of rocksalt

Indium antimonide deposited on the rocksalt cleavage face at about 100°C substrate temperature showed halo type of patterns. Deposits at 200°C substrate temperature showed ring patterns (fig.86). An analysis of the pattern is given in table-XIV. The ring patterns which conformed to f.c.c. structure showed 111 reflection to be strongest whilst 200 reflection was practically absent, 220 and 311 reflections were of medium intensity. The general intensity distribution for different hkl reflections confirms the zinc-blende type of structure of InSb. A few extra reflections were present in the pattern, namely the two weak rings in between 111 and 220 reflections due to free antimony in the deposits. From the table it will be seen that along with the cubic phase of InSb the hexagonal phase of the compound was also present. By tilting the film about an axis perpendicular to the beam, it was noticed that there was neither any change of intensity of the individual ring nor the rings broke into arcs. This suggests that the deposit crystals did not develop any preferred orientation.

At substrate temperature $\sim$ 300°C during the second and third evaporations from the same piece of InSb, the deposits yielded patterns (fig.87) by reflection which were

predominantly due to the presence of cubic crystallites. For this pattern the beam direction was $\langle 100 \rangle$ of the rock-salt crystal. The pattern consisted of reflections forming centred square network. It is seen that 400, 800 etc. reflections were in the plane of incidence. The centred square was formed by 000, 400, 440 and 040 reflections at the corners with 220 reflection at the centre. When the beam direction was changed to $\langle 110 \rangle$ direction of the rocksalt crystal the patterns shown in fig.88 were obtained. It is noticed that the 200 reflection which was very weak in the previous case became prominent and the disposition of spots with 000, 200, 222 and 022 at the corners from a centred rectangular array, the sides being in the ratio of $1 : \sqrt{2}$ with 111 reflection at the centre. This clearly suggests that InSb developed 2-d $\{100\}$ orientation of the cubic phase as discussed in details in the chapter-III. Thus InSb grew epitaxially with parallel orientation on (100) faces of rocksalt crystal. The transmission pattern (fig.89) for the same film is quite interesting. This pattern mainly consisted of rings and sharp spots. The spots were joined by streaks which were due to either stacking fault of the crystallites or due to the curvature of the film caused by placing it on the wire gauge support. This pattern is due to the presence of both the f.c.c. and hexagonal phases, but with different orientations. Here 000, 022, 040 and $02\bar{2}$ reflections formed a square network which clearly indicates

the development of 2-d $\{100\}$ orientation confirming 2-d $\{100\}$ orientation observed by the reflection method. There were twelve equidistant spots lying on the innermost ring, no doubt, due to 10.0 reflection of the hexagonal phase of InSb. The appearance of 12 equidistant spots on 10.0, 11.0 and 20.0 reflections suggest the development of 2-d $\{00.1\}$ orientation of the hexagonalphase rotated by 30° as was discussed in the case of HgSe and HgTe films. Further 12 spots lying on 111 reflection of the cubic phase very close to 10.0 reflection and also equal number on 220 and 311 reflections showed that f.c.c. crystallites developed 2-d $\{211\}$ orientation. The spots, twelve in number, on 111 reflection were not equidistant suggesting that 2-d $\{211\}$ orientation was rotated by 90°.

It is further interesting to note that all the 12 spots over 220 reflection of cubic or 11.0 of hexagonal phase were not of equal intensity. Four out of the twelve spots were stronger than the rest. This increase of intensity of four spots can be explained as due to the rotation of 2-d $\{100\}$ orientation of the cubic form by 30°, 2-d $\{00.1\}$ orientation of hexagonal phase by 30° and 2-d $\{211\}$ orientation by 90°. When all the orientations were superimposed it would be found that the superimposition of the reflections would be only on the four spots of 220 of the cubic or 11.0 of the hexagonal modification. This explains why four out of 12 spots on 220 or 11.0 reflection were stronger.

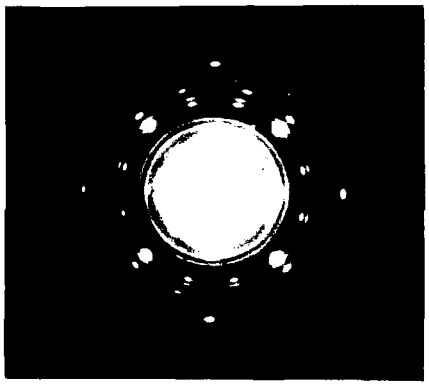

Fig. 90. InSb on (100) NaCl deposited at ~ 350°C.

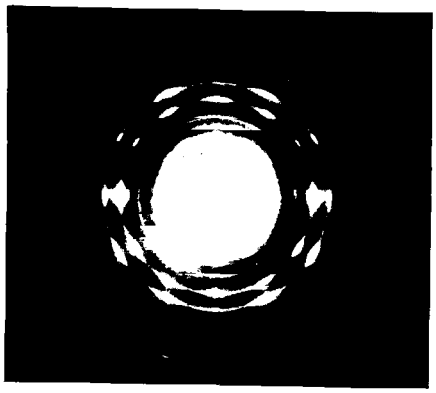

Fig. 91. InSb on (110) NaCl deposited at ~ 300°C

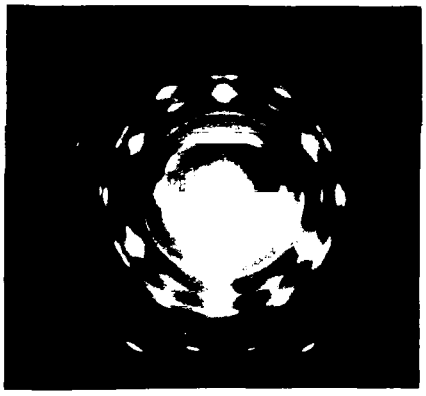

Fig. 92. InSb on (111) NaCl deposited at ~ 300°C.

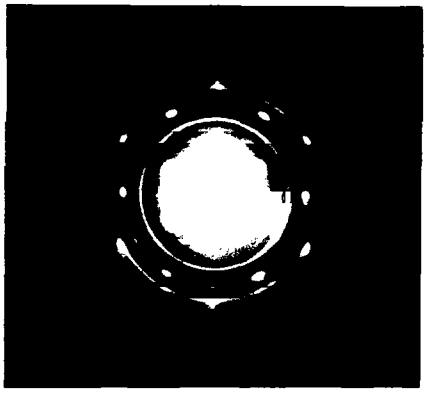

Fig. 93. Same as fig 92. but deposited at ~ 350°C.

Deposits formed at 350°C substrate temperature showed similar patterns. Occasionally films obtained from a fresh piece of InSb showed antimony reflections as shown in fig.90.

On (110) face of rocksalt

InSb deposits on the rocksalt (110) face yielded polycrystalline patterns up to a substrate temperature about 250°C. Deposits at substrate temperature about 300°C did not yield clear pattern when examined by reflection. The transmission patterns (fig.91) from these films consisted of rings as well as spots. There were 12 spots on 111 reflection of the cubic phase which along with equal number of spots on 220 and 311 formed a rectangular array. Such an arrangement of reflection can arise only when the beam direction for the crystallites is $\langle 211 \rangle$. Thus 2-d $\{211\}$ orientation developed on (110) face of rocksalt which is rotated by 30°. Further, it can be seen that the appearance of 400 and its higher orders cannot be accounted for with the above orientation only. These reflections would appear only when the InSb crystallites developed another orientation, namely 2-d $\{100\}$. Thus InSb developed 2-d $\{211\}$ orientation rotated by 30° 2-d $\{100\}$ orientation. The ring in between 111 and 220 reflection is due to antimony.

On (111) face of rocksalt

Indium antimonide deposited on (111) face of rocksalt showed no clear pattern when examined by the reflection method.

Up to substrate temperature about 250°C the patterns observed by the transmission method consisted of rings due to both cubic and hexagonal forms of InSb. 2-d oriented patterns (fig.92) were obtained when evaporations were carried out at substrate temperature about 300°C. The 111 reflection comprised of 12 equidistant spots, out of which 6 were strong. The strong spots were connected by fine streaks with six strong spots of 220. It can be seen that 111, 311 and 220 reflections along with undeflected spot formed a rectangular array as mentioned in the case of deposits on (110) face of rocksalt. This is due to 2-d $\{211\}$ orientation. The appearance of six weak spots was due to the fact that some of the crystallites developing 2-d $\{211\}$ orientation were rotated by 30°. When the deposition was carried out at substrate temperature about 350°C the patterns (fig.93) became more distinct. Strong six spots over 111 reflection along with 220, 311 etc. formed rectangular array similar to that discussed before. This very clearly showed the development of 2-d $\{211\}$ orientation of InSb crystallites These two patterns at the first sight appear to be due to hexagonal type of crystallites. In the case of 2-d $\{00.1\}$ orientation, the innermost spot will be 10.0 reflection and double of its ring radius will correspond to 20.0 of hexagonal or 311 of the cubic phase. In the present case if the ring radius of the innermost reflection is doubled it coincides exactly with 222 of cubic phase instead of 311. Thus it is

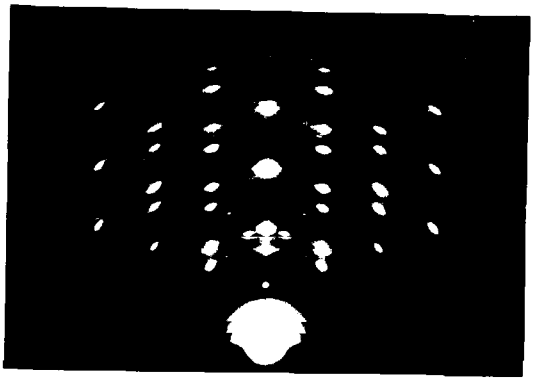

Fig. 94. 2-d {111} + {115} orientation of InSb on cleavage face of mica deposited at 350°C

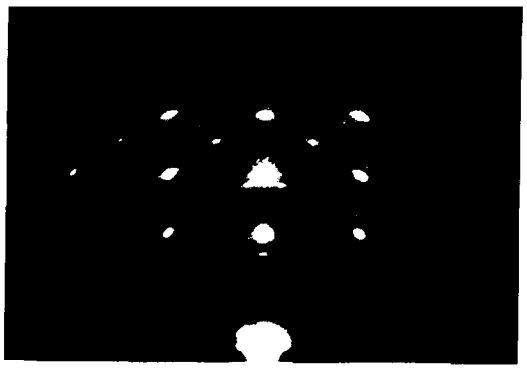

Fig. 95. same as above but the specimen rotated by 30° w.r.t. beam direction of fig. 94.

confirmed that the crystallites developed 2-d $\{211\}$ orientation which only allows 111 reflection and its higher orders to appear. These considerations have already been discussed in details in the cases of HgSe and HgTe films. The additional rings in the pattern (fig.93) are due to antimony.

(4) On cleavage face of mica

Deposits of InSb on cleavage face of mica up to about 300°C substrate temperature yielded very poor patterns. At about 350°C substrate temperature oriented overgrowth on mica substrate was observed. These patterns (figs.94,95) are very similar to the patterns obtained for HgSe over mica substrate at $\sim$ 150°C. The patterns (fig.94) consisted of 111 reflection and its higher orders in the plane of incidence and its nature changed to fig.95, on changing the beam direction by 30° with respect to the position for the previous pattern. This suggests the development of normal and anti 2-d $\{111\}$ orientation. Along with the reflections forming rectangles with sides in the ratio of $\sqrt{3} : \sqrt{24}$ and $\sqrt{3} : \sqrt{8}$ the other symmetrical reflections also appeared which were due to $\{111\}$ twinning as discussed in the case of HgSe deposits on mica at $\sim$ 150°C. Further there were weak reflections of 220 and its higher orders in the plane of incidence suggesting the development of weak 2-d $\{110\}$ orientation. Thus it can be concluded that InSb deposited on the mica cleavage face at substrate temperature $\sim$ 350°C grew epitaxially with a mixture

of normal and anti 2-d $\{111\}$, 2-d $\{115\}$ due to twinning on $\{111\}$ and 2-d $\{110\}$ orientations of the cubic phase.

D. DISCUSSION

It is well-known that indium antimonide has zinc-blende type of structure with lattice parameter equal to 6.4796 Å. The compound prepared in this laboratory by heating pure indium and antimony in vacuo in stoichiometric proportions was examined by X-ray powder method. It was found that the compound formed has got zinc-blende type of structure.

On collodion support at higher temperature a mixture of InSb + Sb was obtained whilst up to about 100°C halo type of pattern was observed. This halo pattern might be due to amorphous antimony.

At substrate temperature 300°-400°C, 2-d $\{100\}$ orientation was observed by reflection method whilst by transmission 2-d $\{100\}$ + 2-d $\{211\}$ + 2-d $\{00.1\}_H$ rotated by 30° were observed. The observation of these orientations was, no doubt, due to the growth faults associated with the crystal growth process as discussed in the case of HgSe and HgTe deposits.

In the case of the deposits on (110) face of rocksalt 2-d $\{110\}$+$\{100\}$ along with $\{211\}$ orientations were observed.

For the deposits on (111) face of rocksalt 2-d $\{211\}$ orientation rotated by 60° was often observed, while in some cases rotation by 30° was also observed. These sorts of orientations and their developments were similar to those discussed in the case of HgSe and HgTe deposits.

Deposits on mica also showed similar orientation namely 2-d $\{111\}$ orientation along with 2-d $\{115\}$, no doubt, due to twinning on $\{111\}$ face.

The lattice misfit is calculated for $\langle 100 \rangle$ direction of the NaCl substrate and found to be 13.8 %. It is seen that even with that misfits the deposits grew epitaxially at appropriate substrate temperature. Further the phase transition from cubic to hexagonal (C.P.) was analogus to that observed in the case of HgSe and HgTe. It may be emphasised here that even though in the bulk form there was no hexagonal modification the deposits obtained from vapour phase often consisted of the hexagonal phase (a_H = 4.57 Å, c_H = 7.47 Å) along with the cubic form, no doubt, due to the fault developed during the crystal growth process.

--

SUMMARY AND CONCLUSIONS

The present systematic electron diffraction study on vacuum deposited films of selenides and tellurides of Hg, In, Tl and also of InSb on different substrates such as amorphous collodion and glass and single crystal rocksalt faces viz. (100), (110) and (111) faces and the cleavage face of mica i.e. (0001) face has thrown some new light on the crystal growth process, phase transition, development of twinning, change of orientations etc. and these features may account for some of the peculiar electrical and optical properties of thin films.

The results of our studies on vapour phase deposits of all the compounds and alloys on different substrates even when the lattice fits between them are widely different show that the crystal growth process was very much similar in all the cases. The deposit films at the initial stage grew epitaxially on single crystal substrates and at higher substrate temperature the thickness of epitaxial layer was considerable. At room temperature however only a very thin layer of deposits on active substrates was epitaxial. Higher substrate temperature was favourable for the epitaxial growth as mentioned before. Because of the non-ideal condition of deposition

the growth fault increased with the increase of film thickness, thus resulting in defects such as dislocations, twinning, disorientations etc. in the deposits. Such surface layers would progressively hinder the epitaxial growth conforming to the initial substrate surface structure. A stage would ultimately be reached when the incoming deposit-atoms would be completely unaffected by the underneath surface layers thus leading to polycrystalline films. Thickness of the epitaxial layer before the deposits became polycrystalline would be determined both by substrate temperature as well as by the degree of misfit between the deposit-crystal and substrate surface. With the further increase of thickness of the films the deposit (polycrystalline) would tend to develop a preferred orientation entirely determined by the deposition conditions such as rate of evaporation, temperature of the substrate etc., but unaffected by the nature of the substrate. Thus whether the substrates were active (single crystal) or passive (glass and collodion) the development of one degree orientation characteristics of the final stage of growth was the same. With the above picture in view it is possible to explain most of the results obtained in the present investigation.

The results of the above study on evaporated films of selenide and telluride of mercury showed that the films

grew epitaxially on rocksalt (100), (110) and (111) faces and mica (0001) face, at substrate temperature of 80°-150°C whilst at room temperature the majority of the crystallites was randomly disposed. The observation of normal and anti 2-d $\{111\}$ orientation by reflection and 2-d $\{100\}$ $\{211\}$ $\{0001\}_H$ by transmission from the same film suggested that the deposit initially grew with parallel orientation as well as $\{111\}$ orientation and later on developed $\{211\}$ due to the double twinning process on $\{111\}$ plane of the crystallites. Simultaneously a hexagonal phase with $\{0001\}$ orientation also developed due to the stacking fault associated with the crystal growth process. On the cleavage face of mica 2-d $\{116\}$ along with $\{111\}$ orientation, no doubt, due to the twinning on $\{111\}$ plane was observed, both for HgSe and HgTe films. On glass and collodion substrates thin films were polycrystalline in nature. Thicker films had a tendency to develop 1-d $\{111\}$ orientation.

In_2Te_3 deposits showed 2-d $\{111\}$ orientation by reflection and $\{100\}$ $\{211\}$ $\{0001\}_H$ by transmission. The development of $\{211\}$, $\{0001\}$ orientations was, no doubt, due to the growth faults. In_2Se and In_2Te grew epitaxially on all the faces of rocksalt with 2-d $\{001\}$ orientation. It was noticed that the orientation was such that $\langle 110 \rangle$ of the rocksalt face was parallel to $\langle 001 \rangle$ of the deposits.

This shows that even though there was a large difference in lattice parameters the two compounds grew epitaxially on rocksalt faces.

Tl_2Se and Tl_2Te developed 2-d $\{001\}$ orientation when deposited on rocksalt (100) face. By transmission, patterns characteristic of $\{310\}$ twinned structure were observed. This was the first time such a new type of twinning on a tetragonal crystal was noticed. The electron diffraction studies for the first time revealed that Tl_2Te film was also tetragonal and its lattice parameters were found to be a = 8.88 Å and c = 13.20 Å. Further Tl_2Te also developed twinned structure similar to Tl_2Se on $\{310\}$ plane.

InSb deposits at higher substrate temperature showed extensive $\{111\}$ twinned structure similar to those observed for HgSe, HgTe and In_2Te_3. The orientations observed were 2-d $\{211\}$, $\{100\}$ and $\{0001\}$ of hexagonal phase. On the (111) face, extensive twinning took place and 2-d $\{211\}$ orientation was observed. It may be mentioned here that the crystal growth in the vapour phase deposits is similar to those of cathodic (Finch, Wilman, Young, 1948; Banerjee and Goswami, 1959), anodic (Goswami, 1956) and chemically grown deposits (Goswami et al., 1956, 1958).

Though the above study on different compounds from vapour phase has clarified many aspects of crystal

growth process, the change of orientation from one to another, phase transition etc. during the growth process, it is yet not possible to predict the exact orientation that deposits will take up for a given combination of deposit and substrate pair. Even the orientation developed does not always conform to the best fit of atoms between the deposit and the substrate. Further recent ultra high vacuum work shows that a very 'clean' surface has a considerable influence in epitaxial growth of deposits from vapour phase. Investigations on the cathodic, anodic and chemically grown deposits on single crystal substrates in aqueous media, on the other hand show that even the so called 'unclean' substrate surface does not at all hinder the epitaxial growth. Thus a much more intensive work on crystal growth process with the help of other tools especially electron microscope is desirable to have a unified and clear picture of the growth of epitaxial layers for all cases of crystal growth processes whether anodic, cathodic or chemically grown layers or vapour phase deposits.

--

A C K N O W L E D G E M E N T S

The author is much indebted to Dr. A. Goswami for supervision, many helpful discussions, interest and encouragement received from him during the present study.

The author wishes to thank the Director, National Chemical Laboratory, Poona-8, for permission to submit this work in the form of a thesis.

Finally the author is thankful to the Council of Scientific and Industrial Research, New Delhi, for the award of Junior Research Fellowship which enabled him to devote his whole time to carry out the present investigation.

Kamal Chandra Barua

REFERENCES

Agalarzade, P.S. and Semiletov, S.A. (1963) Soviet Phys. Cryst. (USA), 8, 231.

Aggarwal, P.S. and Goswami, A. (1963a) Indian J. Pure and Appl. Phys., 1, 366.

Akhundov, G.A. and Abdullayev, G.B. (1958) Dokl. Akad. Nauk SSSR, 119, 267.

Akhundov, G.A., Abdullayev, G.B. and Guseynov, G.D. (1960) Fiz. Tverdogo Tela, 2, 1518.

Alieyev, M.I. and Dzhangirov, A.Yu. (1963) Fiz. Tverdogo Tela, 5, 3338.

Alieyev, M.I. and Dzhangirov, A.Yu. (1965) Soviet Phys. Solid State, 6, 1916.

Andrievskii, A.I., Nabitovich, I.D. and Voloshchuk, Ya.V. (1963) Soviet Phys. Cryst. (USA), 7, 704.

Averkin, A.A., Sergeeva, V.M. and Shelykh, A.I. (1960) Soviet Phys. Solid State, 2, 319.

Avery, D.G., Goodwin, D.W. and Rennie, A.E. (1957) J. Sci. Instrum., 34, 394.

Badachhape, S.B. and Goswami, A. (1964) Indian J. Pure and Appl. Phys., 2, 250.

Baev, I.A. (1966) Soviet Phys. Solid State (USA), 7, 2100.

Bakhyshov, A.E. and Abdullaev, G.B. (1960) Dokl. Akad. Nauk SSSR, 16, 437.

Banerjee, B.C. and Goswami, A. (1959) J. Electrochem. Soc., 106, 20.

Banus, M.D., Hanneman, R.E., Mariano, A.N., Warekois, E.P., Gatos, H.C. and Kafalas, J.A. (1963) Appl. Phys. Letters (USA), 2, 35.

Barret, C.S. (1952) "Structure of Metals" (McGraw Hill, London and N.Y.).

Bate, G. and Taylor, K.N.R. (1960) J. Appl. Phys., 31, 991.

Bauer, E. (1964) "Single Crystal Films" Ed. M.H. Francombe and H. Sato. Pergamon.

Bausch, W., Pinkenrath, H.F., Pagnia, H. and Schafer, G.H. (1965) Z. Angew. Phys. (Germany), 19, 42.

Becker, R. and Doring, W. (1935) Ann. Phys., 24, 719; (1949) Disc. Faraday Soc., 5 (Crystal Growth), 55.

Belashov, Yu.G. and Belashova, L.V. (1961) Optic and Spectrosc. (USA), 11, 282.

Black, J., Ku, S.M. and Minden, H.T. (1958) J. Electrochem. Soc., 105, 723.

Blair, J. and Smith, A.C. (1961) Phys. Rev. Letters (USA), 7, 124.

Blue, M.D., Garfunkel, J.H. and Kruse, P.W. (1961) Optical Soc. Amer. J., 51, 1408.

Bok, J. and Guthmann, C. (1964) Phys. Status Solidi (Germany) 6, 853.

Borets, A.N. and Stakh'yra, I.M. (1964) Ukrain Fiz. Zh. (USSR), 9, 1074 .

Brach, B.Ya., Zhdanova, V.V. and Lev, E.Ya. (1961) Soviet Phys. Solid State (USA) 3, 571.

Brice, J.C., Newman, P.C. and Wright, H.C. (1958) Brit. J. Appl. Phys., 9, 110.

Brown, F.C. (1913) Phys. Rev., 1, 237.

Bublik, A.I. (1952) Dokl. Akad. Nauk SSSR, 87, 215.

Buchsbaum, S.J., Chynoweth, A.G. and Feldmann, W.L. (1965) Appl. Phys. Letters (USA), 6, 67.

Burton, W.K. and Cabrera, N. (1949) Disc. Faraday Soc. No.5 (Crystal Growth).

Burton, W.K., Cabrera, N. and Frank, E.C. (1951) Trans. Roy. Soc. (London), A243, 299.

Busch, G. and Steigmeier, E. (1961) Helv. Phys. Acta (Switzerland), 34, 1.

Carlson, R.O. (1958) Phys. Rev., 111, 476.

Chizhevskaya, S.N. and Glazov, V.M. (1962) Dokl. Akad. Nauk SSSR, 145, 115.

Cowley, J.M. (1953) Acta Cryst., 6, 516;
9, 397.

Cowley, J.M. and Rees, A.L.G. (1958) Reports on Progress in Phys., 21, 166.

Cruceanu, E. Neulescu, D., Stamatescu, I., Nistor, N. and Ionescu-Bujor, S. (1966) Soviet Phys. Solid State, 7, 1646; ibid, (1965) Soviet Phys. Solid State, 7, 1456.

Curie, P. (1885) Bull. Soc. Franc. Miner., 8, 145.

Dale, E.B. and Senecal, G. (1962) J. Appl. Phys. (USA), 33, 2526.

Damon, R.W. and Redington, R.W. (1954) Phys. Rev., 96, 1498.

Dana, J.D. and Dana, E.S. (1951) "System of Mineralogy" Vol.II New York. John Wiley & Sons, Inc. Chapman and Hall Ltd. London.

Davisson, C.J. and Germer, L.W. (1927) Phys. Rev., 30, 705; (1928) Proc. nat. Acad. Sci. Wash, 14, 317.

Delves, R.T. and Lewis, B. (1963) J. Phys. Chem. Solids, 24, 4.

de Jong, W.F. (1926) Z. Krist., 63, 466.

Elleman, A.F. and Wilman, H. (1948) Proc. Phys. Soc. (London), 61, 164.

Elpat'evskaya, O.D. (1958) Zh. Tekh. Fiz., 28, 2676.

Ferry, D.K., Young, R.W. and Dougal, A.A. (1965) J. Appl. Phys. (USA), 36, 3684.

Finch, G.I. and Wilman, H. (1937) Erg. Exakt. Naturav, 16, 353.

Finch, G.I., Wilman, H. and Yang, L. (1947) Disc. Faraday Soc., 1, 144.

Finch, G.I., Sinha, K.P. and Goswami, A. (1955) J. Appl. Phys., 26, 250.

Frank, F.C. and van der Merwe, J.H. (1949) Proc. Roy. Soc., A198, 205.

Frenkel, J. (1945) J. Phys. Moscow, 9, 392;
(1946) "Kinetic Theory of Liquids" Clarendon Press, Oxford.

Friedrich, W., Knipping, P. and Laue, M. (1912) S.B. bayer Akad. Wiss, 303.

Furmeron-Rodot, H. and Rodot, M. (1959) C.R. Acad. Sci. (Paris) 248, 937.

Galavanov, V.V. and Erokhima, N.A. (1959) Fiz. Tverdogo Tela, 1, 1198.

Gerasimov, Ya.I., Abbasev, A.S. and Nikol'skaya, A.V. (1962) Dokl. Akad. Nauk SSSR, 147, 835.

Gibbs, J.W. (1878) Collected Works, 1928, p.325 footnote, Longmans Green and Co. London.

Giriat, W. (1964) Brit. J. Appl. Phys., 15, 151.

Gobrecht, H., Gerhardt, U., Peinemann, B. and Tausend, A. (1961) J. Appl. Phys. (Suppl.) 32, 2246.

Gorjunova, N.A. and Fedorova, N.N. (1955) Zh. Tekh. Fiz., 25, 1339.

Goryunova, N.D. and Radautson, S.I. (1958) Dokl. Akad. Nauk SSSR, 121, 848.

Goswami, A. (1954) J. Sci. Indust. Res., 13B, 677;
(1957) Trans. Faraday Soc., 54, 821;
(1962) J. Electrochem. Soc., 109, 365.

Goswami, A. and Trehan, Y.N. (1956) Trans. Faraday Soc., 52, 358.

Grigor'eva, V.S. (1958) Zh. Tekh. Fiz., 28, 1670.

Grochowskii, E.G., Mason, D.R., Schmitt, G.A. and Smith, P.H. (1964) J. Phys. Chem. Solids (GB), 25, 551.

Guliev, T.N. and Medvedeva, Z.S. (1965) Zhurnal Neorganicheskoi Khimii, 10, 1520.

Gunther, K.G. (1958) Z. Naturforch., 13a, 1081.

Guseinov, G.D. and Akhundov, G. (1964) Soviet Phys. Solid State (USA), 6, 497.

Haasen, P. (1957) J. Metals, N.Y., 9, 30.

Hahn, H. and Klinger, W. (1949a,b) Z. Anorg. Chem., 260, 97, 110.

Hall, E.O. (1954) "Twinning" Butterworths, London.

Harman, T.C. and Strauss, A.J. (1961) J. Appl. Phys. (USA) Suppl., 32, 2265.

Henisch, H.K. and Francois, M.L.J. (1950) Nature, London, 165, 891; (1951) "Semiconducting Materials" Ed. H.K. Henisch (Lond: Butterworths Scientific Publications).

Henisch, H.K. and Saker, F.W. (1952) Proc. Phys. Soc. (London), B65, 149.

Henneke, H.L. (1961) Solid State Electronics (GB), 3, 159.

Hirth, J.P., Hruska, S.J. and Pound, G.M. (1964) "Single Crystal Films" Ed. M.H. Francombe and H. Sato, Pergamon.(

Holmes, P.J., Jennings, I.C. and Parrott, J.E. (1962) Phys. Chem. Solids (GB), 23, 1.

Inuzuka, H. and Sugaike, S. (1954) Proc. Imp. Acad. Japan, 30, 383.

Jawson, M.A. and Dove, D.B. (1954) Acta Cryst., 10, 14.

Kafalas, J.A., Gatos, H.C., Lavine, M.C. and Banus, M.D. (1962) Phys. Chem. Solids (GB), 23, 1541.

Kanai, Y. (1958 a) J. Phys. Soc. Japan, 13, 1065;
(1958 b) J. Phys. Soc. Japan, 13, 967.

Kasper, J.S. and Brandhorst, H. (1964) J. Chem. Phys. (USA), 41, 3768.

Kas'yan, V.A. (1964) Soviet Phys. Solid State (USA), 5, 1445.

Katayama, Y. and Tanaka, S. (1966) Phys. Rev. Letters (USA), 16, 129.

Katilene, E.R. and Regel, A.R. (1965) Soviet Phys. Solid State (USA), 6, 2284.

Kolomiets, B.T. and Pavlov, B.V. (1960) Soviet Phys. Solid State (USA), 2, 592.

Kolomiets, B.T. and Nazarova, T.F. (1960) Soviet Phys. Solid State, 2, 369.

Kolomiets, B.T. and Mamontova, T.N., Stepanov, G.I. (1965) Soviet Phys. Solid State (USA), 7, 1320.

Kolosov, E.E. and Sharavskii, P.V. (1966) Soviet Phys. Solid State (USA), 7, 1814.

Konozenko, I.D. and Mikhnov'skyi, S.D. (1956) Ukrayin. Fiz. Zh., 1, 151.

Kornfel'd, M.I. and Sochava, L.S. (1959) Fiz. Tverdogo Tela, 1, 1370.

Kossel, W. (1927) Nachr. Ges. Weiss. Gottingen, 135;
(1928) Quantentheorie und Chemie, p.46, Leipzig.

Krucheanu, E., Nikulesku, D. and Vanku, A. (1965) Soviet Phys. Cryst. (USA), 9, 445.

Kruse, P.W., Blue, M.D., Garfunkel, J.H., and Saur, W.D. (1962) Infrared Phys., 2, 53;
(1959) J.Appl. Phys., 30, 770.

Kurov, P.A. (1957) Zh. Tekh. Fiz., 27, 2181.

Kurov, G.A. and Pinsker, Z.G. (1958 a) Zh. Tekh. Fiz. 28, 29;
(1958b) Zh. Tekh. Fiz. 28, 2130.

Lagrenaudie, J. (1958) J. Chem. Phys., 55, 175.

Lawson, W.D., Nielsen, S., Putley, E.H. and Young, A.S. (1959) J. Phys. Chem. Solids, 9, 325.

Lyubin, V.M. and Fomina, V.I. (1964) Soviet Phys. Solid State (USA), 5, 2472.

Man, L.I. and Semiletov, S.A. (1965) Soviet Phys. Cryst., 10, 328.

Mariano, A.N. and Warekois, E.P. (1963) Science, 142, 672.

Mayer, H. (1959) "Structure and Properties of Thin Films" p.225, Wiley, New York; (1961) Symposium on Electrical and Magnetic Properties of Metallic Thin Layers, Louvin Belg.

Menzer, G. (1938 a,b,c) Naturwiss, 26, 385; Z. Krist., 99, 378, 410.

Monlton, C. (1962) Nature (GB), 195, 793.

Moss, R.J. (1877) Phil. Mag., 3, 67.

Moss, T.S. (1960) Progress in Semiconductors, 5, 189, Ed. A.F. Gibson, I.A. Kroger and R.E. Burgess. London: Heywood and Co.

Mugge, O. (1903) News Jahrb. Min. Beil-Bd, 16, 335.

Ozolin'sh, G.V., Averkieva, G.K., Goryunova, N.A. and Ievin'sh, A.F. (1963) Soviet Phys. Cryst., 8, 207.

Palatnik, L.S., Atroschenko, L.V., Gal'chinetskii, and Koshkin, V.M. (1965) Dokl. Akad. Nauk SSSR, 165, 809.

Paparoditis, C. (1957) C. R. Acad. Sci. (Paris), 245, 1526.

Pashley, D.W. (1956) Phil. Mag., 5,(Suppl.) 173.

Pearson, W.B. (1958) "A Handbook of Lattice Spacings and Structure of Metals and Alloys" Pergamon Press.

Petrusevich, V.A. and Sergeeva, V.M. (1961) Soviet Phys. Solid State (USA), 2, 2562.

Pinsker, Z.G. (1953) "Electron Diffraction" Butterworth, London.

Porowski, S. and Galzazka, R.R. (1964) Phys. Status Solidi (Germany), 5, K71.

Putley, E.H. (1959) Proc. Phys. Soc., 73, Pt.2, 280.

Rabenau, A., Stegherr, A. and Eckerlin, P. (1960) Zeitschrift fur Metallkunde, 51, 295.

Raether, H. (1951) Ergeb. Exakt. Naturw., 24, 54; (1957) Handbuch Der Physik (Ed. S. Flugge) 32, 443, (Berlin, Gottingen, Heidelberg: Springer-Verlag).

Reimer, L. (1958) Z. Naturforch, 13a, 148.

Rhodin, T.N. and Walton, D. (1964) "Single Crystal Films" Ed. M.H. Francombe and H. Sato, Pergamon.

Richards, J.L., Hart, P.B. and Gallone, L.M. (1963) J. Appl. Phys. (USA), 34, 3418.

Rodot, M., Rodot, H. and Triboulet, R. (1961) J. Appl. Phys. (USA), Suppl. 32, 2254.

Rodot, H. and Triboulet, R. (1962) C. R. Acad. Sci. (France) 254, 852.

Rodot, Par M. Michel. (1958) J. Phys. Radium, 19, 140.

Rosenberg, A.J. and Strauss, A.J. (1961) J. Phys. Chem. Solids, 19, 105.

Royer, L. (1928) Bull. Soc. Franc. Min., 51, 7.

Schubert, K.S., Dorre, E. and Gunzel, E. (1954) Naturwissenschaften, 41, 448.

Schulz, L.G. (1951 a) J. Chem. Phys., 19, 504;
(1951 b) Acta Cryst., 4, 487.

Semiletov, S.A. (1958) Soviet Phys. Cryst., 3, 292;
(1961 a) Soviet Phys. Solid State (USA), 3, 544;
(1961 b) Soviet Phys. Cryst.(USA), 5, 673;
(1961 c) Soviet Phys. Cryst.(USA), 6, 158.

Semiletov, S.A. and Rozsibal, M. (1957) Soviet Phys. Cryst., 2, 281.

Shalyt, S.S. and Tamarin, P.V. (1965) Soviet Phys. Solid State (USA), 6, 1842.

Shneider, A.D. and Gavrischak, T.V. (1961) Soviet Phys. Solid State (USA), 2, 1865.

Slavnova, G.K., Luzhnaya, N.P. and Medvedeva, Z.S. (1963) Zhurnal Neoganicheskoi Khimi, 8, 153.

Slavnova, G.K., Yeliseyev, A.A. (1963) Zhurnal Neorganicheskoi Khimi, 8, 1654.

Smith, P.L. and Martin, J.E. (1963) Nature (GB), 196, 762.

Sorokin, O.M. (1961) Soviet Phys. Solid State (USA), 2, 2091.

Spencer, P.M., Pamplin, B.R. and Wright, D.A. (1962) Proc. International Conf. Phys. and Semiconductors, p.244, Exeter, England.

Spencer, P.M. (1964) Brit. J. Appl. Phys., 15, 625.

Stakhira, I.M. (1963) Ukrayin Fiz. Zh. (USSR), 8, 970.

Stasova, M.M. and Vainshtein, B.K. (1958) Soviet Phys. Cryst., 3, 140.

Stranski, I.N. (1928) Z. Phys. Chem., 136, 259;
(1949) Disc. Faraday Soc., No.5(Crystal Growth), p.13.

Straumanis, M.E. and Kim, C.D. (1965) J. Appl. Phys. (USA), 36, 3822.

Swanson, H.E., Gilfrich, N.T. and Cook, M.I. (1957) Nat. Bur. Standards Circular, 7, 539.

Terpilowski, J. and Zaleska, E. (1963) Roczniki Chemii, Warsaw, 37, 193.

Thomson, G.P. (1928) Proc. Roy. Soc., A117, 600;
(1928) Proc. Roy. Soc., 119, 651.

Thomson, G.P. and Cochrane, W. (1939) "Theory and Practice of Electron Diffraction" (McMillan, London).

Tisdale, W.E. (1918) Phys. Rev., 12, 325.

Tittmann, B.R., Darnell, A.J., Bommel, H.E. and Libby, W.F. (1964) Phys. Rev., Pt.A, 135, A1460.

Trehan, Y.N. and Goswami, A. (1958), Trans. Faraday Soc., 54, 1703; (1958) Trans. Faraday Soc., 55, 2162;
(1959) Proc. National Inst. Sci. India, 25A, 210.

Uphoff, H.L. and Healy, J.H. (1963) J. Appl. Phys., 34, 390.

Vainshtein, B.K. (1964) "Structure Analysis by Electron Diffraction" Pergamon Press, N.Y.

van der Merwe, J.H. (1964) "Single Crystal Films" Ed. M.H. Francombe and H. Sato, Pergamon.(

Vodopyanov, L.K. and Kurdiani, N.I. (1966) Soviet Phys. Solid State (U.S.A.) 7, 2224.

Volmer, M. (1939) Kinetic der Phasenbildung, Steinkopff, Dresden and Leipzig.

von Borcke, U., Martens, H. and Weiss, H. (1966) Solid State Electronics (GB) 8, 365.

Walleraut, F. (1902) Bull. Soc. Franc. Min., 25, 180.

Wilman, H. (1948 a) Proc. Phys. Soc. (London), 60, 341;
(1948 b) Proc. Phys. Soc. (London), 61, 416;
(1949) Research, 2, 352;
(1952) Acta Cryst., 5, 782.

Williams, A.L. and Thompson, L.E. (1941) J. Instn. Elect. Engrs., 88, 353.

Williamson, W.J. (1966) "Solid State Electronics" Pergamon Press, 9, 213.

Woolley, J.C. and Ray, B. (1960) J. Phys. Chem. Solids (GB), 13, 151; ibid, 15, 27.

Woolley, J.C. and Pamplin, B.R. (1959) Jour. of the Less-Common Metals, 1, 362.

Woolley, J.C., Gillett, C.M. and Evans, J.A. (1960) J. Phys. Chem. Solids (GB), 16, 138.

Woolley, J.C. and Pamplin, B.R. (1961) Electrochem. Soc. J., 108, 874.

Wright, D.A. (1965) Brit. J. Appl. Phys., 16, 939.

Wulff, G. (1901) Z. Kristallogr., 34, 449.

Wyckoff, R.W.G. (1931)"The Structure of Crystals" (New York: Chemical Catalog Co.)

Zachariasen, W.H. (1925) Nork geol. tidssk, 8, 302;
(1926) Zeits. Phys. Chem., 124, 436.

Zaslavskii, A.I. and Sergeeva, V.M. (1961) Soviet Phys. Solid State (USA), 2, 2556.

Zaslavskii, A.I., Sergeeva, V.M. and Smirnov, I.A. (1961) Soviet Phys. Solid State, 2, 2565.

Zhuze, V.P., Sergeeva, V.M. and Shelykh, A.I. (1961) Soviet Phys. Solid State (USA), 2, 2545.

Zhuze, V.P. and Shelykh, A.I. (1965) Fiz. Tverdogo Tela, 7, 1176.

Zhad'ko, I.P., Rashba, E.I., Romanov, V.A., Stakhira, I.M. and Tovstyuk, K.D. (1965) Soviet Phys. Solid State (USA), 7, 1432.

Zorll, U. (1954) Z. Phys., 138, 167.

Zuze, V.P., Zaslavskii, A.I., Petrusevic, V.A., Sergeeva, V.M., Smirnov, I.A. and Selykh, A.I. (1960) Proc. International Conf. on Semiconductor Phys. Prague. New York and London. Academic Press (1961) p.871.

--